Einführung in die Rastersondenmikroskopie

Ernst Meyer
Ernst.Meyer@unibas.ch

SPM/SXM: Scanning Probe Microscopy
STM: Scanning Tunneling Microscopy
AFM: Atomic Force Microscopy
SFM: Scanning Force Microscopy
SNOM: Scanning Nearfield Optical Microscopy

1) G. Binnig, H. Rohrer, Ch. Gerber and E. Weibel, Phys. Rev. Lett. 49, 57 (1982)

(2) G. Binnig, C.F. Quate, and Ch. Gerber, Phys. Rev. Lett. 56, 930 (1986)

(3) E. Meyer, H. Hug and R. Bennewitz, Scanning Probe Microscopy: The Lab on a Tip, Springer Verlag, 2003

Scanning Probe Microscopy

Invention of the Scanning Tunneling Microscope 1982 by Gerd Binnig and Heinrich Rohrer: Begin of a new era of microscopy
Invention of the Atomic Force Microscope in 1986: Extension to surfaces of insulators.
New members of the family of probe microscopes:

- scanning near-field optical microscope (SNOM)
- magnetic force microscope (MFM)
- magnetic resonance force microscope (MRFM)
- scanning thermal microscope
- scanning potentiometry microscope
- ballistic electron emission microscope (BEEM)
- scanning capacitance microcope
- scanning ion conductance microscope
- ……...

(1) G. Binnig, H. Rohrer, Ch. Gerber and E. Weibel, Phys. Rev. Lett. 49, 57 (1982)
(2) G. Binnig, C.F. Quate, and Ch. Gerber, Phys. Rev. Lett. 56, 930 (1986)

Scanning Tunneling Microscope

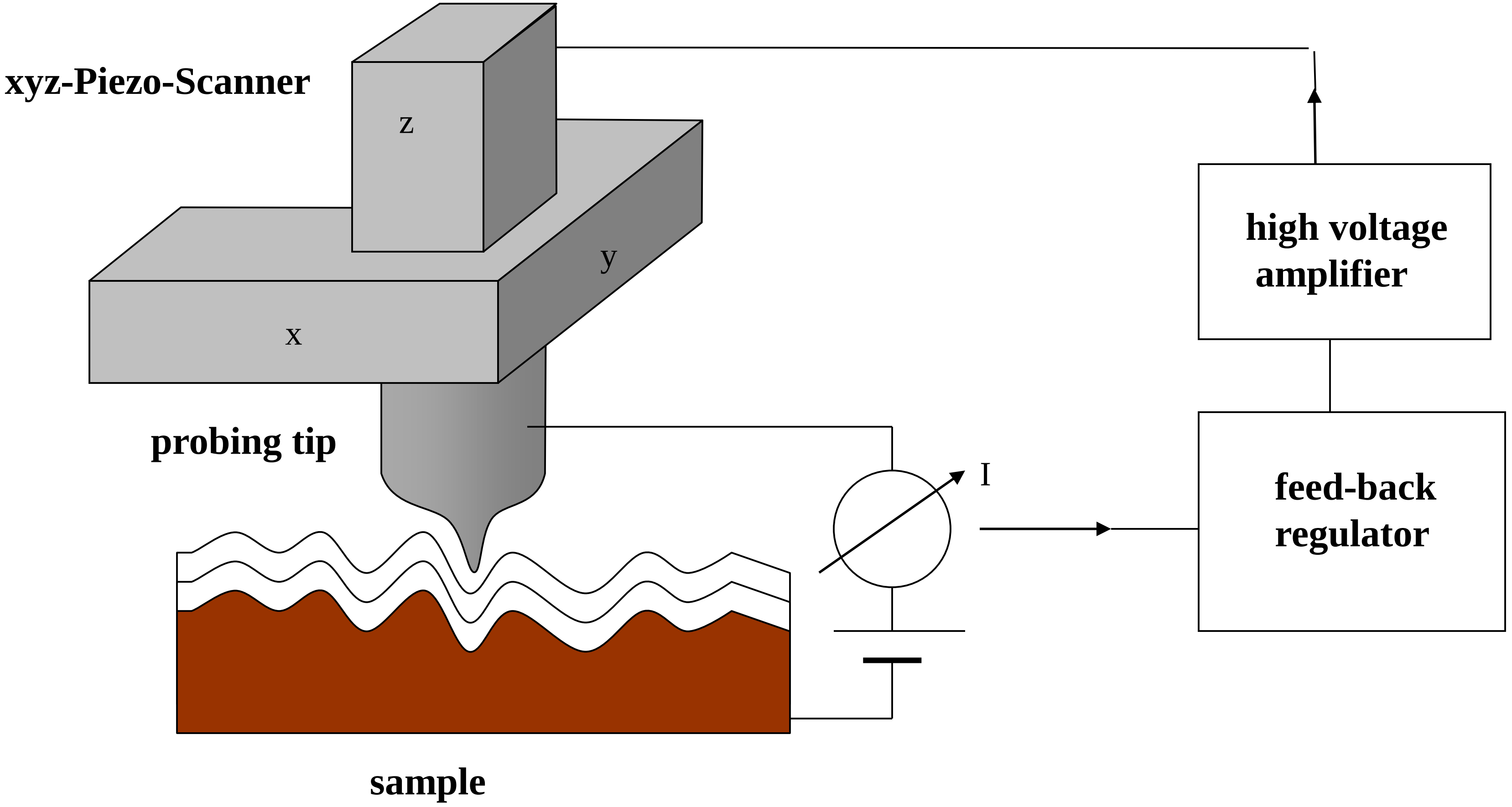

Feed-back regulator keeps current (pA-nA) constant.
Contours of constant current are recorded.

STM for Schools

Nanosurf AG, Liestal: Start-up from the University of Basel

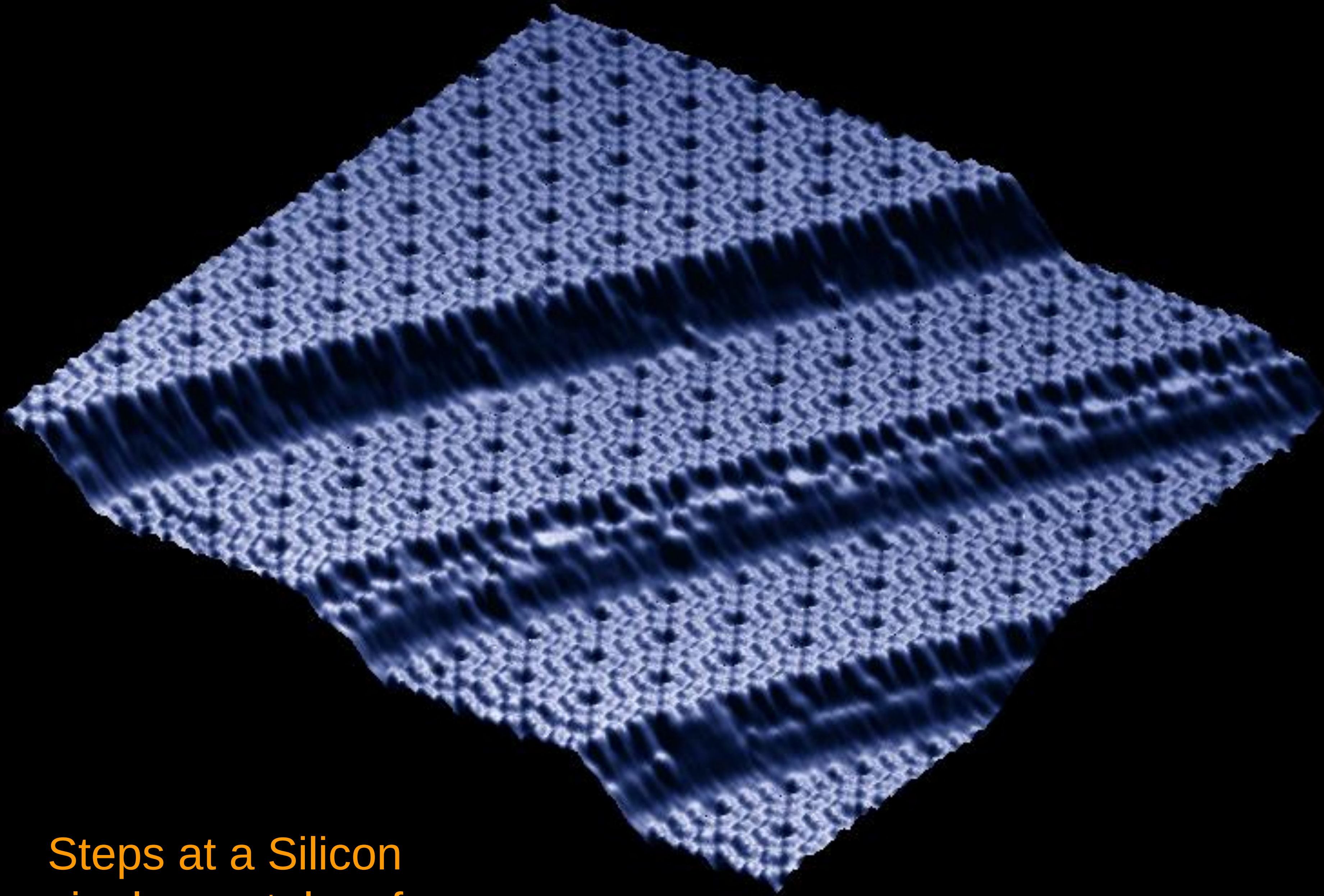

Steps at a Silicon
single crystal surface.

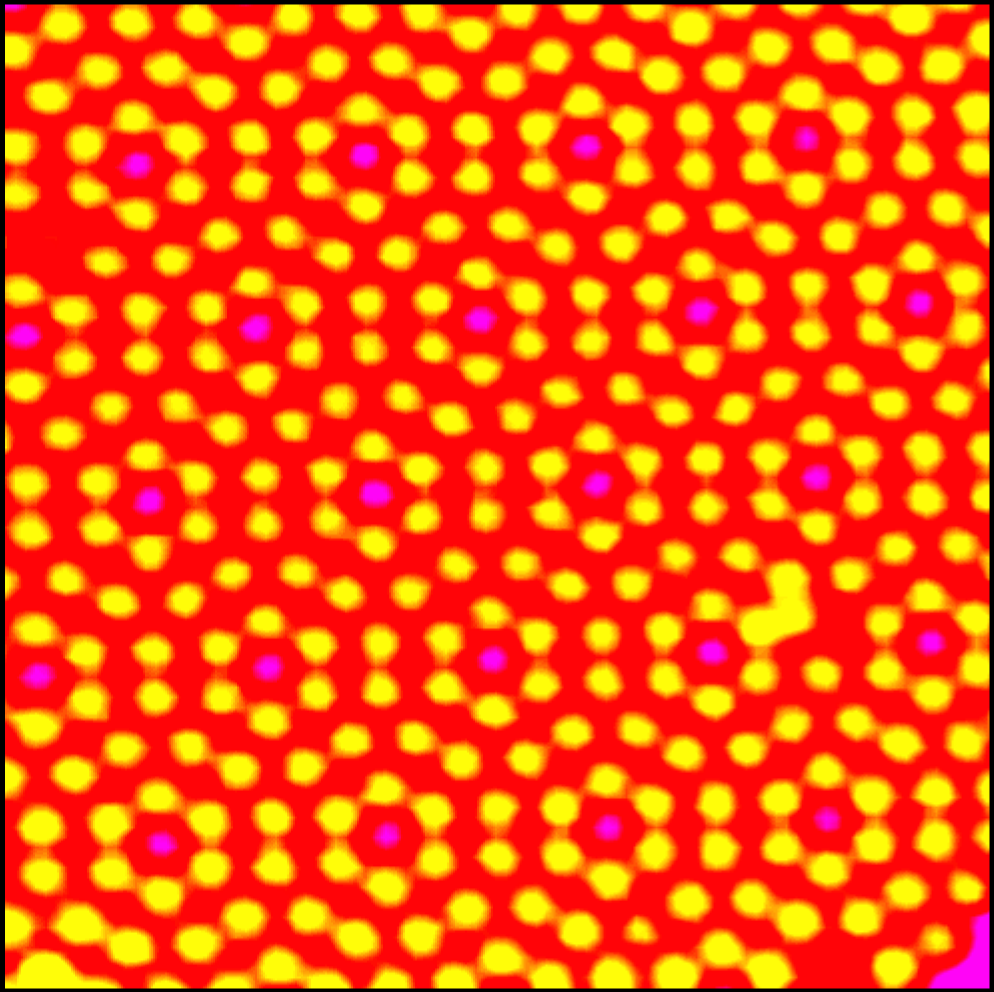

Si(111)7x7 reconstructed surface

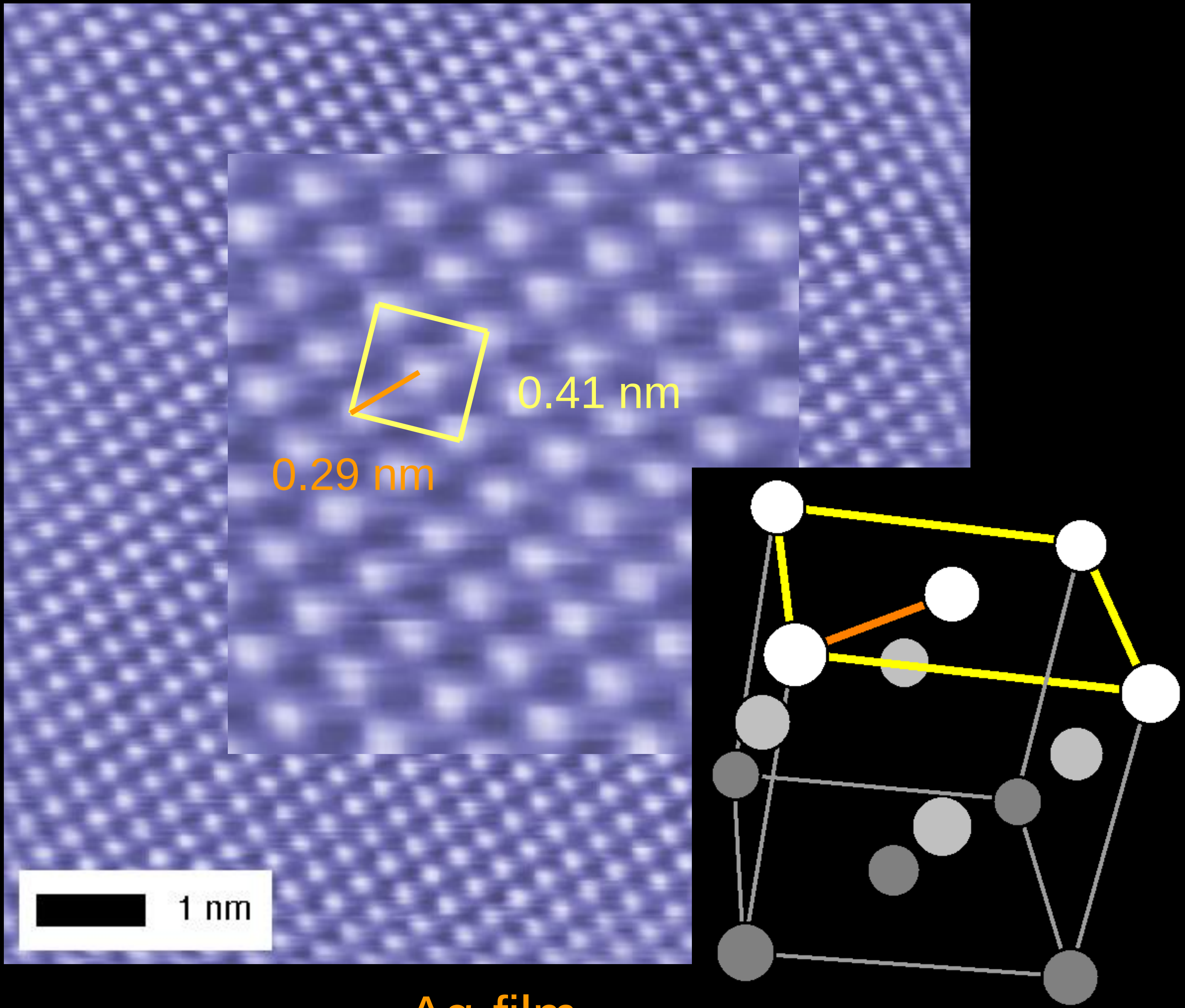

Ag-film

Elements of STM

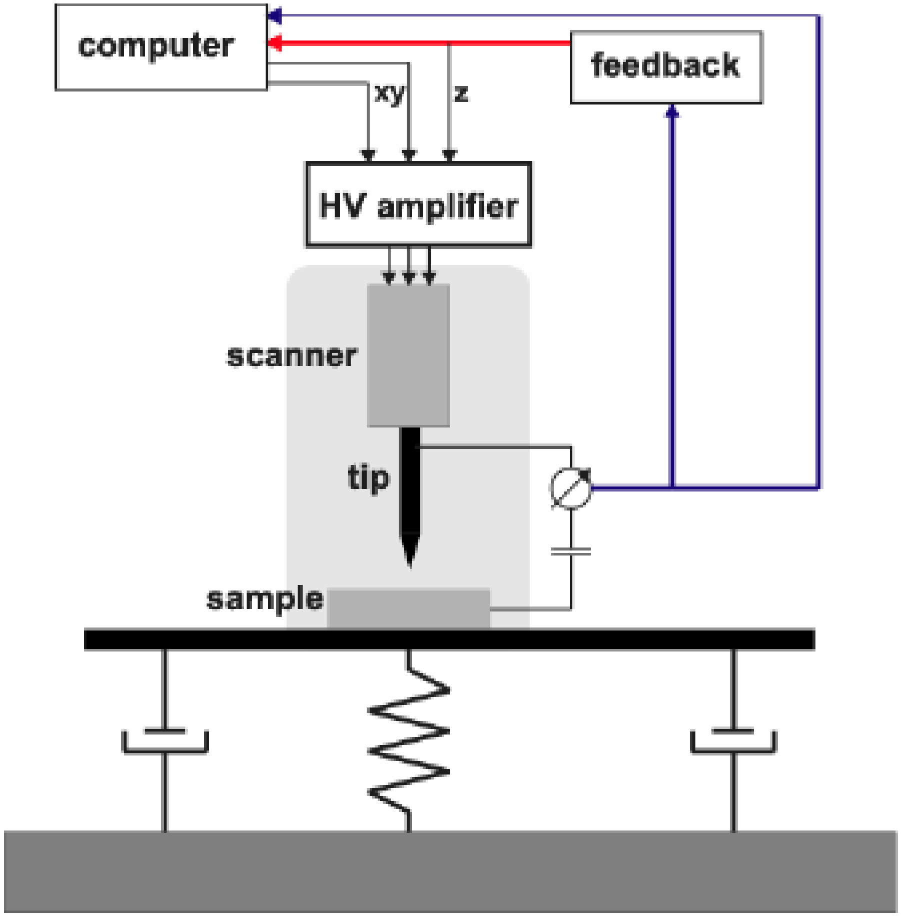

- the tip is moved in three dimensions by piezoelectric actuators
- good vibration isolation
- mechanical stability of the experimental setup turns out to be a prerequisite for successful measurements on the atomic scale
- a high-voltage amplifier is required to drive the piezoelectric scanner
- the tunneling current is used to control the tip-sample distance z via a feedback circuit that keeps the tunneling current constant
- the distance z is recorded by a computer as function of the scanned coordinates x,y

Piezoelectric effect

Piezoelectric scanners work with the transversal piezoelectric effect. The crystal is elongated perpendicular to the applied electric field.

$$\Delta L = d_{31} \cdot L \cdot \vec{E}$$

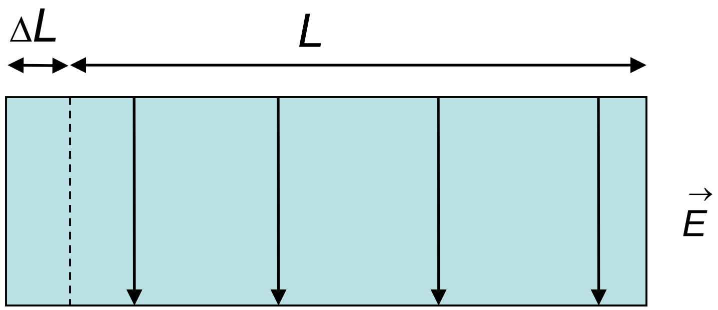

$\vec{E}$ electric field, *L* length, Δ*L* elongation, d_{31} transversal piezoelectric coefficient

Typical material is PZT (Lead Zirkonium Titanat). The relation between Lead and Zirkonium determines the Curie-temerature and the piezoelectric coefficient.

Example: PZT-5H: d_{31}=-2.62Å/V i.e. L=1 cm, ΔL = 1 μm, E=380 V/mm

Piezoelectric scanners

For a thre-dimensional movement 3-leg scanners or tube scanners are employed:

Sensitivity of the tube scanner:

$$\Delta z = d_{31} \cdot V \cdot \frac{L}{H}$$

***V*: applied voltage, *L* length, *H* thickness und d_{31} transversal piezoelectric coefficient.**

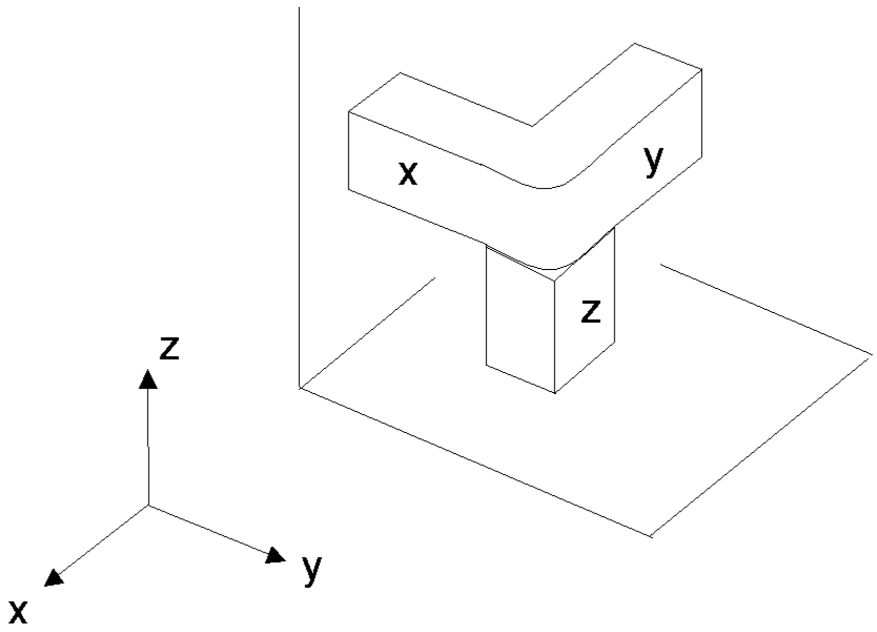

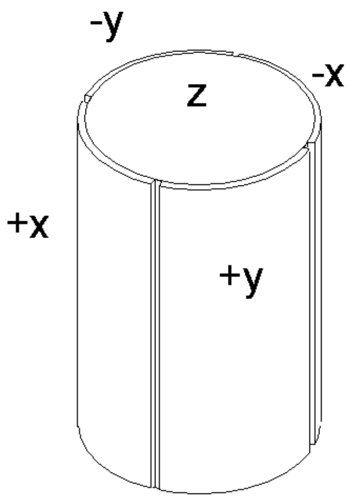

Piezotubes

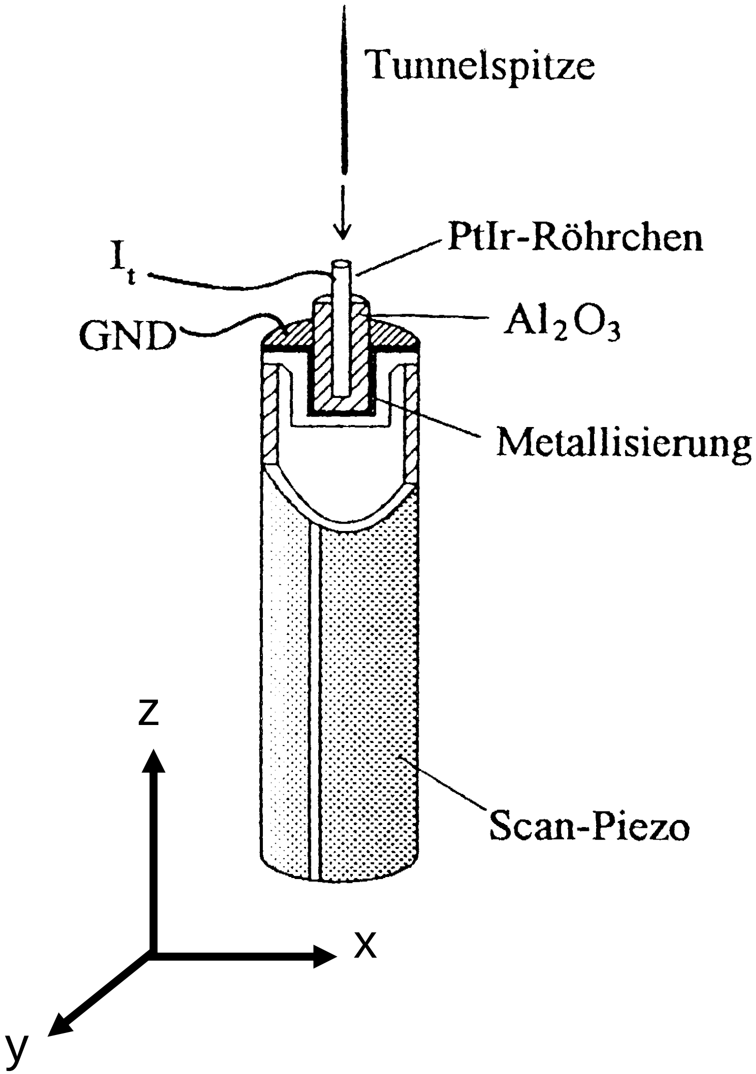
Tunnelspitze
PtIr-Röhrchen
I_t
GND
Al_2O_3
Metallisierung
Scan-Piezo
z
x
y

Calibration of scanners

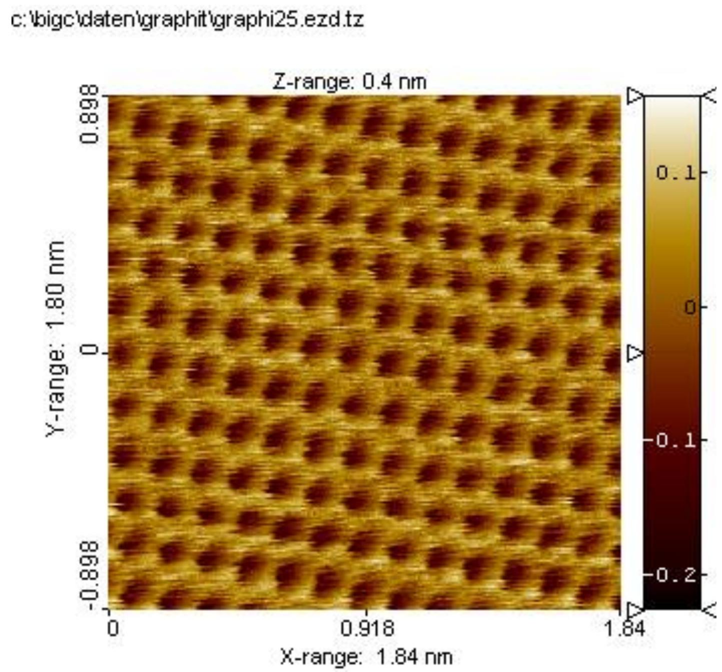

Highly oriented pyrolitic graphite (HOPG) is a common sample.
The distance between atoms is 1.42Å. However, the observed s
pacing between protrusions is 2.56 Å, which corresponds to the distance between the hexagons. Every other atom is imaged equally.
LDOS-contrast is influenced by the layer below.
➔Calibration in x-y-direction. (Drift rates have to be optimized)

Z-Calibration

c:\bigc\daten\graphit\graphi15.ezd.tz

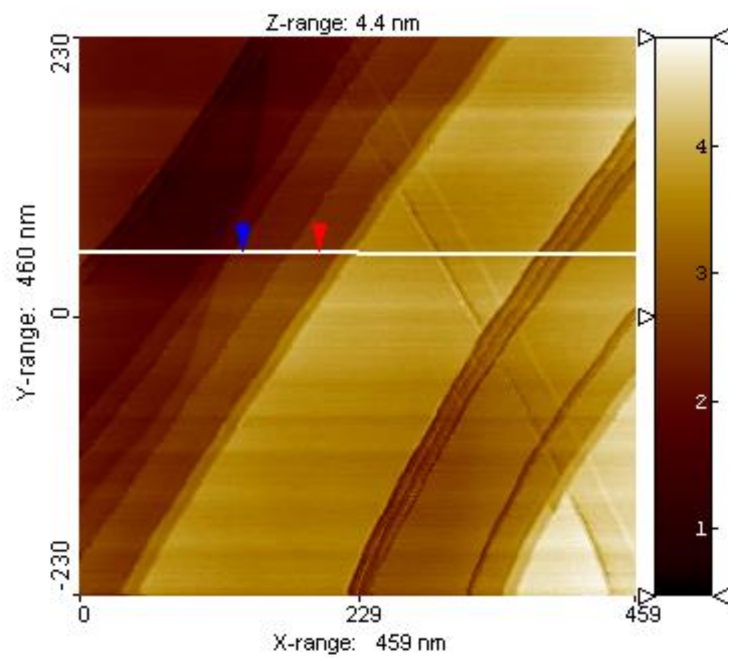

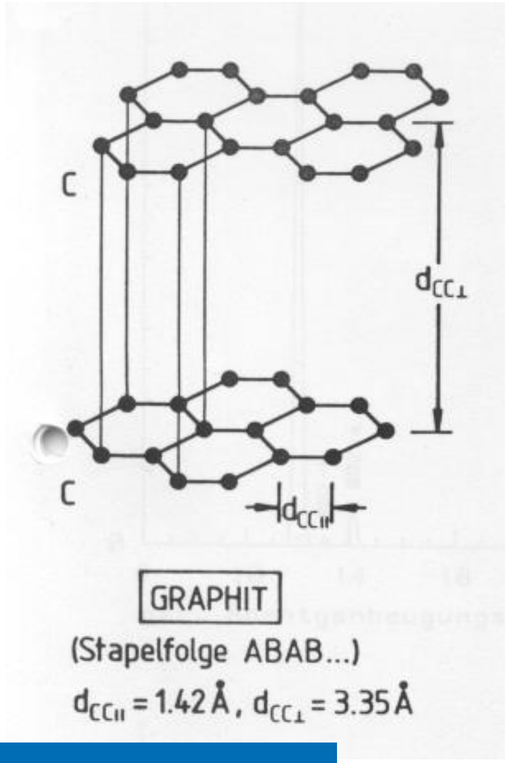

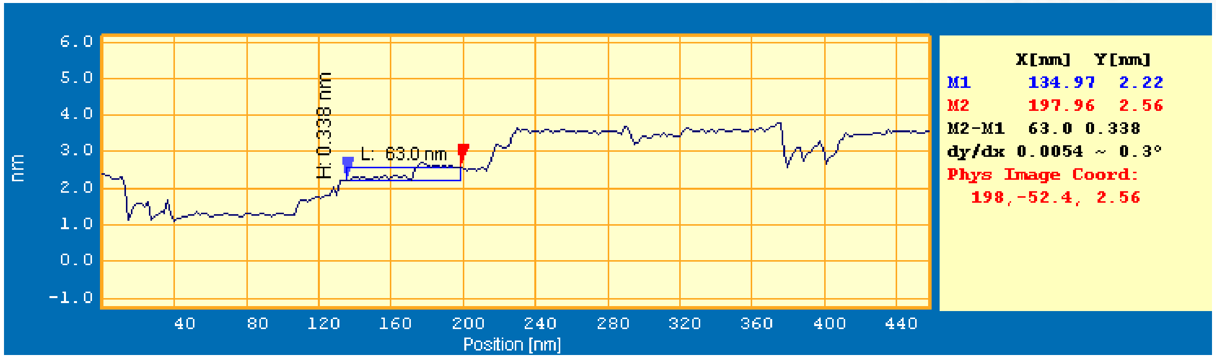

Calibration of Scanner

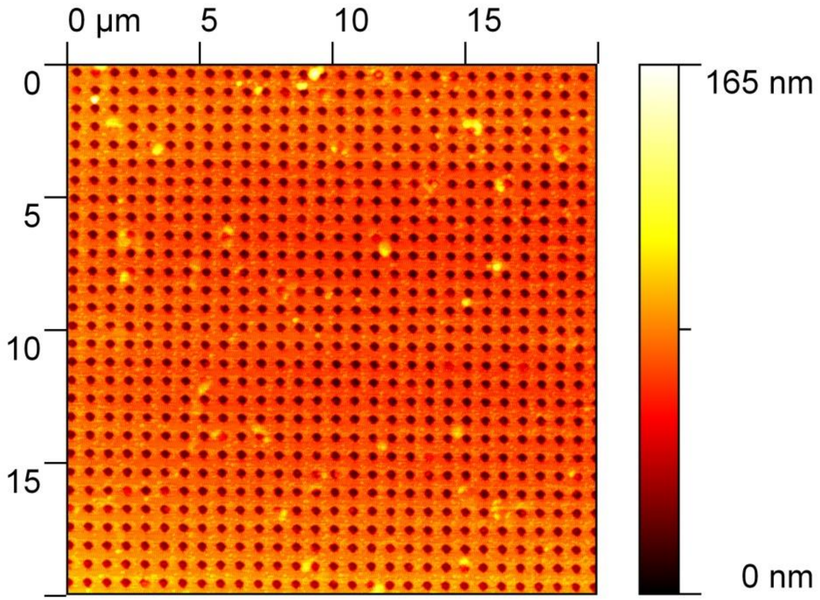

P=660nm

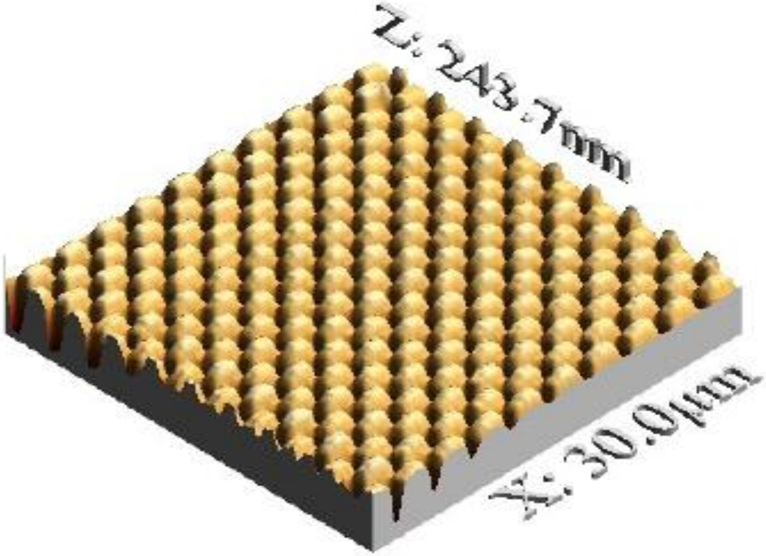

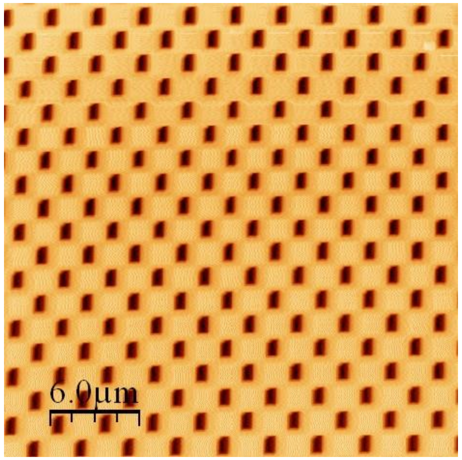

Gratings: Periodicity and z-height are known.

P=3µm

Vibration damping

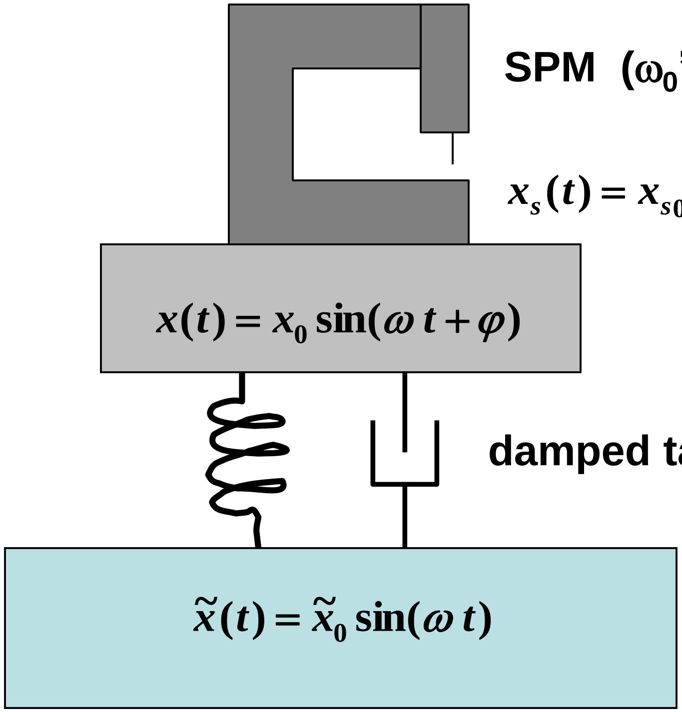

SPM (ω_0' , Q')

$$x_s(t) = x_{s0} \sin(\omega t + \varphi')$$

damped table (ω_0 , Q)

$$T_S = \frac{|x_{s0}|}{|x_0|} = \frac{\left(\frac{\omega}{\omega'_0}\right)^2}{\sqrt{\left(1-\left(\frac{\omega}{\omega'_0}\right)^2\right)^2 + \left(\frac{\omega}{Q'\omega'_0}\right)^2}}$$

transfer function of the SPM

$$T = \frac{|x_0|}{|\tilde{x}_0|} = \sqrt{\frac{1+\left(\frac{\omega}{Q\omega_0}\right)^2}{\left(1-\left(\frac{\omega}{\omega_0}\right)^2\right)^2 + \left(\frac{\omega}{Q\omega_0}\right)^2}}$$

total transfer function: $T_T = T \cdot T_S$

transfer function of the table

Amplitude transformation

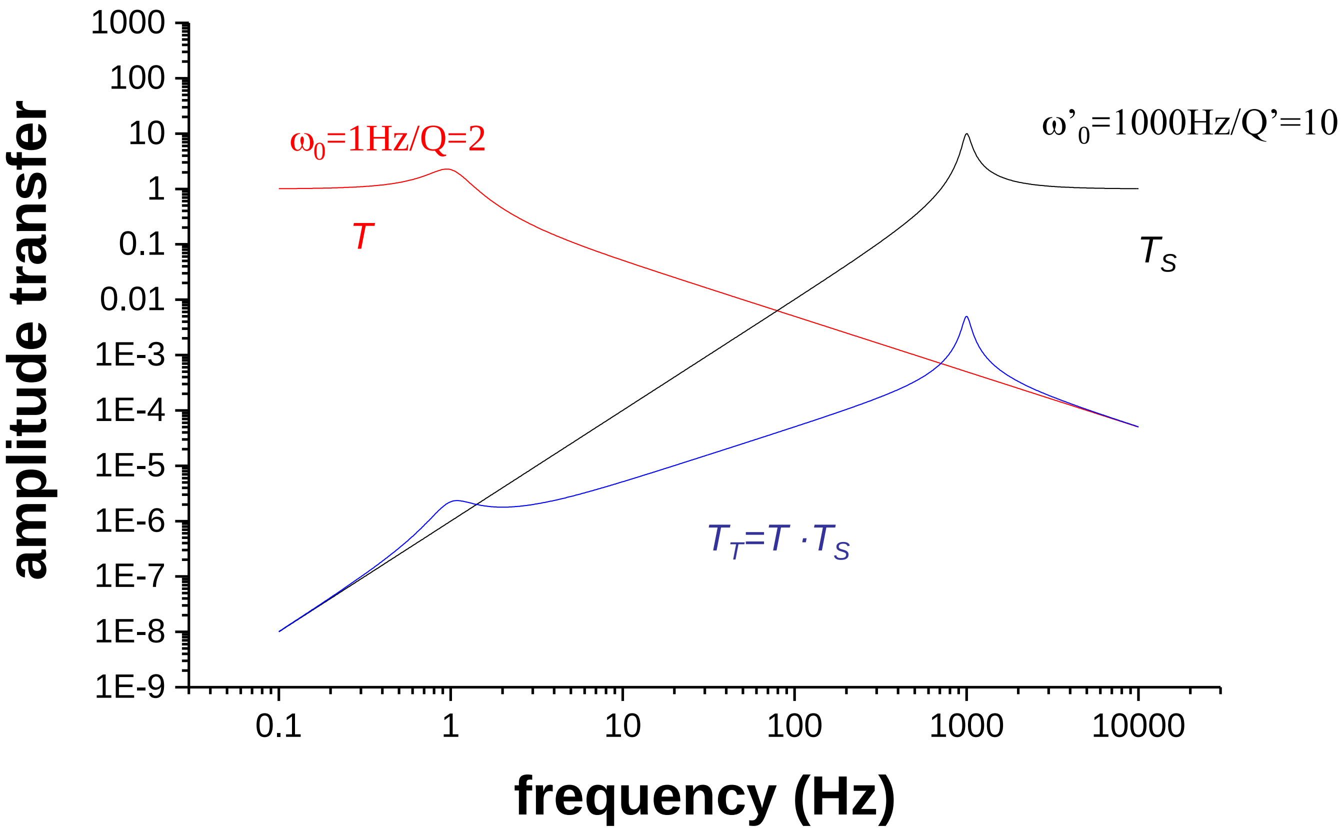

table: ω_0 =1Hz, Q=2 SPM: ω_0' =1000 Hz, Q'=10

Two-step damping

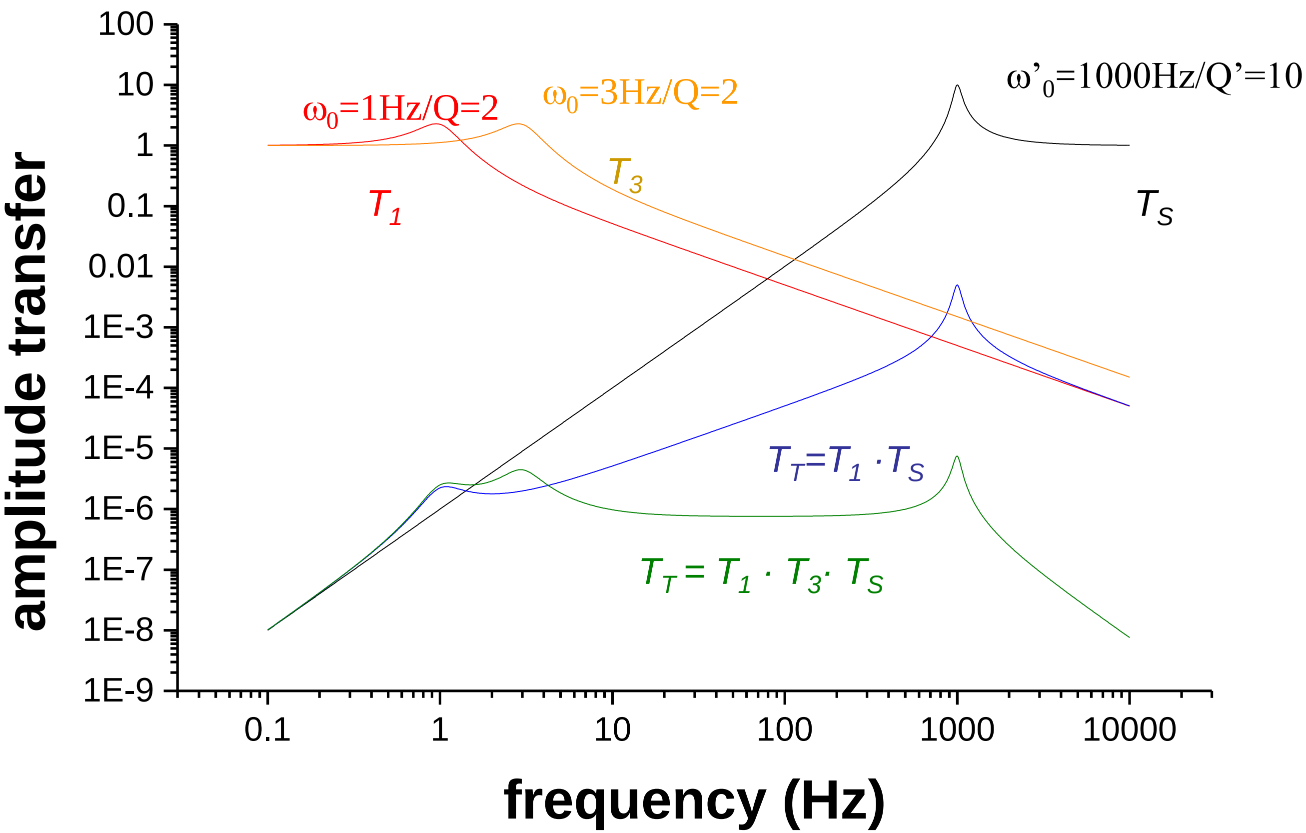

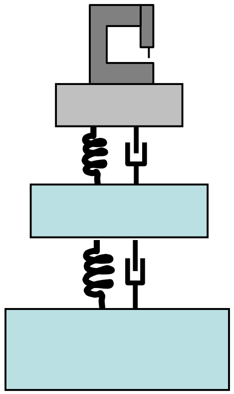

Eddy current damping

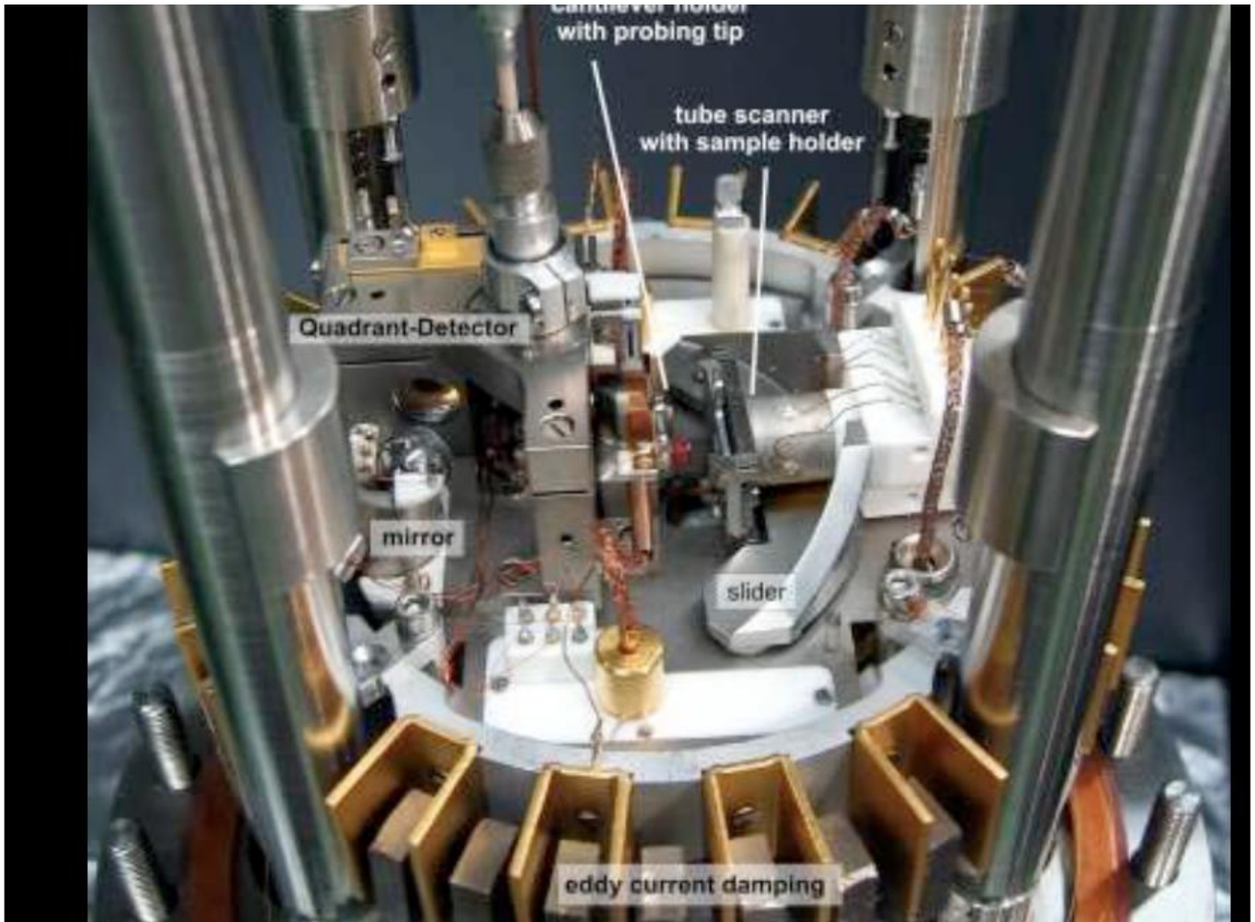

Pneumatic damping systems

Preparation of STM tips

Cutting PtIr wires

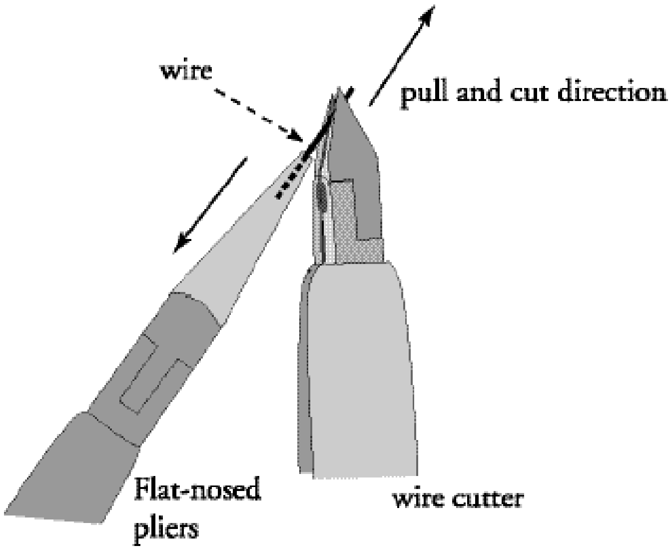

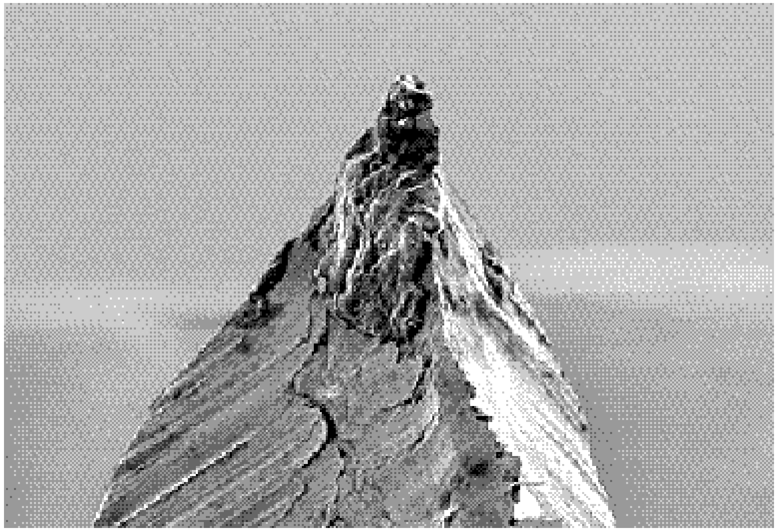

Electrochemically Etching

Tungsten tips are etched in KOH

cutoff time is essential parameter

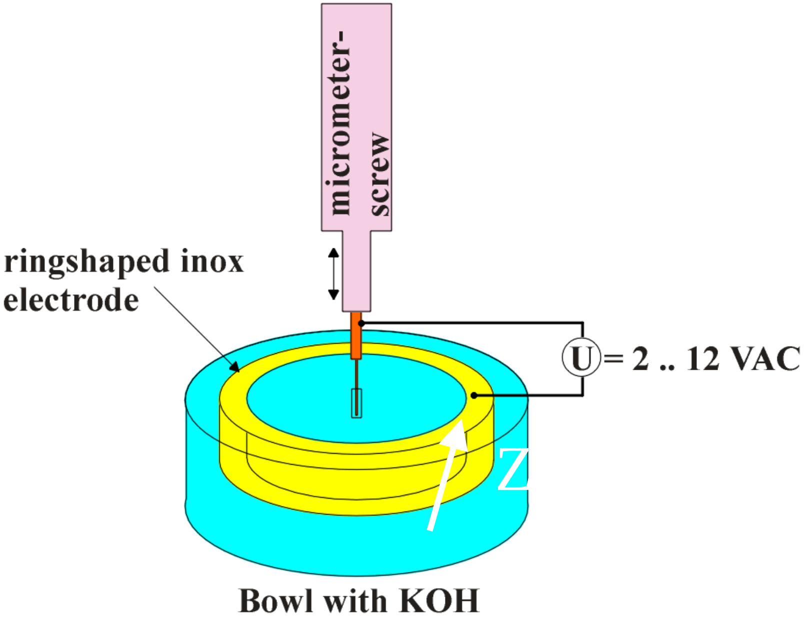

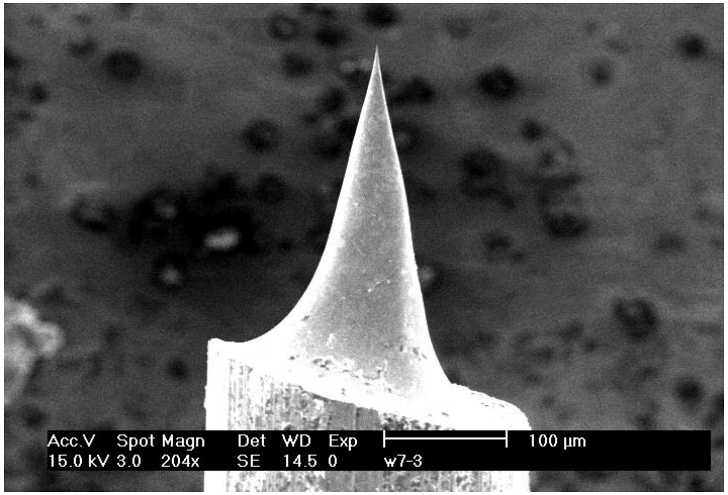

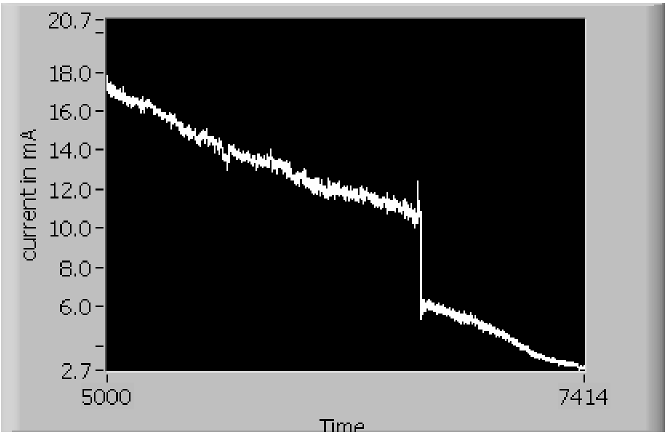

Electrochemical etching

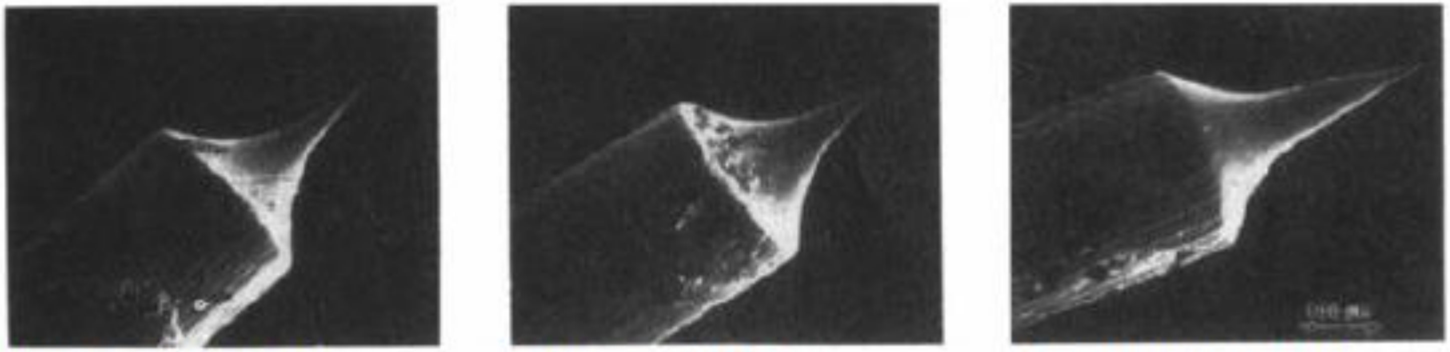

600ns, with 32nm | 140ms, with 58nm | 640ms, with 100nm.

- A 0.25mm tungsten wire is immersed in 1M acqueous solution of NaOH.
- the counterelectrode is a piece of stainless steel or platinum
- a positive voltage of 4-12V is applied to the wire.
- etching occurs at the liquid-air interface and a neck is formed
- the weight of the lower part of the wire pulls the neck and naturally fractures it.
- **cutoff time** after the tip has fractured is important parameter
- cleaning in boiling water to remove residuals of NaOH.
- problem: formation of a surface oxide during etching, which has to be removed before tunneling.
- remove the oxide by resistive heating or electron bombardment

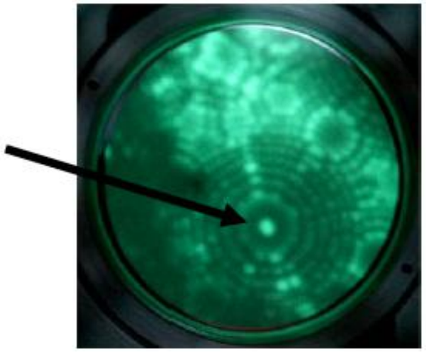

FIM-image

Tip shape artifacts

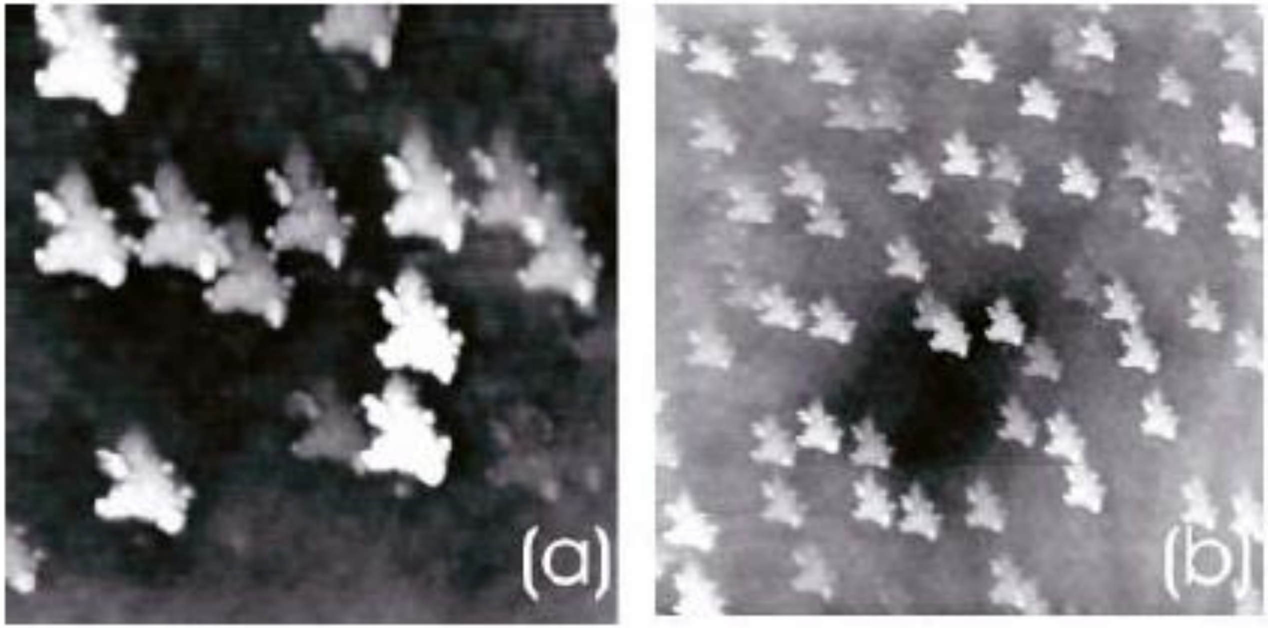

The image of a sample with needle-like structures (here an Al2O3 surface imaged by AFM) shows tip artifacts. The (blunter) tip is imaged by the sharp(er) needle-like structures existing on the sample.

Tip artifact vs. real sample structure

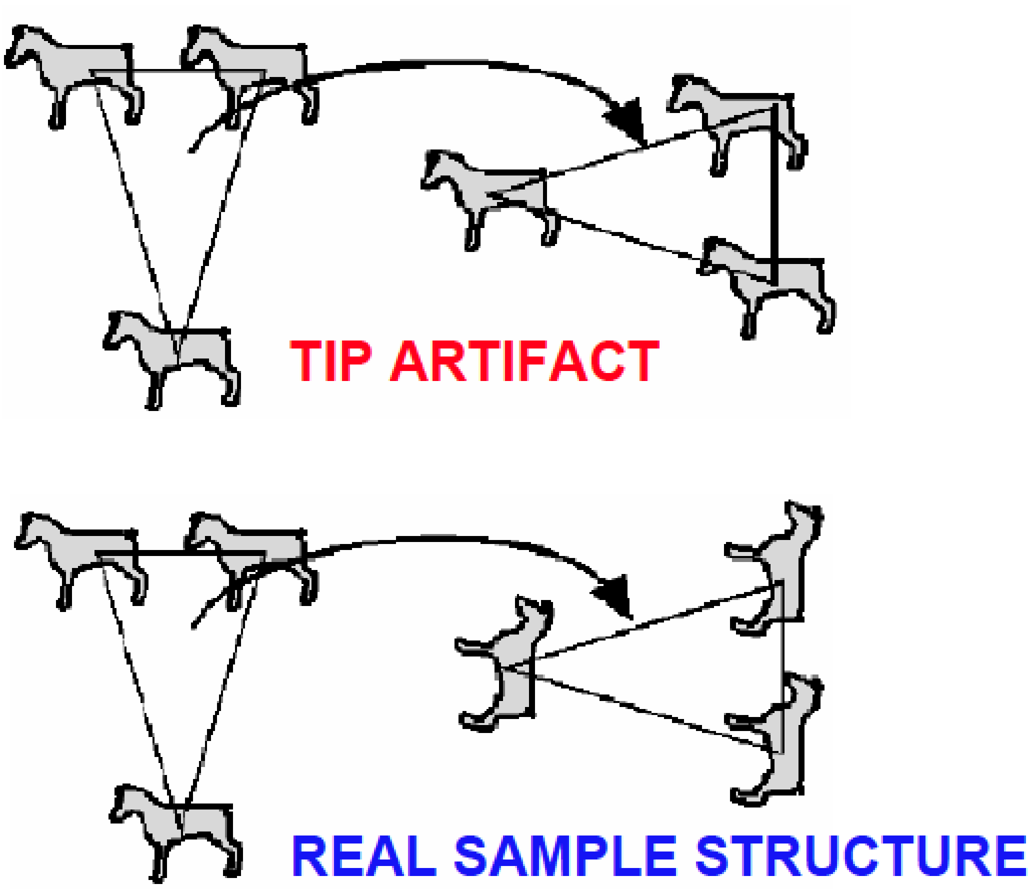

Rotation of sample shows rotation of she features for real sample structures

Quantum tunneling

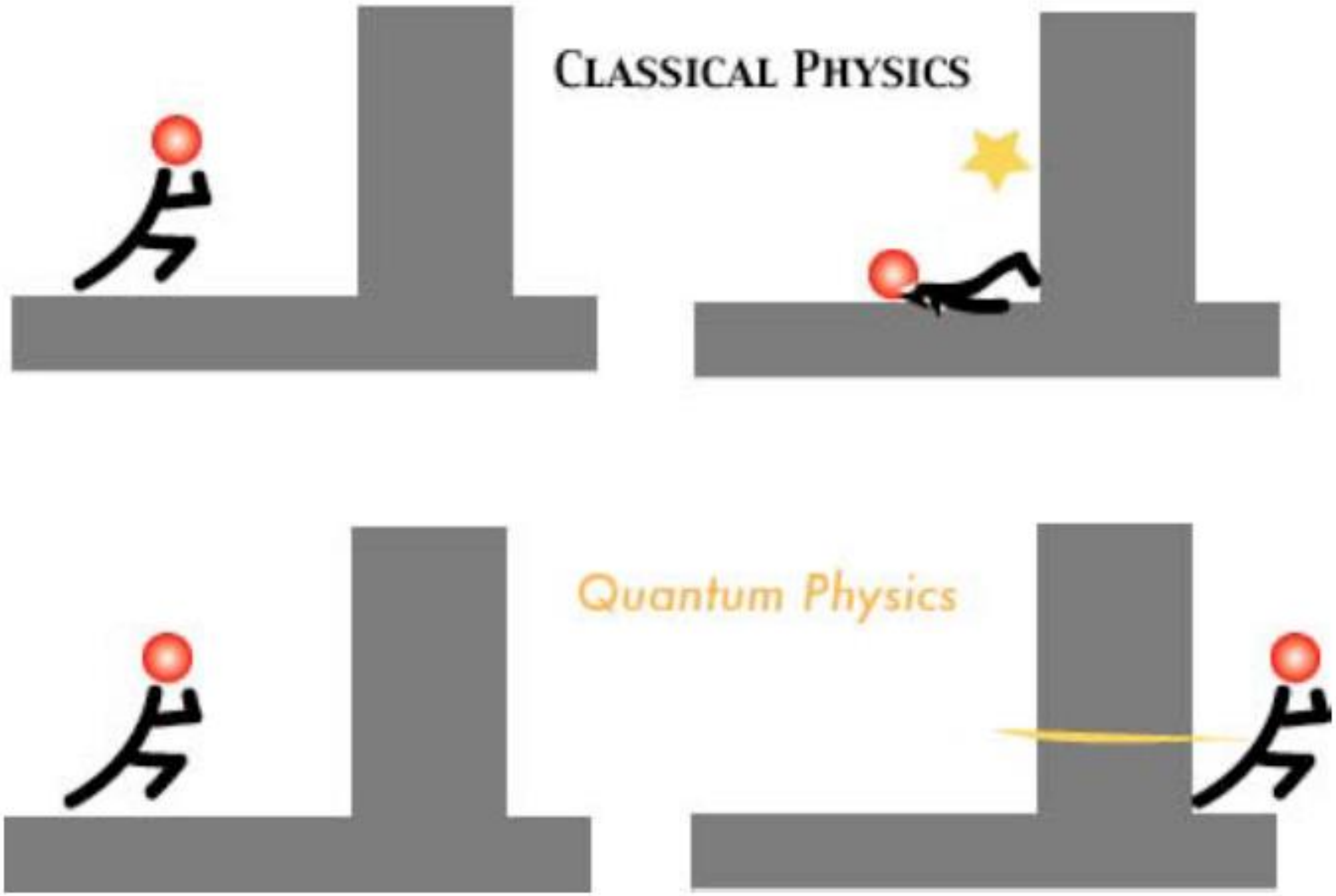

Tunneling effect

Quantum mechanics predict the tunneling effect:
A current flows between two metals separated by a thin insulating oxide layer.

J. Frenkel, *Phys. Rev.* **B 36**, 1604 (1930

$$I = f(U)\exp(-A\sqrt{\phi}s)$$

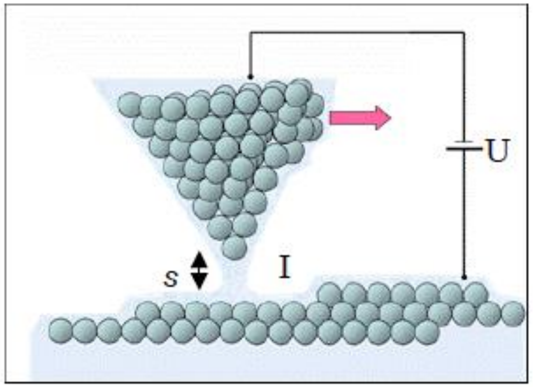

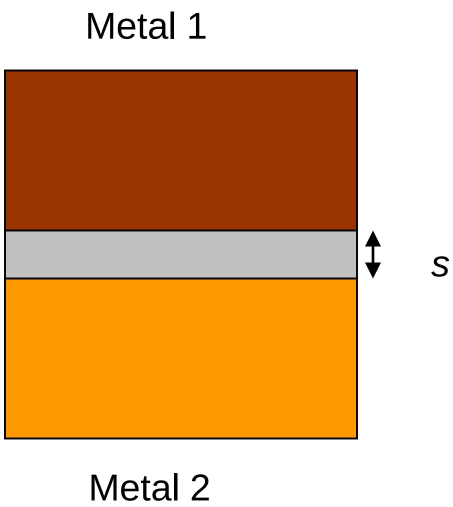

***I*: tunneling current**
***U*: applied bias voltage**
***s*: thickness of oxide**
ϕ: barrier height

$$\phi \approx \frac{\phi_1 + \phi_2}{2}$$

ϕ_1, ϕ_2 work functions of Metal 1 and Metal 2

$$A = 2\sqrt{\frac{2m}{\hbar^2}} = 1.025\ \text{Å}^{-1}\text{eV}^{-1/2}.$$

***f* (U) : function of the electronic structure, for free electrons *f* (U) ~ U**

For typical work functions of ϕ =4.5eV the current changes by one order of magnitude if the distance is changed by 1Å.

Scanning Tunneling Microscope (STM)

Source: IBM

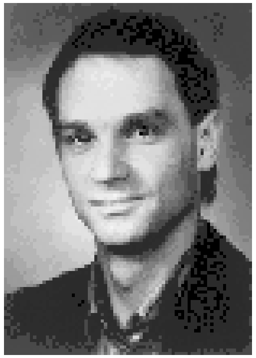

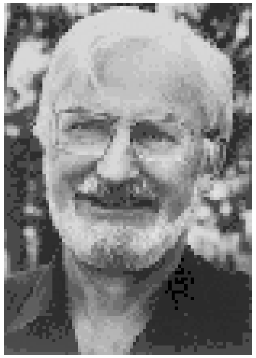

G. Binnig and H. Rohrer
Nobelprice1986

IBM Rüschlikon
Switzerland

UNI BASEL

Scanning Tunneling Microscopy (STM)

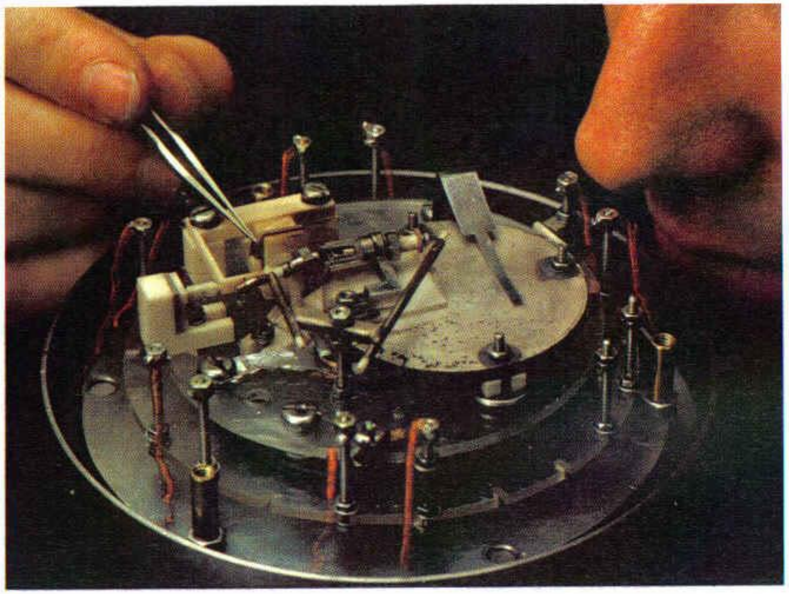

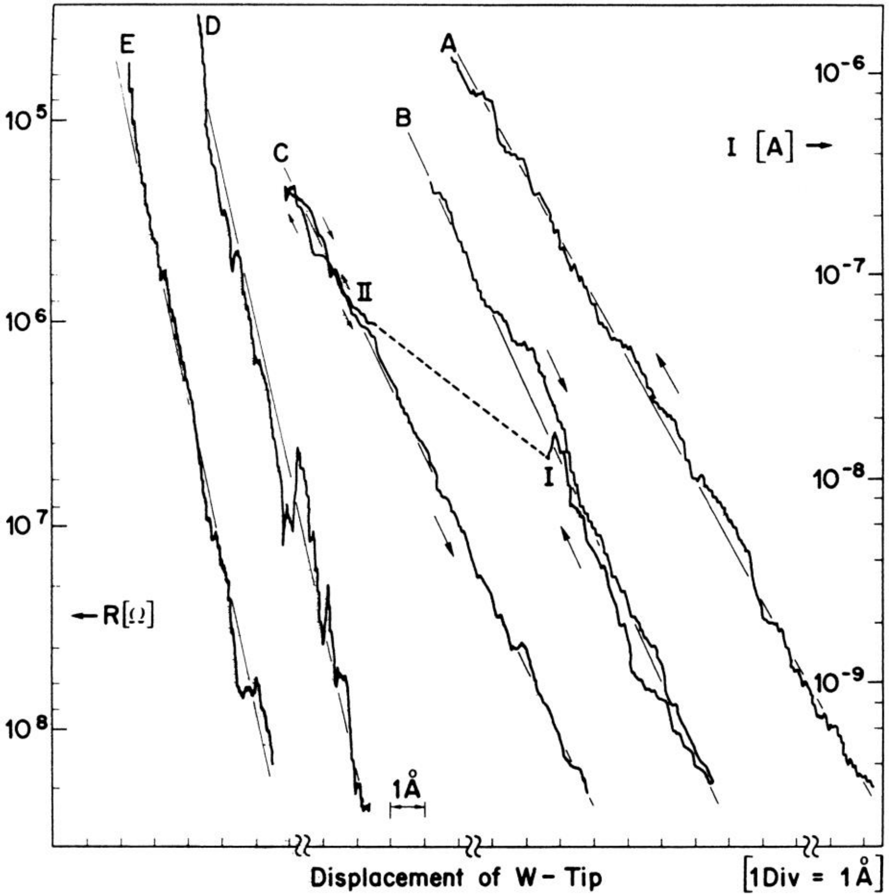

Exponential decay of current with distance

G. Binnig et al. Appl. Phys. Lett. 40, 179 (1982)

First STM imaging of Si(111)7x7

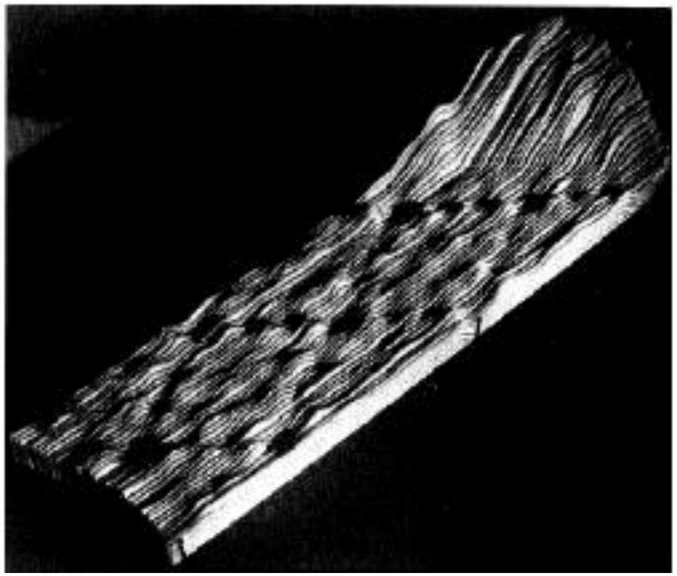

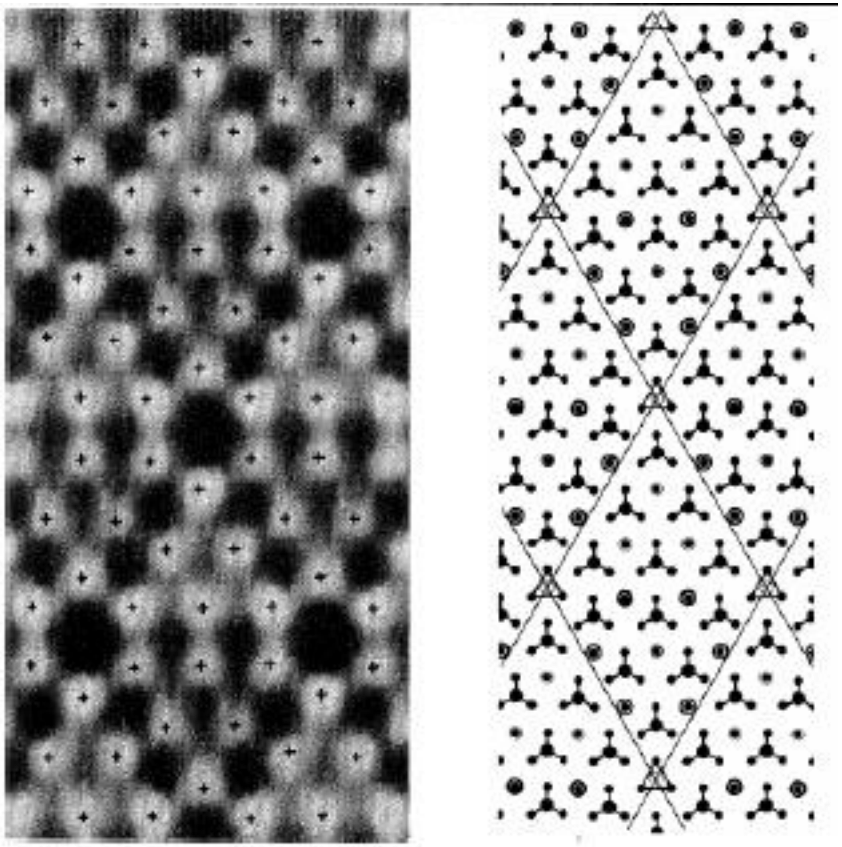

Observation of adatoms on the Si(111)7x7 reconstruction
Per unit cell 12 atoms are visible
G. Binnig et al. PRL50 120 (1983).

STM on GaAs(110)

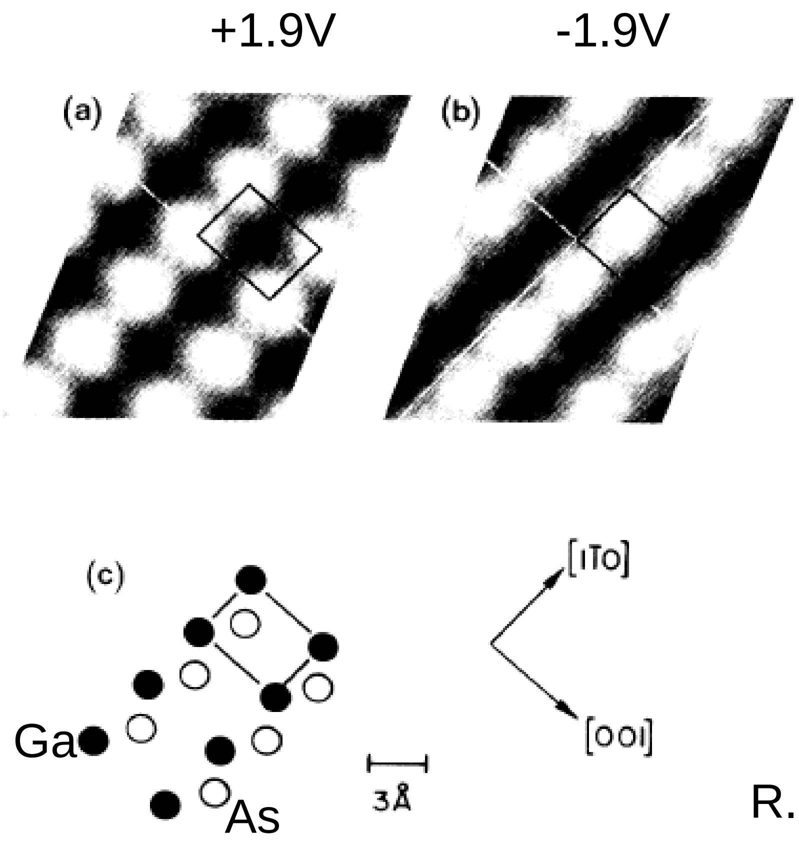

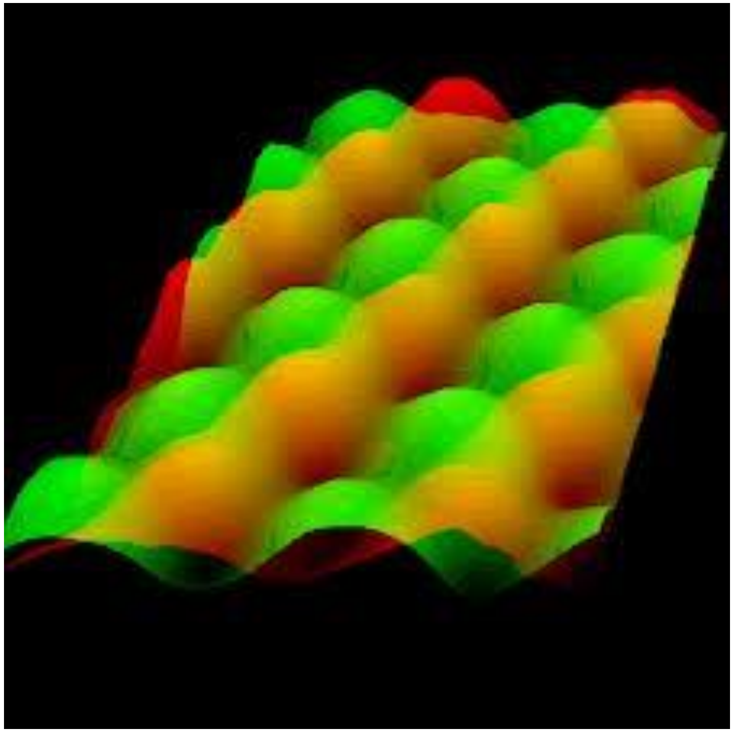

R. Feenstra, Phys. Rev. Lett. 58, 1192 (1987)

Depending on the polarity Ga or As are imaged.
LDOS-effect! As-atoms have higher LDOS for occupied states (-1.9V)
Ga for unoccupied states (+1.9V).

dI/dV/(I/V)-Spectra of GaAs(110)

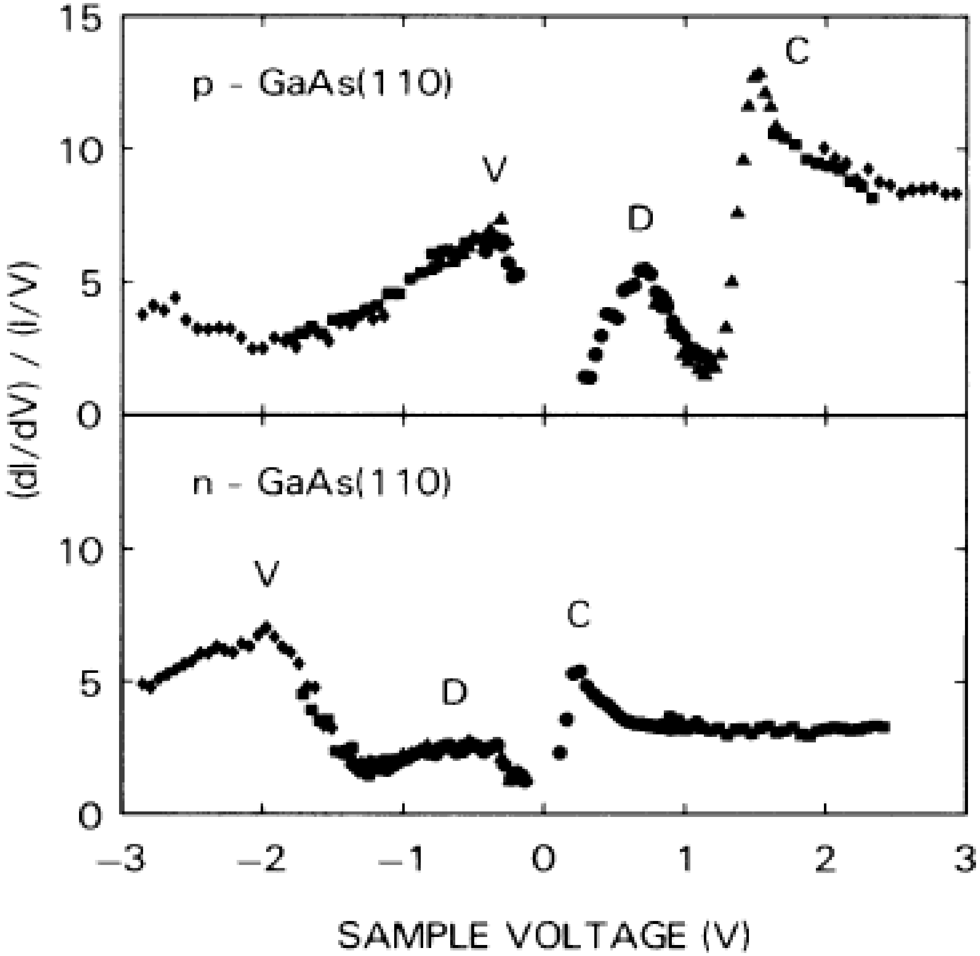

E_g=1.43eV

R. Feenstra, Phys. Rev. Lett. 58, 1192 (1987)

STM on metals

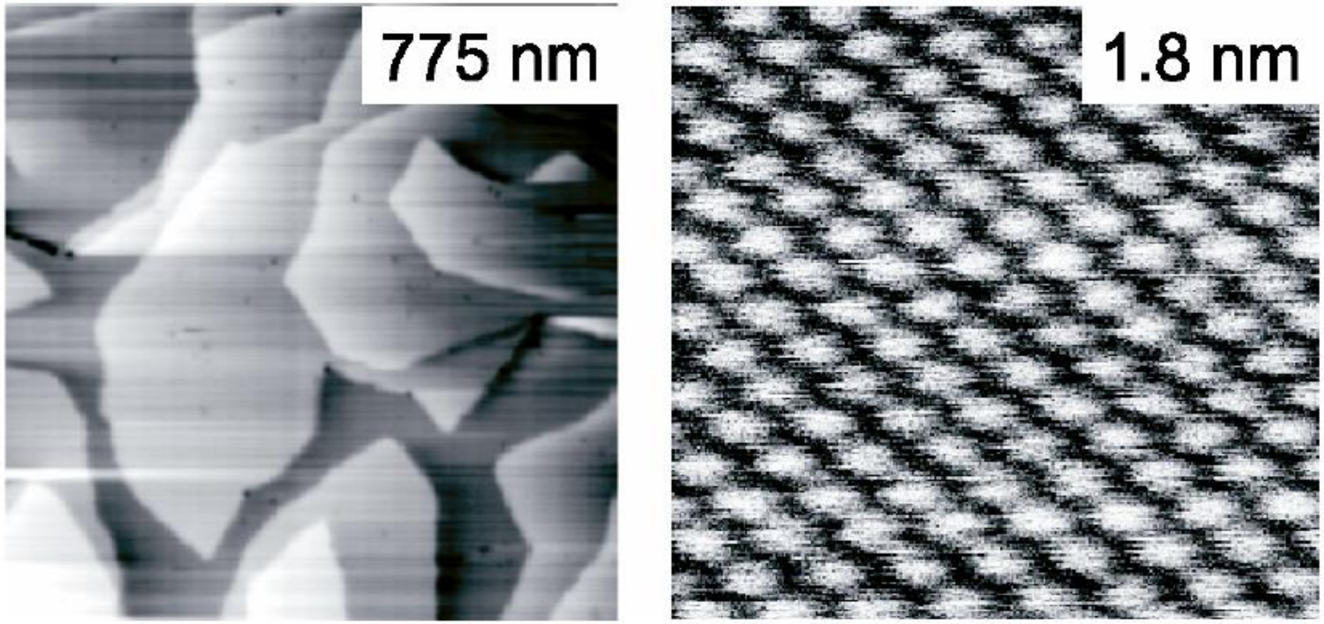

STM images of the Cu(111) surface in constant current mode. (left) Overview image with monatomic steps (right) Atomic resolution on Cu(111). The spacing between the protrusions is 2.5A.

• first resolved by Binnig and Rohrer 1982 [1] (Au(110)-2x1 and Au(110)3x1 reconstructions)
• atomic resolution on a close-packed Au(111) by Hallmark et al. [2] in 1987
• today, a large number of clean metal surfaces could be resolved, such as Cu(111), Cu(110), Cu(001), Pt(111), Pt(001), Ru(0001), Ni(001) and Ni(110)
• spacing between the atoms of the close-packed surfaces is 2-3A.
• corrugation heights are found to be rather large of the order of tenths of A
• corrugation in contradiction with results from He scattering
• contradiction explained by force induced variation of tip-sample distance

High resolution of metallic alloys

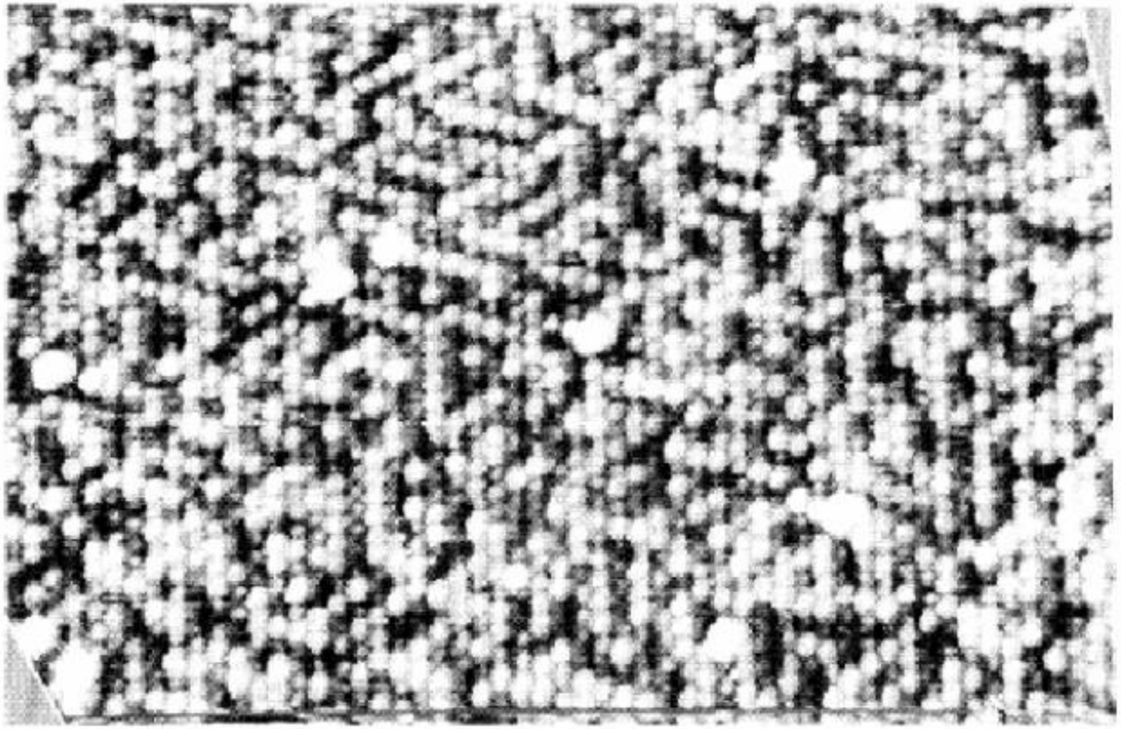

An impressive example of the resolution capabilities is given by Schmid et al., where Pt-atoms and Ni-atoms could be distinguished on a $Pt_{25}Ni_{75}(111)$-surface. The best resolution was observed with small tunnel resistances of (50-300kOhms), which was attributed to the interaction between adsorbates at the tunneling tip and the surface atoms.

M. Schmid et al. PRL70 1141 (1993)

UNI BASEL

Giant currugations: STM on layered materials

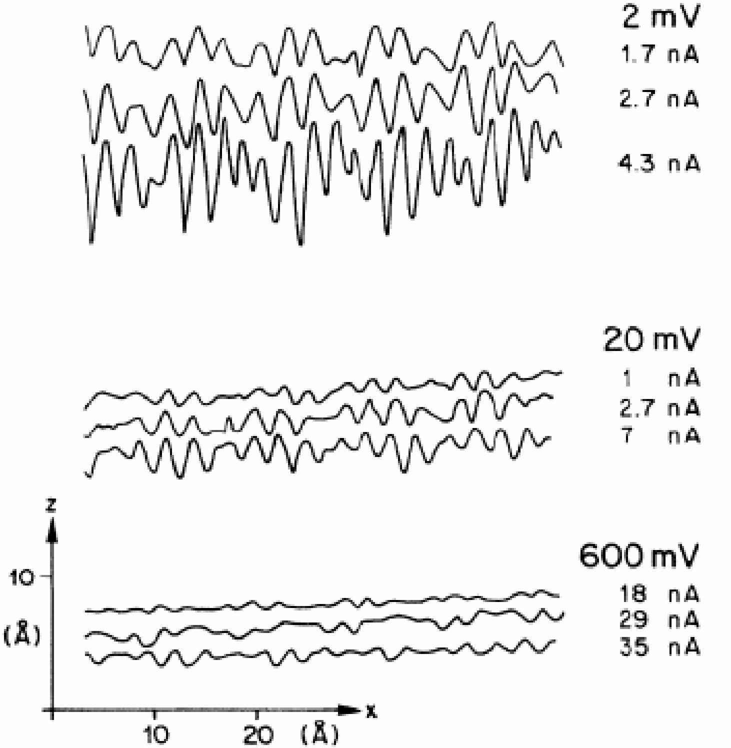

FIG. 1. Graphite STM traces obtained at ambient-air pressure and room temperature with a "pocket-size" STM (Ref. 14) with scanning speeds between 1 and 5 sec per scan. The varying corrugation within a scan is due to the mismatch between crystallographic and scanning directions (Ref. 3); plateaus in the traces indicate the saddle points in the LDOS (Refs. 3 and 11).

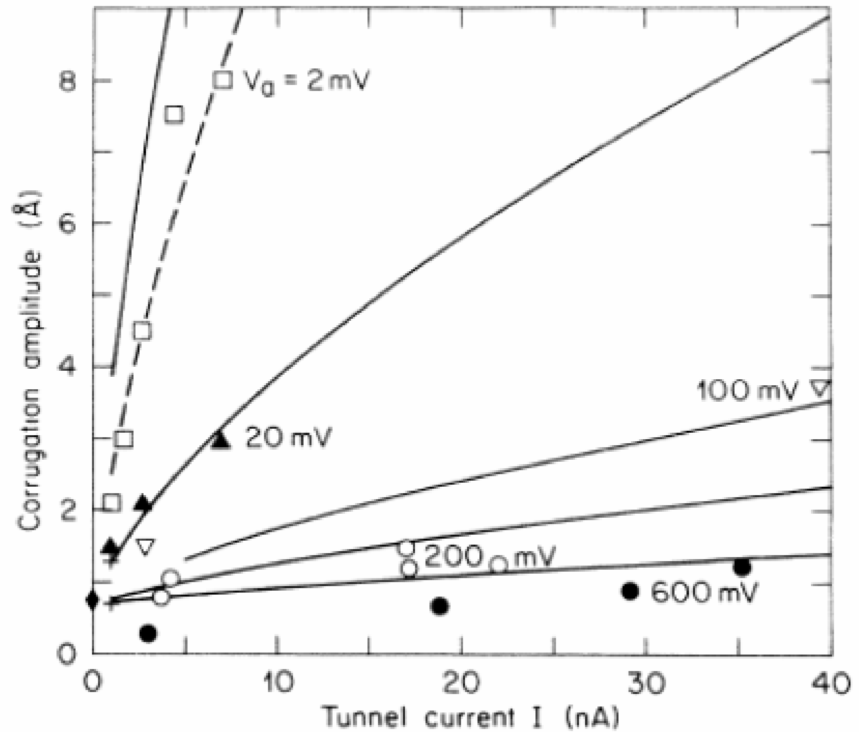

FIG. 4. Measured (symbols) and calculated (solid lines) corrugations as a function of tunneling current and voltage. The dashed line was obtained with $d^* = 0.4$ Å. The two crosses at 1 nA correspond to the measured corrugations at 50 and 400 mV, respectively, of Ref. 3; the diamond at zero current indicates the corrugation of the LDOS at the Fermi level (Ref. 11).

Refs.:[1] Soler et al. PRL57 444 (1987)
[2] R.V. Colemann et al. Adv. Phys. 37 559 (1988)

STM on molecules

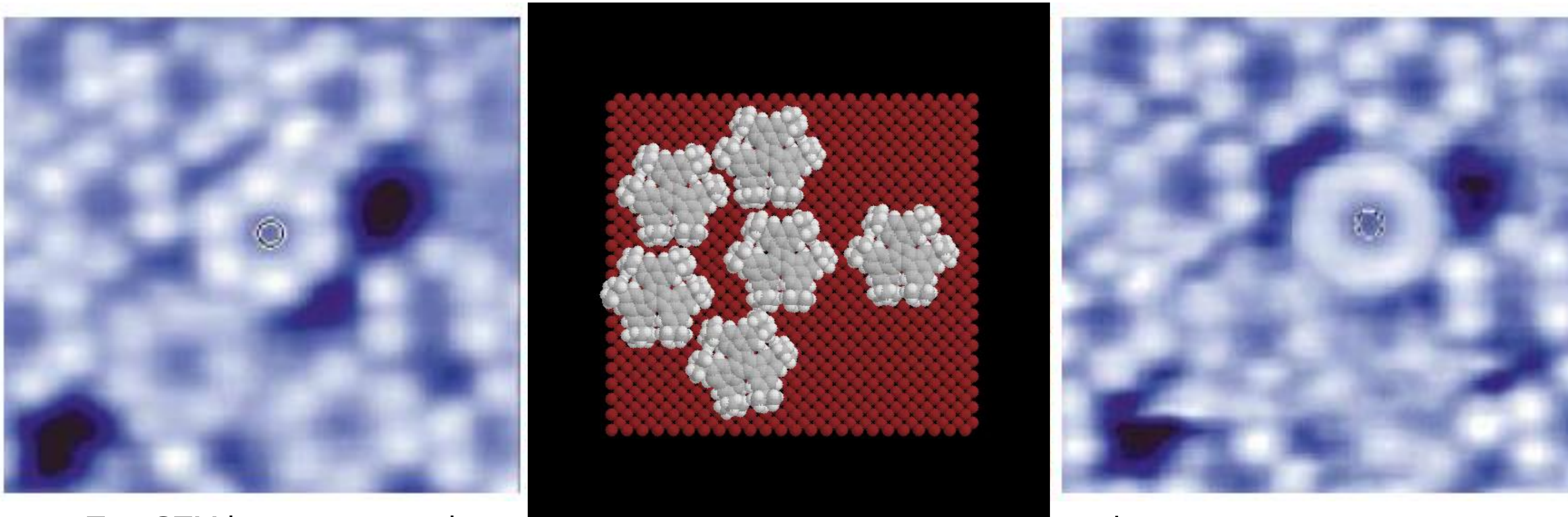

Two STM images on top show a six-lobed "propeller" marked by an inner ring
in an immobilized state close to four sister molecules (a) and in an rotating
state when shifted away by one-fourth of a nanonometer (c) The graphical view of the computer
simulation (b,d) illustrates the structure and the two positions of the molecular wheel. (J. Gimzewski).

Generally, the mechanisms of tunneling through molecules are rather complicated, e.g., resonant tunneling may occur. Adatoms or small molecules (e.g., benzene molecules) which lie .at on a surface can be imaged in
most cases. Larger molecules can be more difficult to be imaged, because of poor conductivity. Especially, molecules which are oriented perpendicular to the surface may cause problems. E.g., alkylthiols on Au(111) can be best imaged with small currents of some pA. Larger currents lead to strong distortions of the image.

C_{60} on Ag(111)

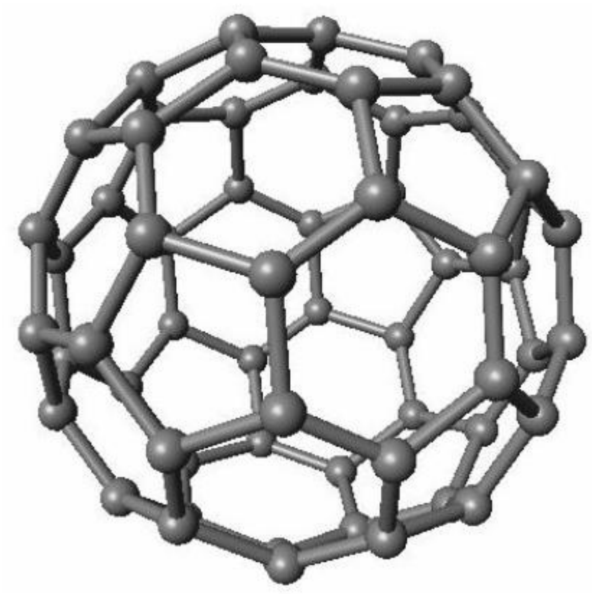

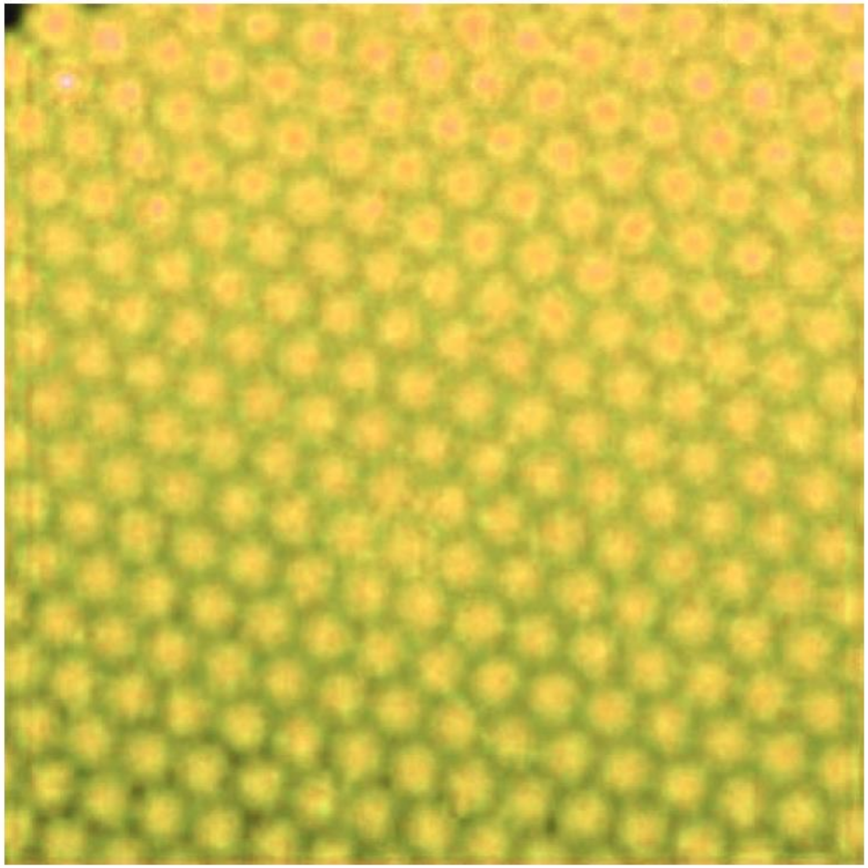

T. Jung et al.

Chloro-[subphthalocyaninato]boron(III) on Ag(111)

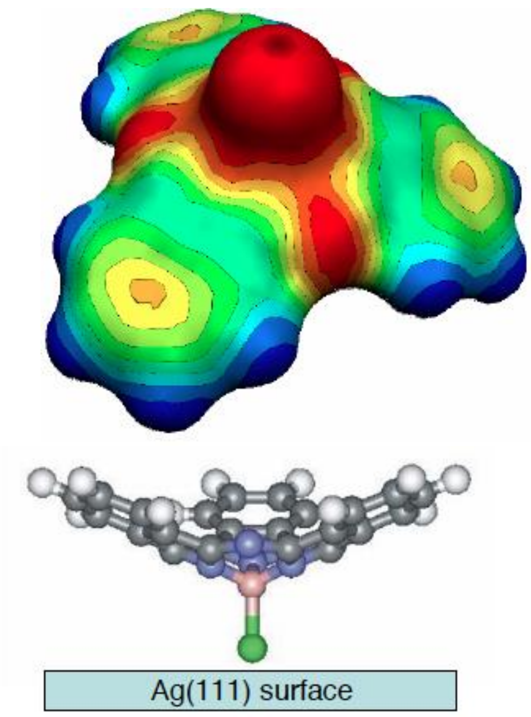

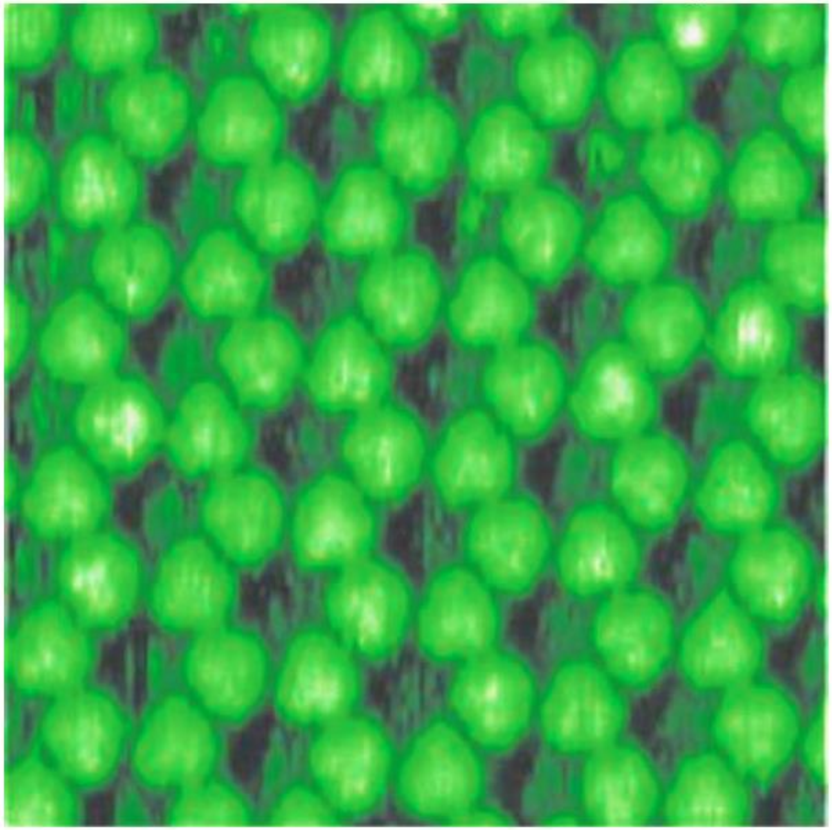

angle resolved photoemission
reveals that molecule sits
with polar Cl on Ag(111) surface

T. Jung et al.

Mixtures of C60 and SubPC

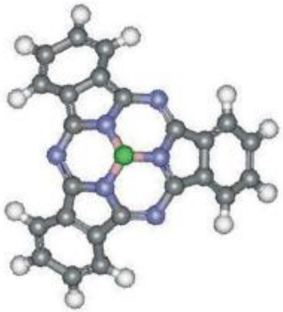

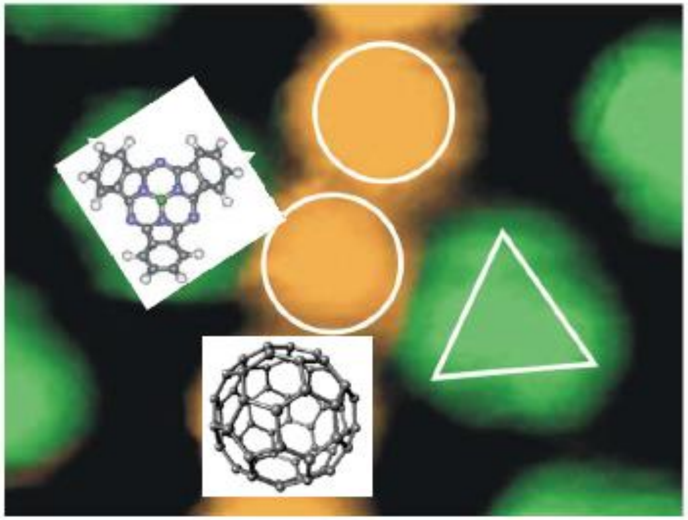

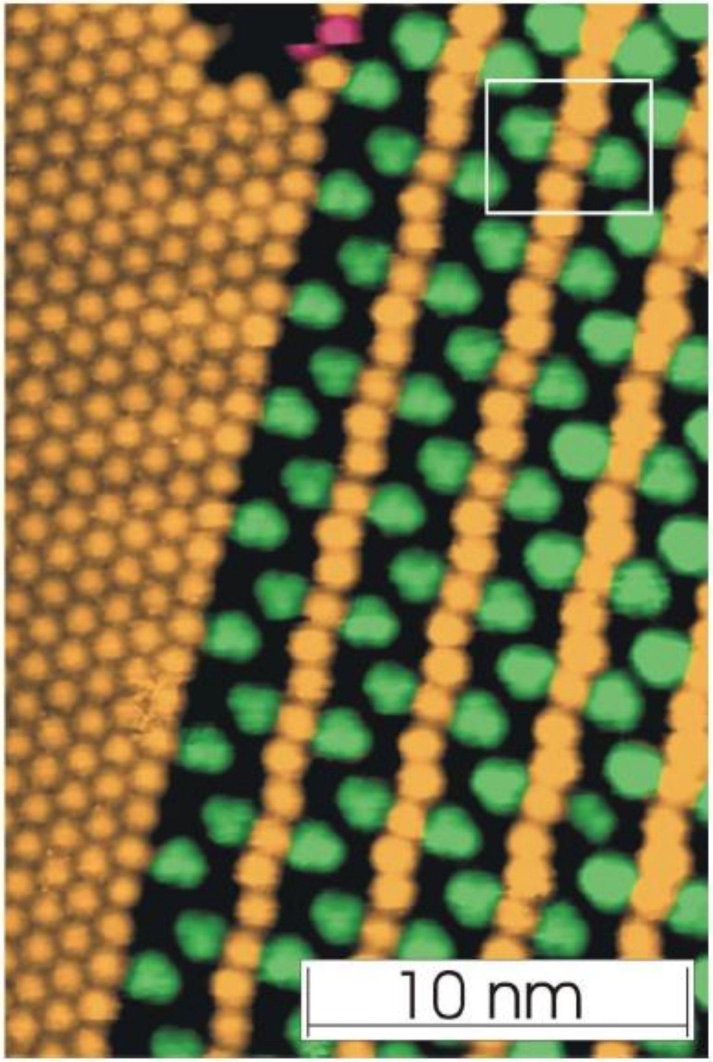

T. Jung et al.

Binary phase diagram

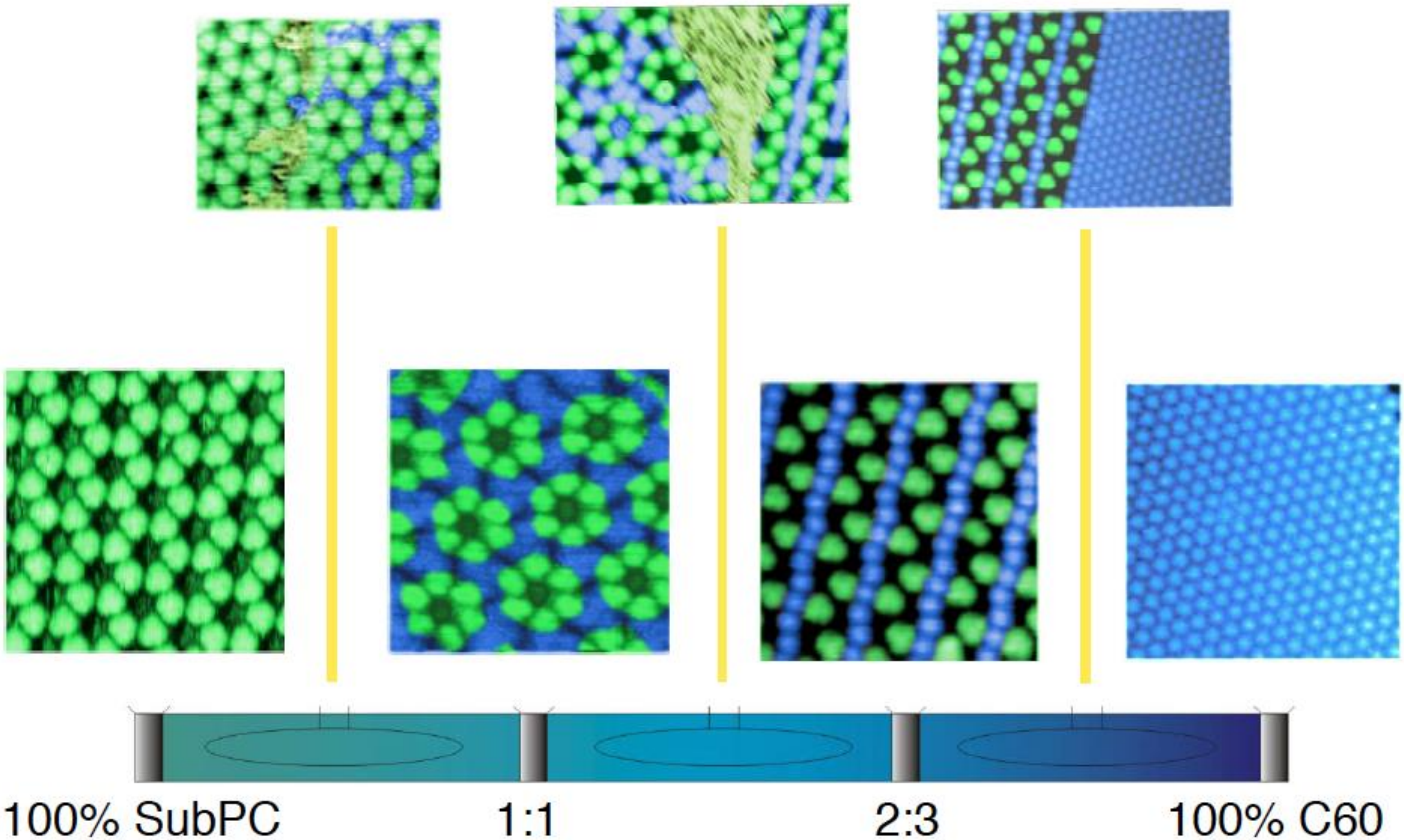

T. Jung et al.

Constant current mode

$$\ln(I) = \text{konst.} \quad \Rightarrow \quad \sqrt{\phi}\, s = \text{konst.}$$

If barrier height constant ⇨ **s=constant**

If barrier height varies ⇨ **ϕ(x,y), *s*(x,y) affect topography z(x,y)**

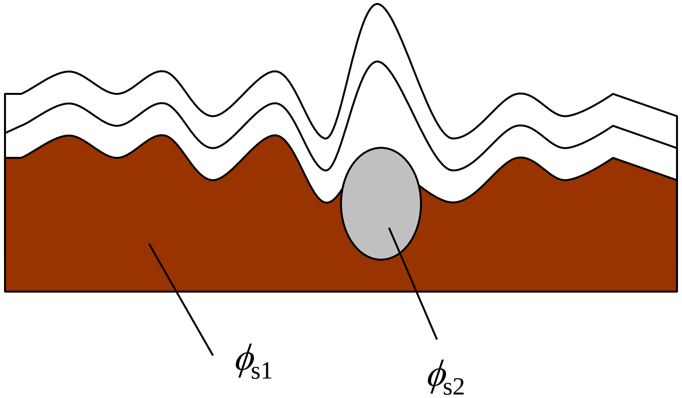

Contour z(x,y)
at constant current

Topography or not?

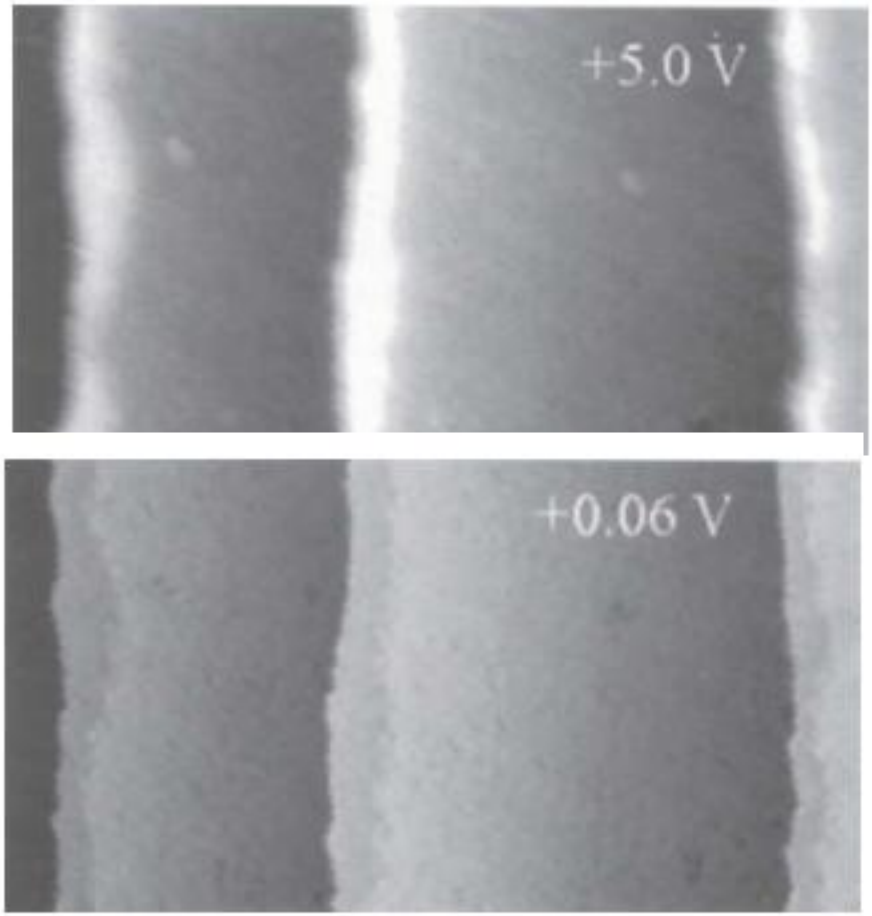

Th. Jung et al., Phys. Rev. Lett. 74, 1641 (1995)

Image of Cu nanowire running along a step of Mo(110), recorded with different bias voltages. An image state produces a strong contrast (left) .

Feed-back regulator

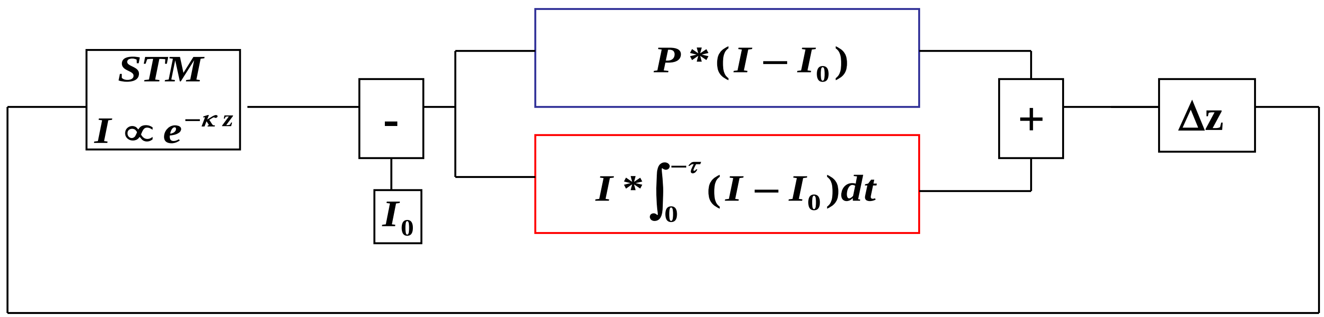

response without feed-back

response with feed-back

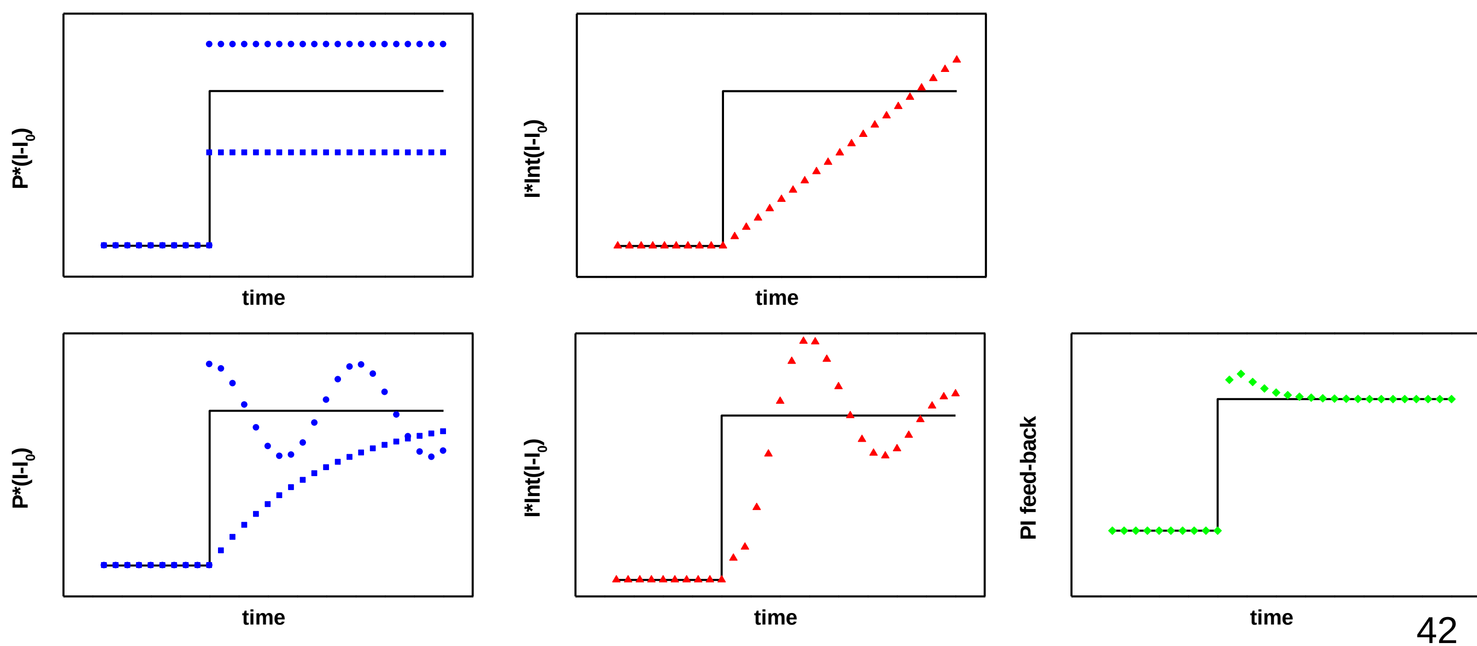

Influence of feed-back parameter

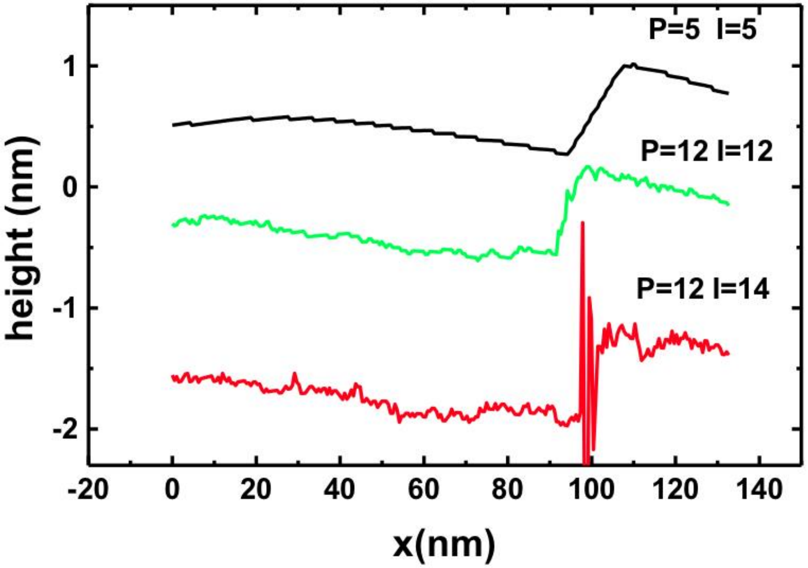

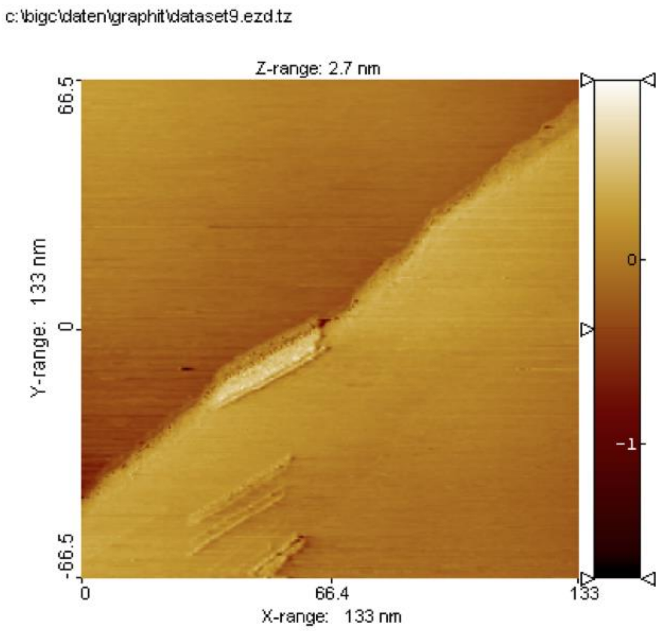

Feedback parameters depend on the state of the probing tip sample conditions and have to be optimized for each experiment. Oscillations are mostly due to the resonance of the scanner (typically 0.5-10kHz)

Selection of feedback parameters

How to select the feedback parameters?

Ziegler-Nichols procedure:
-increase P-part until small oscillations are observed
-reduce P-part to $0.45P_{krit}$
-measure oscillations period (T_{krit}) and set I-part to $0.85T_{krit}$

J. Ziegler, N. Nichols, Trans. ASME 64, 759 (1942)

UNI BASEL

Principle modes of SPM

1. **Imaging** a “surface or surface properties” with high lateral (atomic) and vertical (pm) resolution. The tip-sample distance z adjusted to keep interaction constant or measurement of varying interaction at (controlled) z.

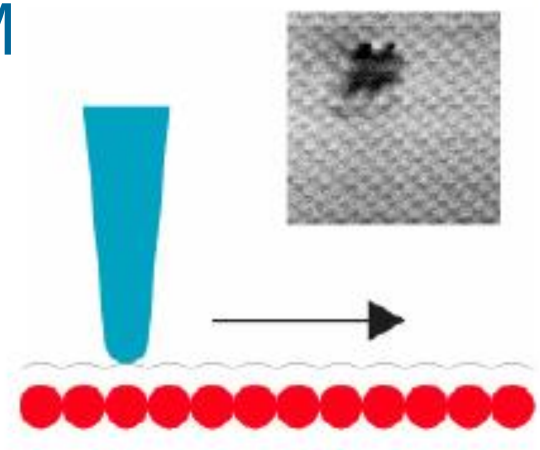

2. **Local spectroscopy** on selected sites. The interaction (i.e. tunneling current) is measured as a function of other parameters,
i.e. tip-sample distance z or potential V_{tip}.

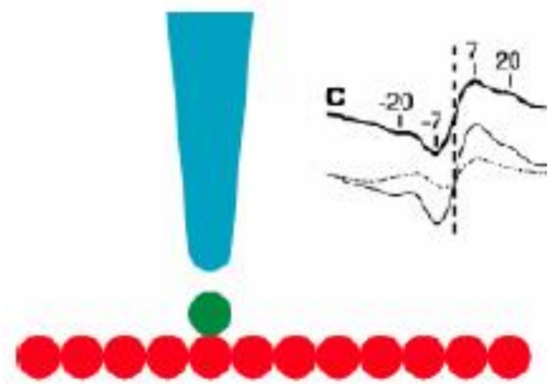

3. **Manipulation** of surface structures and surface states. Manipulation of atoms and molecules on surfaces. Transfer of atoms between tip and sample and vice versa. Lithography, deposition of charges, bleaching of fluorescing molecules … .

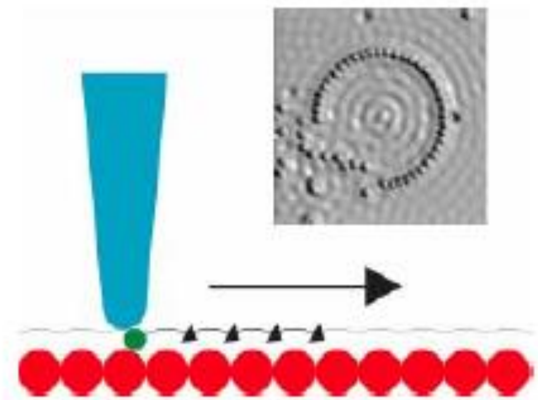

Manipulation modes

a) Vertical manipulation (transfer of the surface atom to the tip and back to the sample):

b) Lateral manipulation mode (adsorbate is kept adsorbed to the surface and moved laterally along surface)

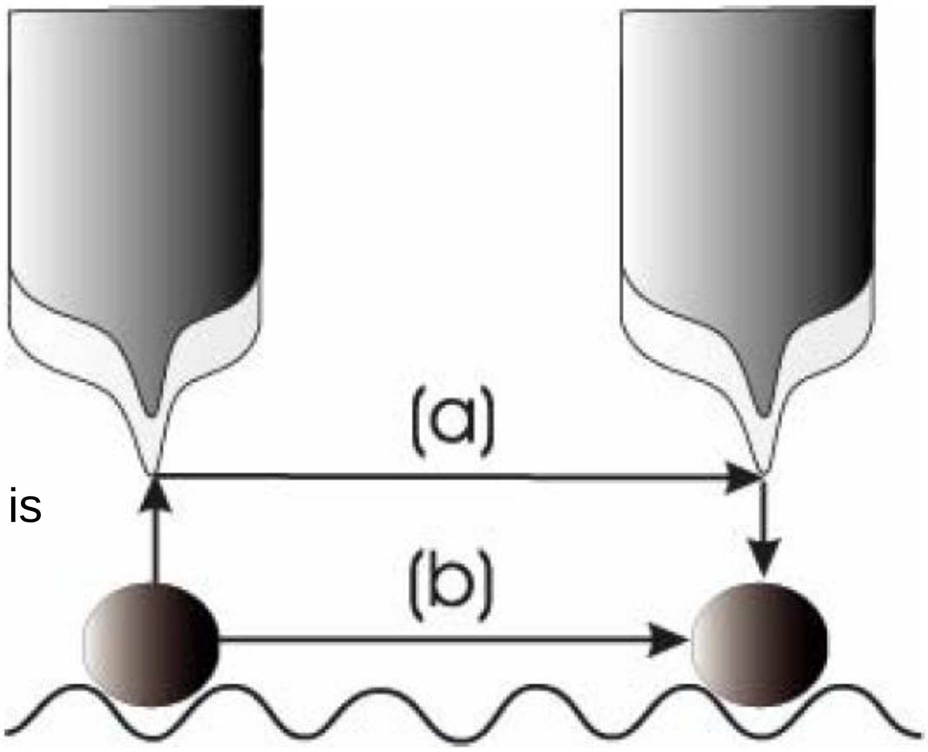

D. Eigler, E. Schweizer: Nature 344, 524 (1990)

Manipulation of Xe-atoms on Cu(111)

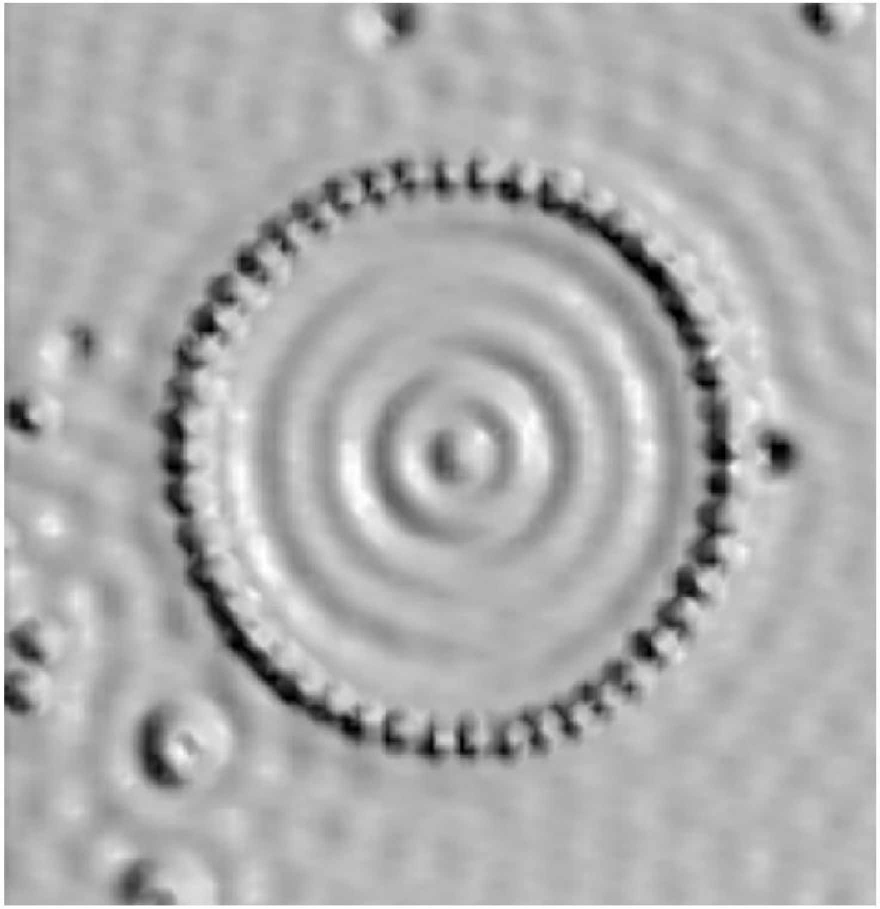

Don Eigler, IBM Almaden Research Center

D. Eigler, E. Schweizer: Nature 344, 524 (1990)

Lateral manipulation traces

Tip height curves are shown during manipulation of a Cu atom (a), a Pb atom (b,c), a CO molecule (d), and a Pb dimer (e)-(g) along the [110] of the Cu(211) surface. The tip movement is from the left to the right, and the tunneling resistances are indicated. The vertical dotted lines correspond to fcc sites next to the step edge. The initial sites of the manipulated species are indicated by small sphere models. On the right part STM images of the different adparticles are shown. The arrows indicate the direction of tip movement.

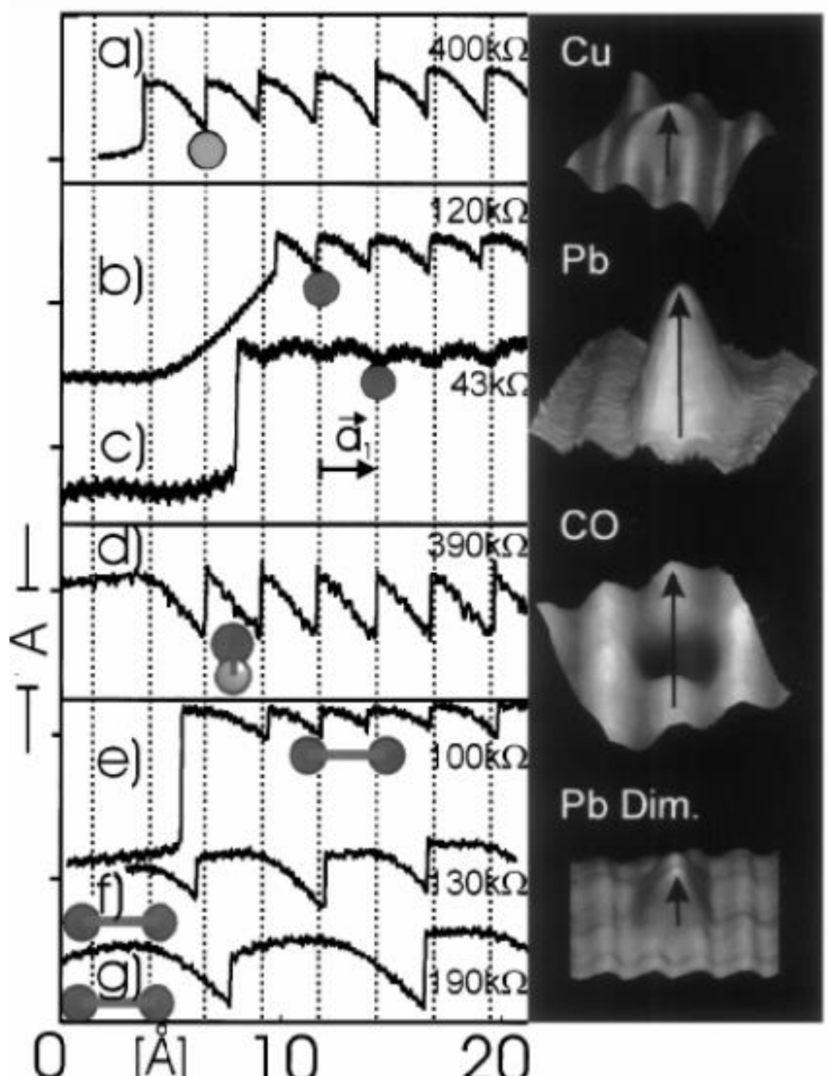

L. Bartels et al., Phys. Rev. Lett. 79, 697 (1997)

Desorption of Hydrogen by STM

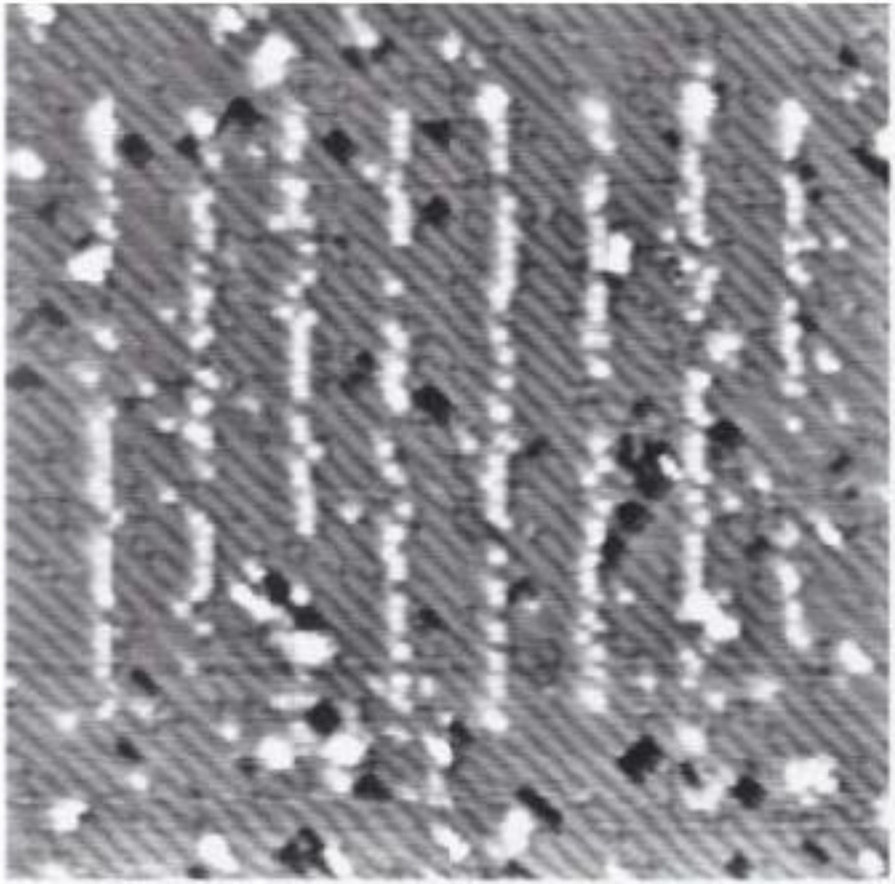

Hydrogen passivated Si-surface. Application
of high voltages (5V) leads to desorption
of hydrogen. Possibly related to inelastic tunneling

J. W. Lyding et al. Appl. Phys. Lett. 64, 2010 (1994)

Atomic Force Microscope (AFM)
Scanning Force Microscopy (SFM)

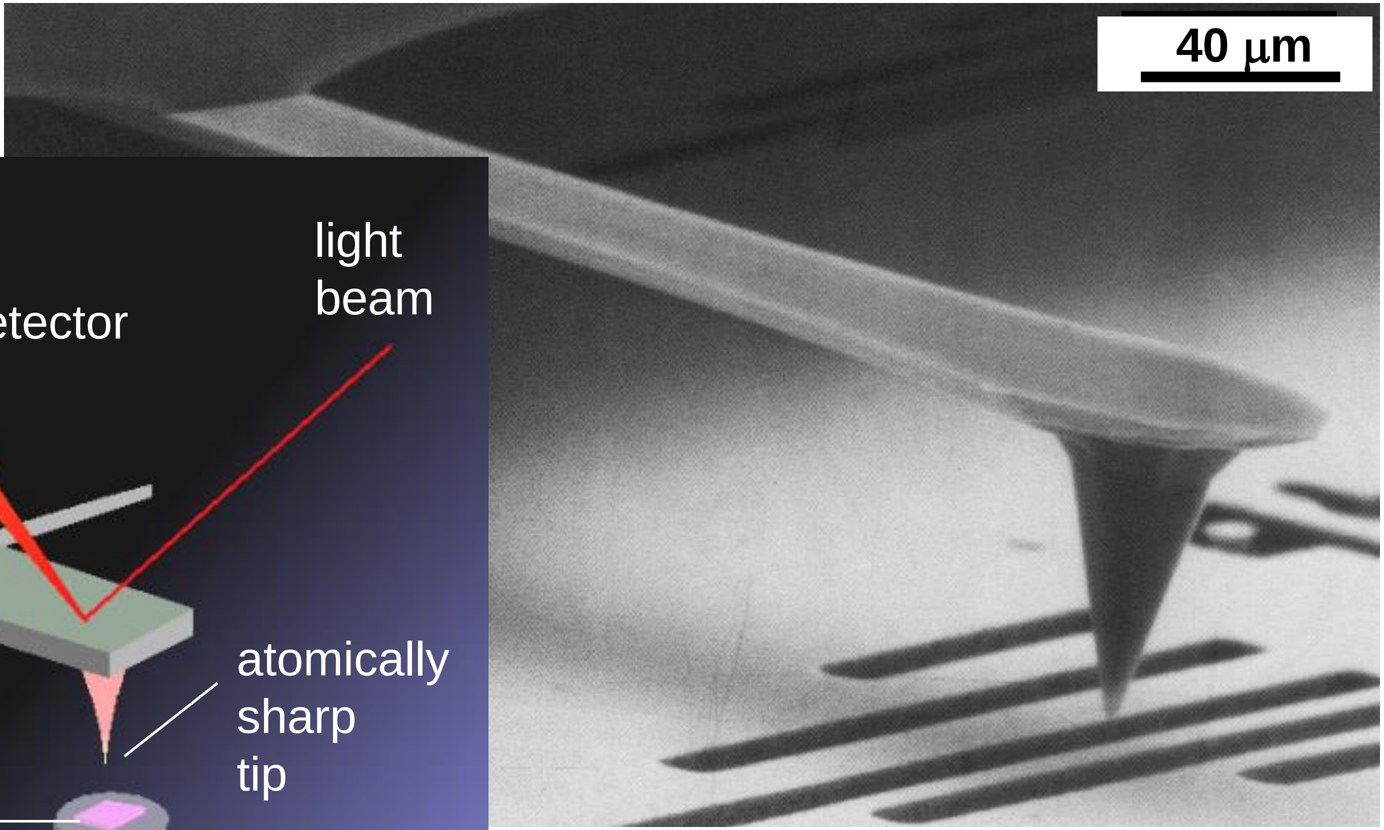

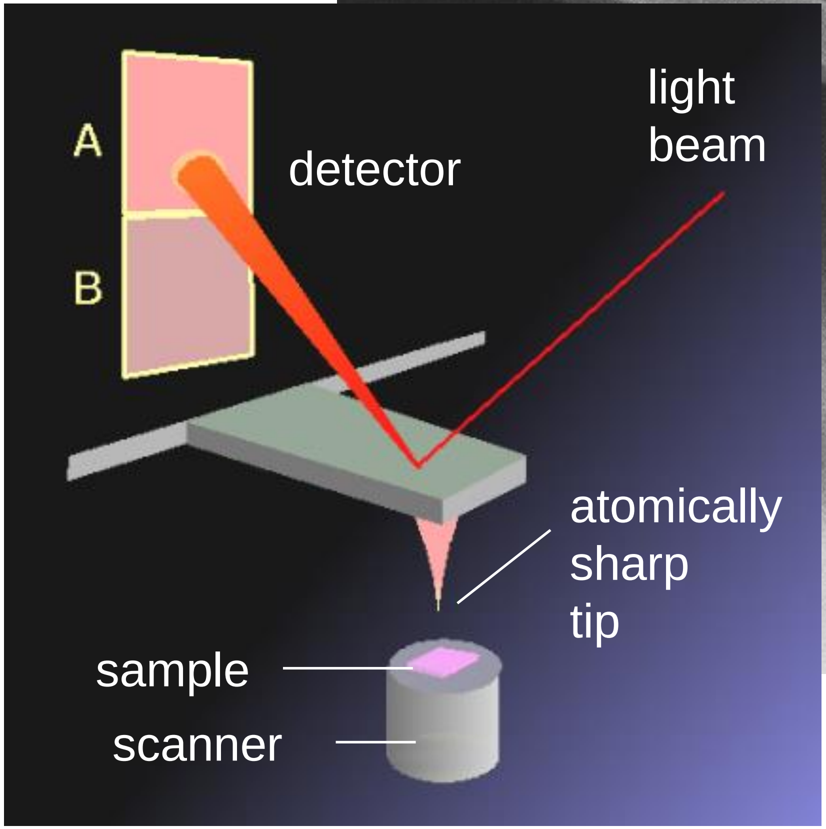

Atomic Force Microscopy (AFM)

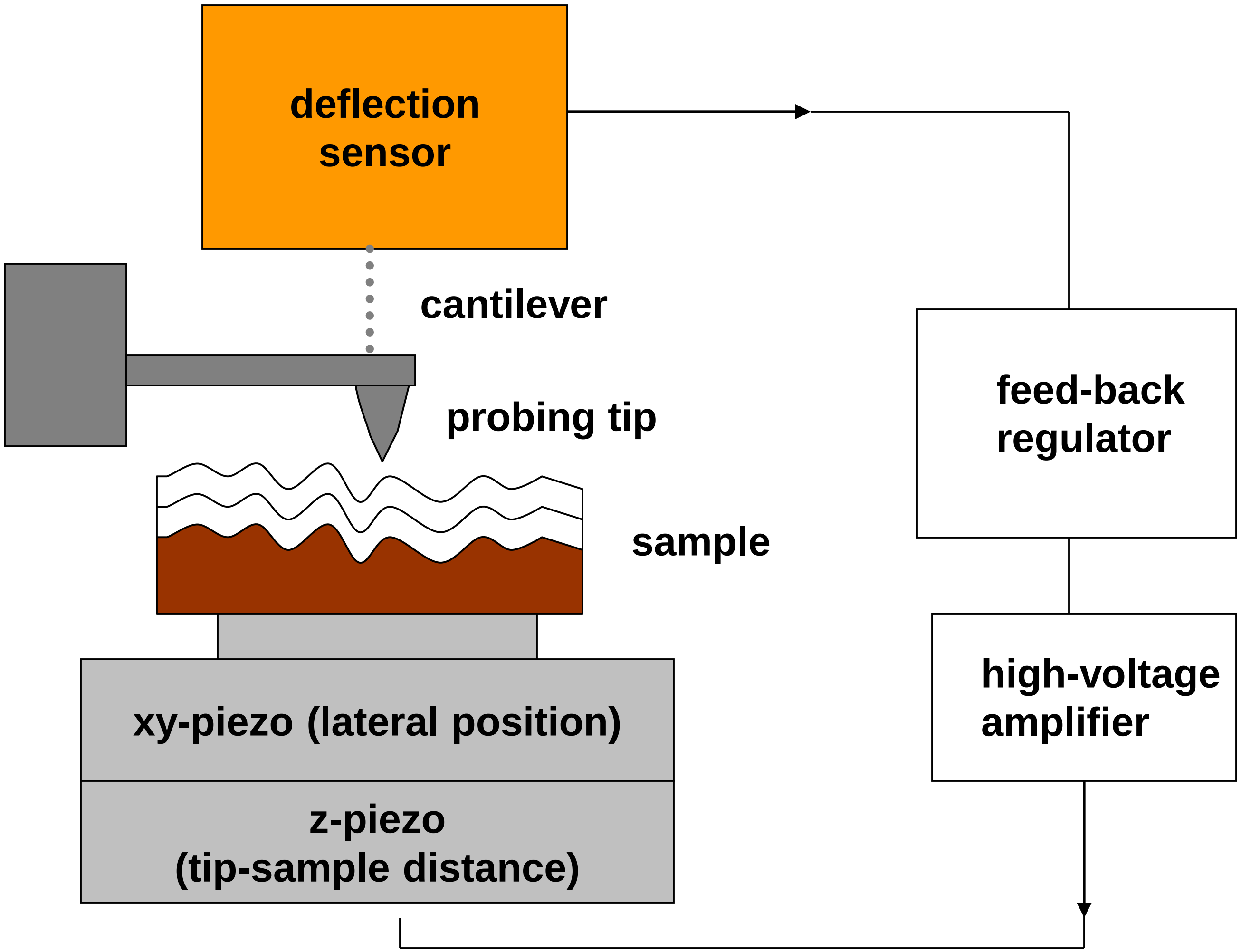

Microfabricated cantilever with integrated tip

Si-Cantilever (1.5x45x450μm)

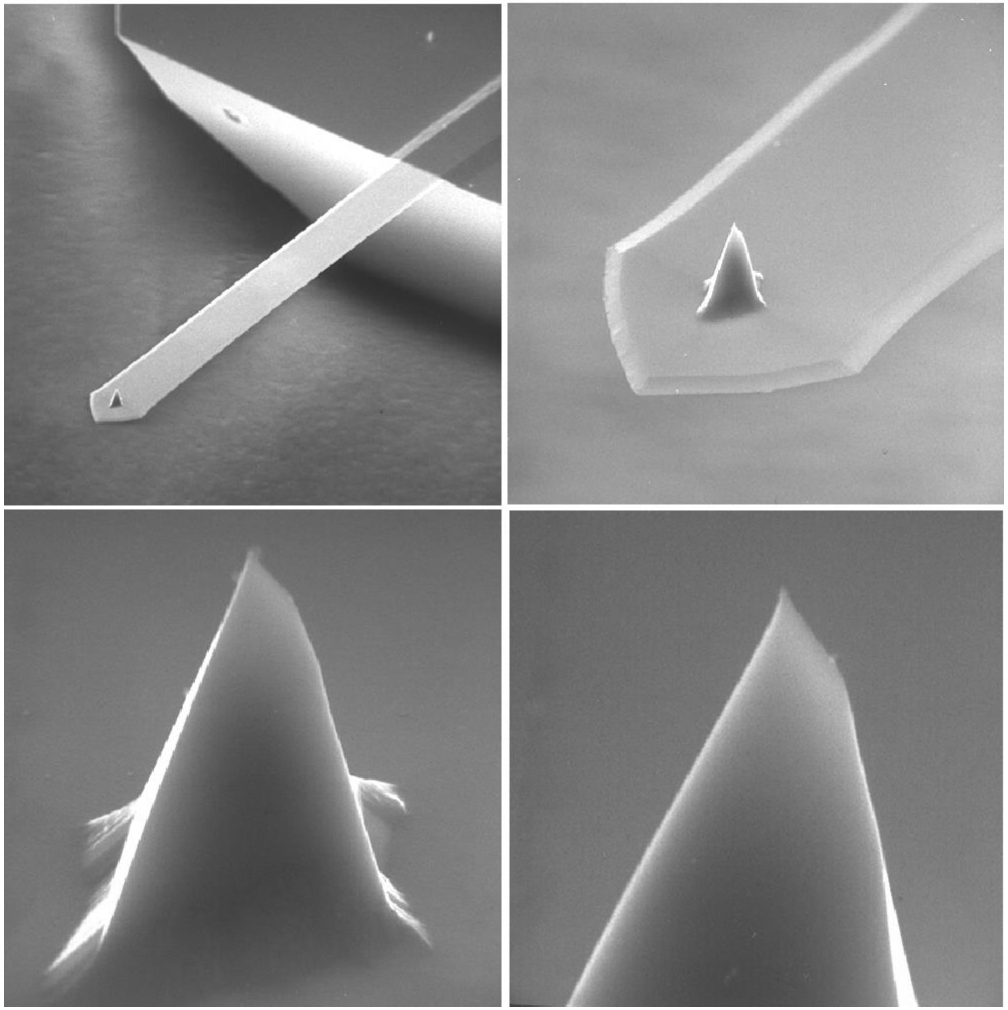

Geometry of cantilevers

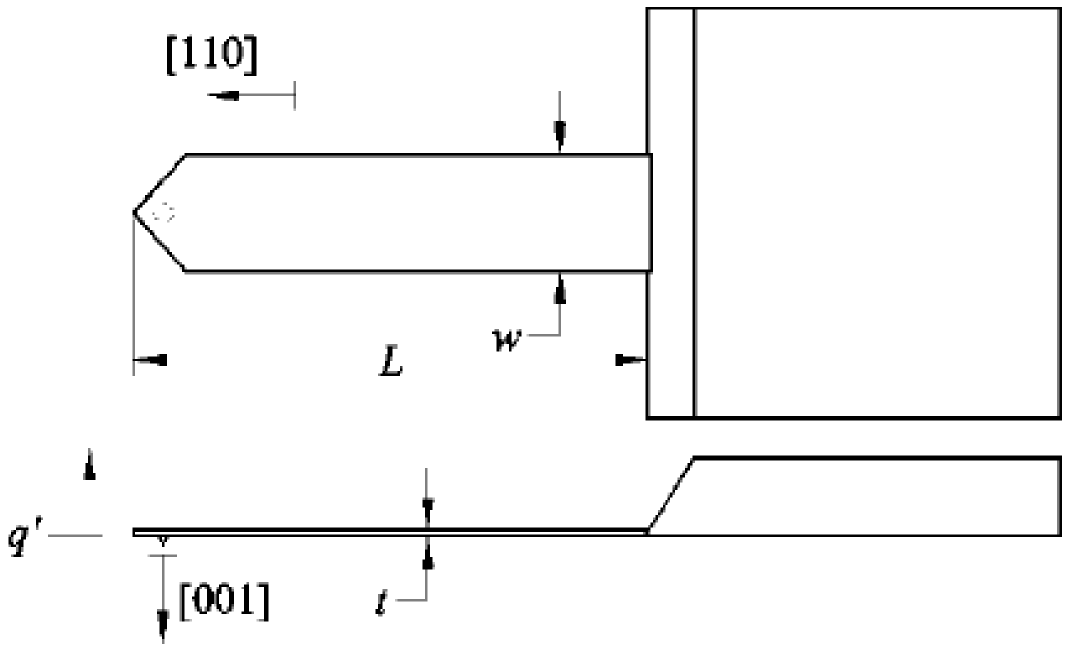

length : l = 450 μm
width : w = 45 μm
thickness: t = 1.5 μm
E=1.69 10^{11}N/m^2

Tip heigth: 12 μm
Tip radius: ≈10 nm

Spring constant k:

$$k = \frac{Ewt^3}{4l^3} = 0.15\,\mathrm{N/m}$$

Wafers are oriented in [001]-direction

Deflection sensors

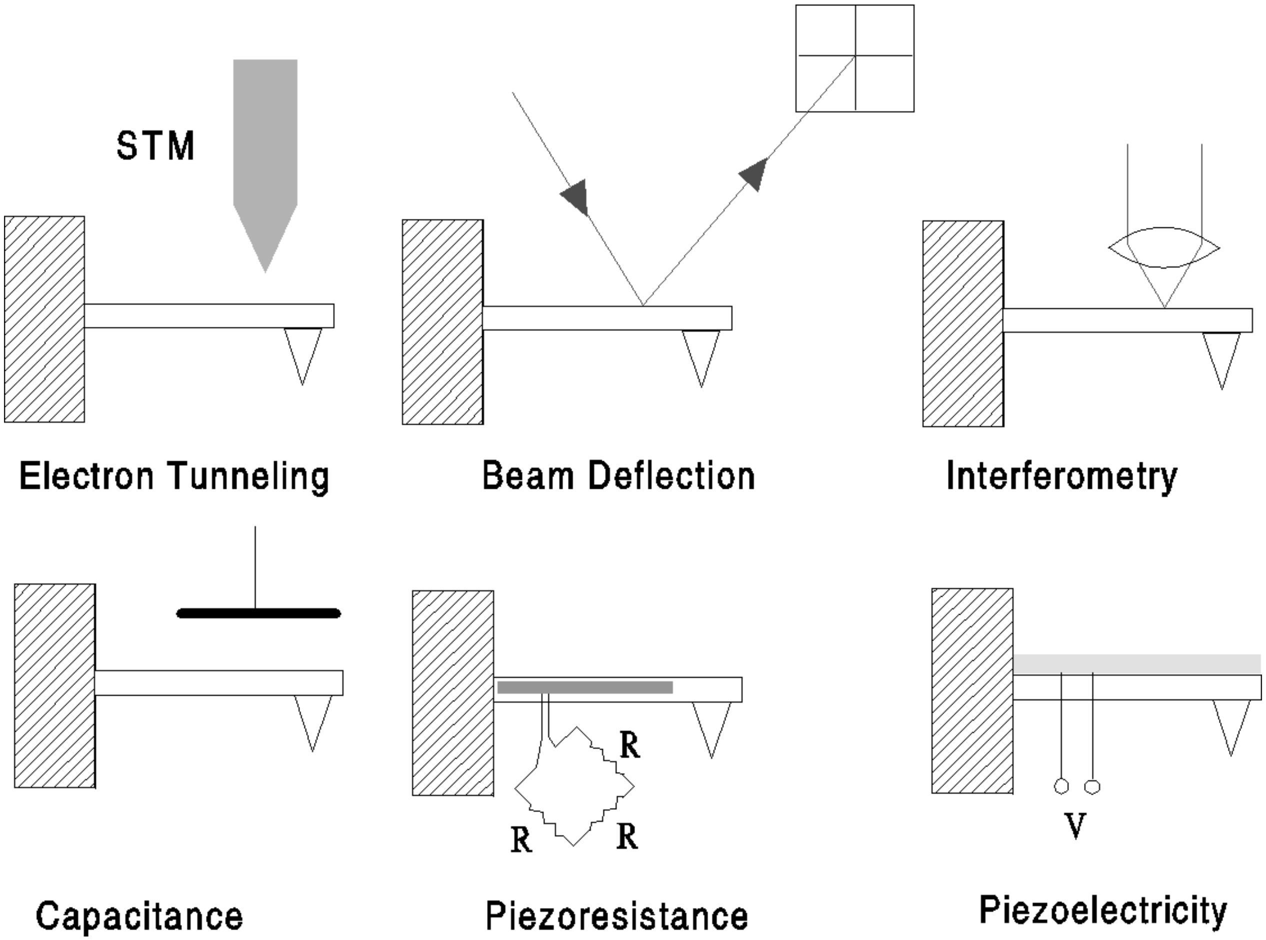

Tuning fork sensors

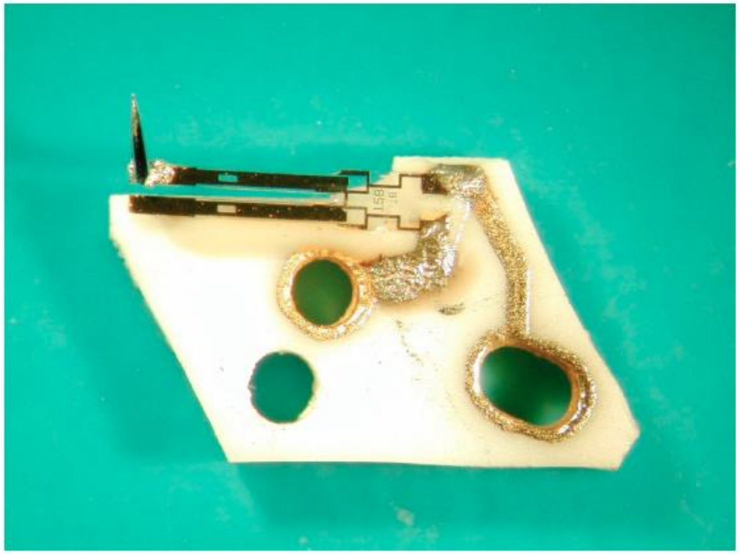

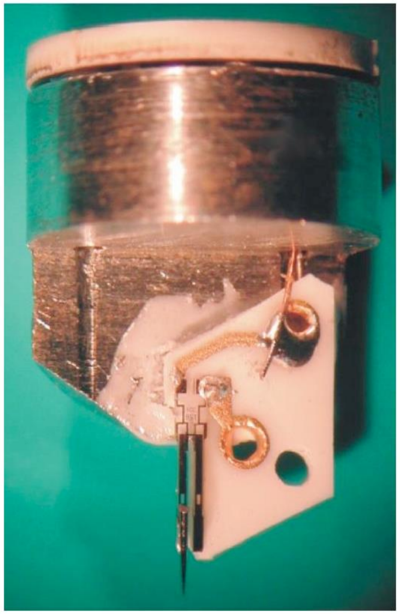

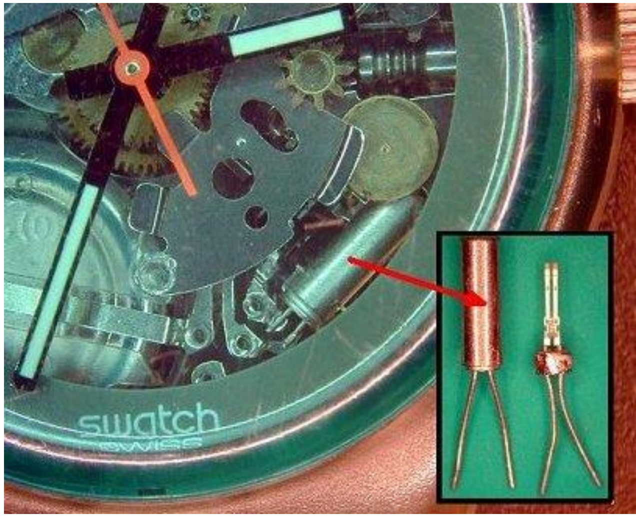

F. Giessibl, Rev. Mod. Phys. 75, 949 (2003)

Quartz tuning forks are based on piezoelectric response.
Advantage: No positioning required, compatible with low temperature
The most common sensor originates from watch industry
Frequency of about 32kHz and high spring constant 1800N/m
Disadvantage: -Limited bandwidth and only operational in dynamic mode,
-Tip has to be attached manually
-either normal or lateral force information

UNI BASEL

Piezoresistive sensor

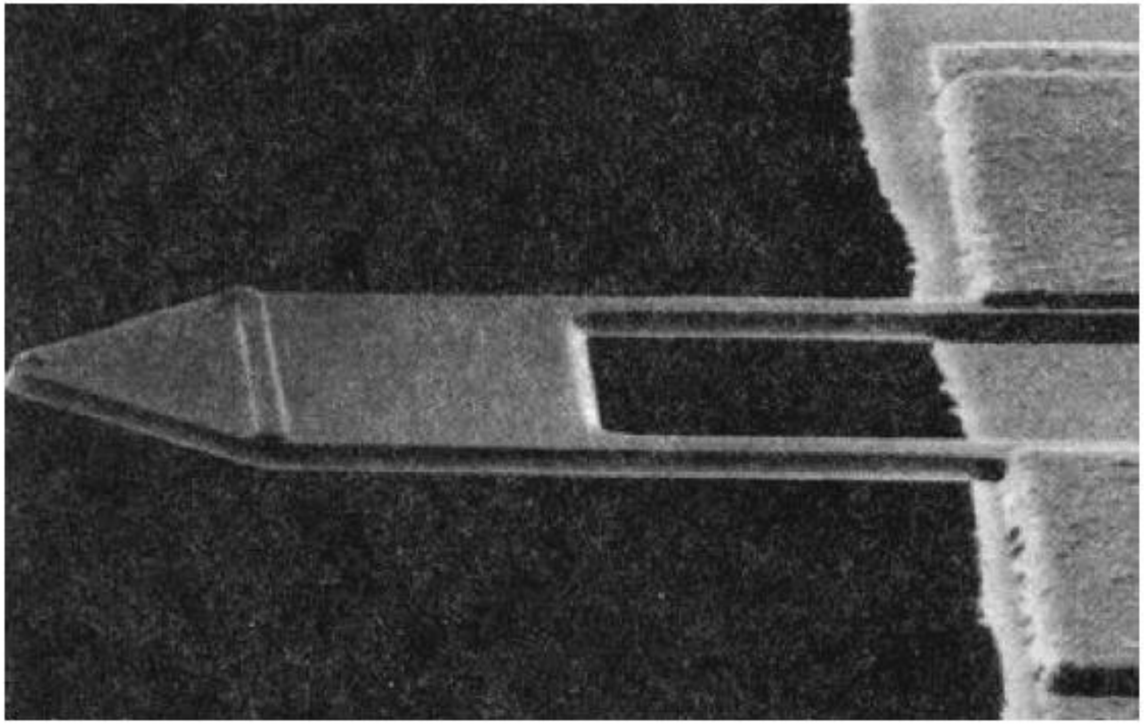

M. Tortonese et al., Appl. Phys. Lett. 62, 834 (1993)

Electrical current is passed through highly doped region. The current depends on strain. Commercially not available at the moment.

Fiber-optical interferometer

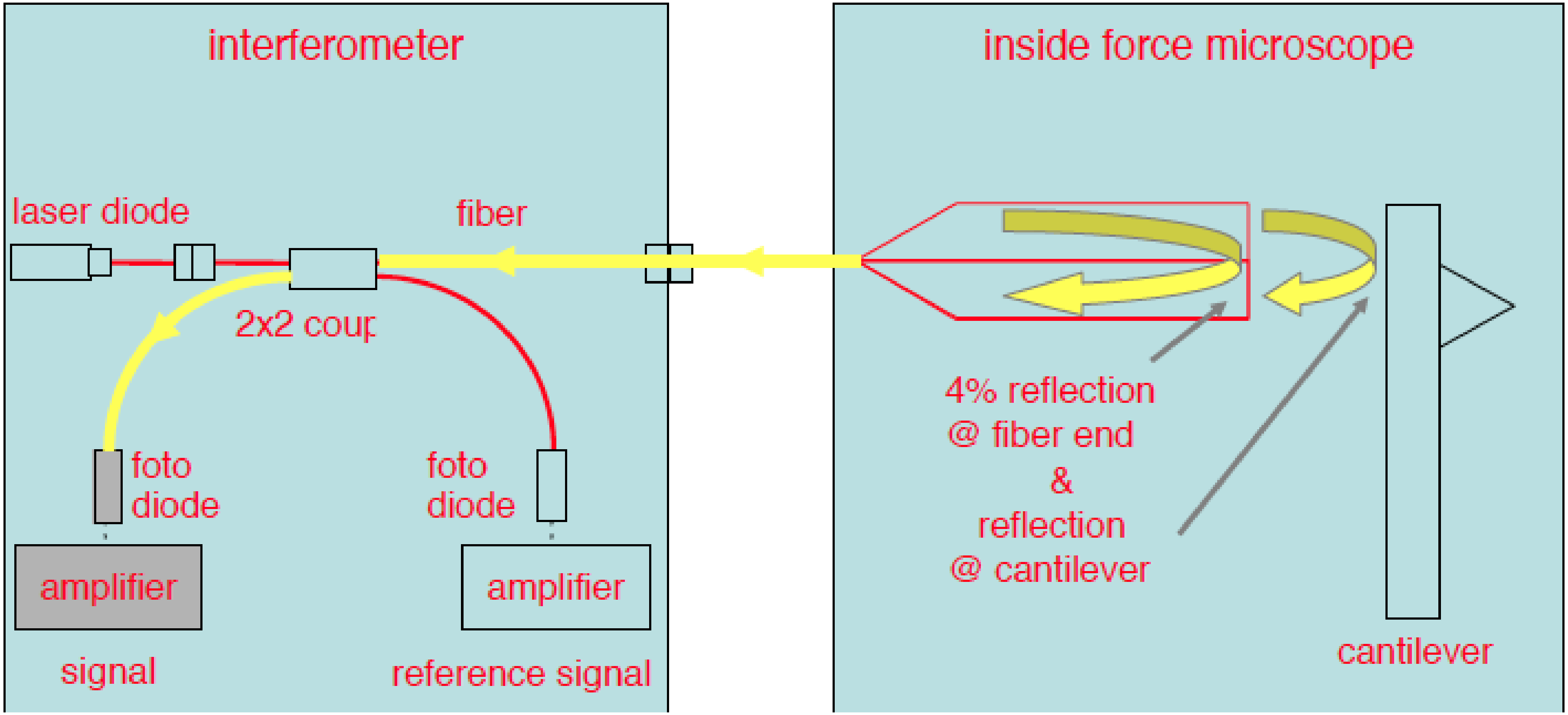

Ref.: D. Rugar, H. Mamin, P. Güthner: Appl. Phys. Lett. 55, 2588 (1989)
A. Moser, H. J. Hug, Th. Jung, U. D. Schwarz, and H.-J. Güntherodt, Meas. Sci. Technol. 4, 769-775 (1993).

Beam-deflection method

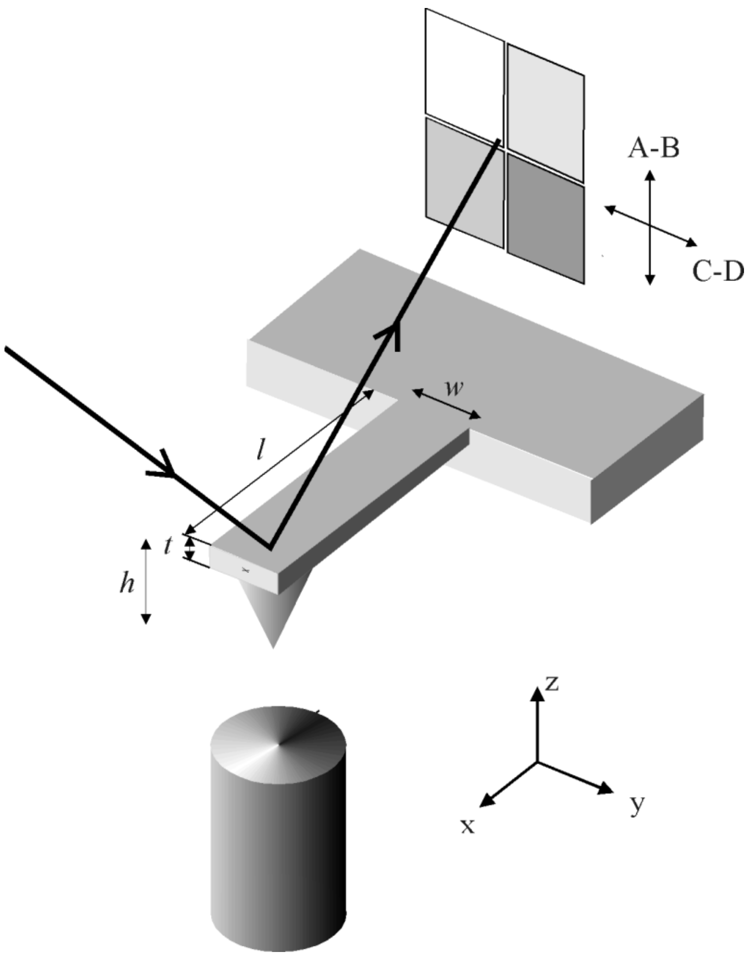

A light beam is reflected from the cantilever onto a segmented photo-diode.
The difference signal A-B is proportional to the normal deflection
The difference signal C-D is proportional to the torsional bending of the cantilever.
Both deflections are proportional to forces and, therefore, normal and lateral forces can be mesured simulaneously.

Spring constants of the cantilever:

$$k_N = \frac{E \cdot w}{4}\left(\frac{t}{l}\right)^3$$

$$k_t = \frac{G \cdot w \cdot t^3}{3 \cdot l \cdot h}$$

Spring constants of triangular cantilevers: Neumeister et al., *Rev. Sci. Instr*. 65 2527 (1994)

Examples

Ultrahigh vacuum force microscopy

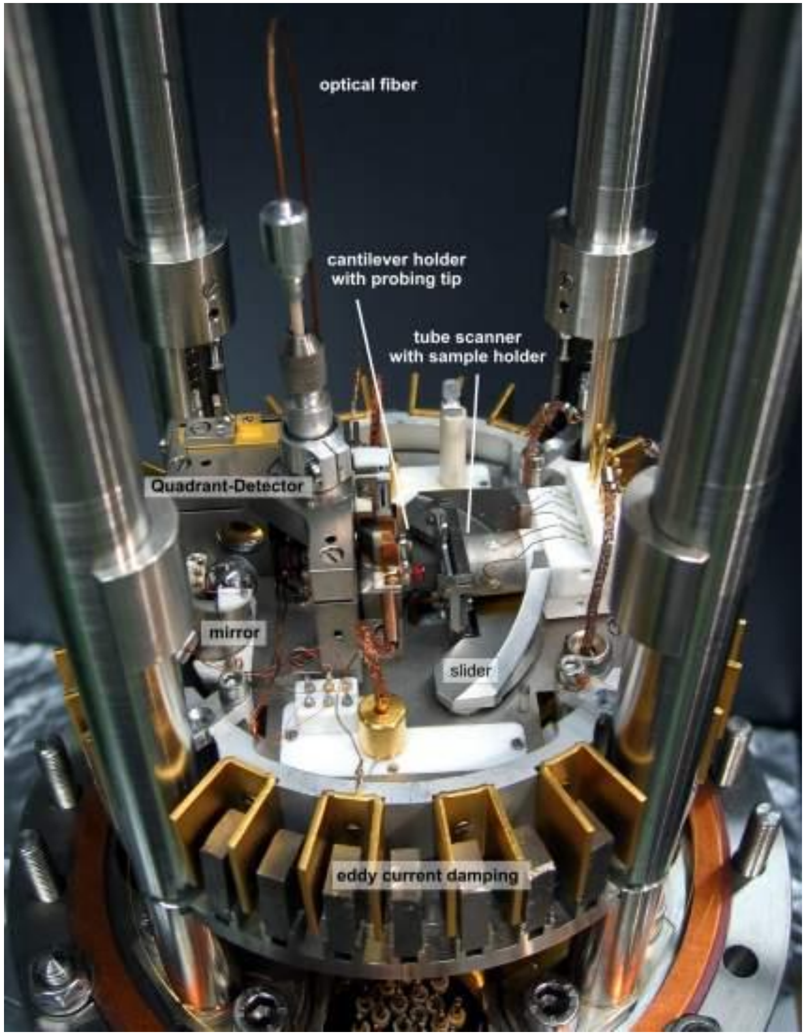

- Pressure: p < 10 $^{-10}$ mbar
- room temperature
- Fast in-situ preamplifier (<3MHz)

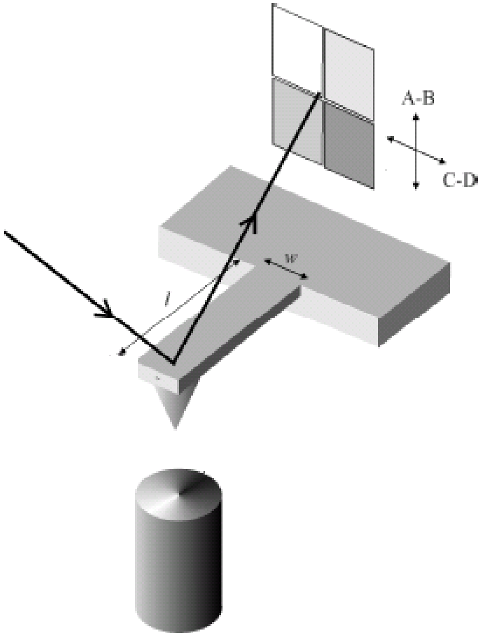

Low temperature force microscopy

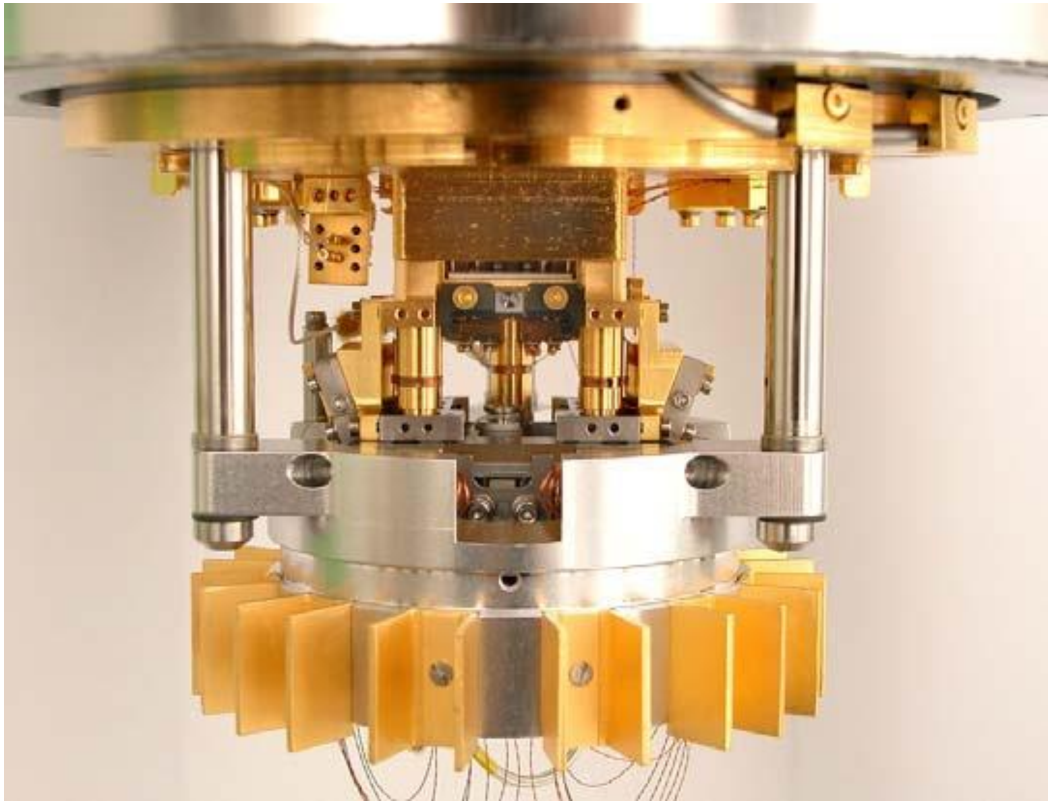

Low temperature measurement (5K-77K).

Large scan UHV SPM (SSRM,KPFM,SCFM,nc-AFM)

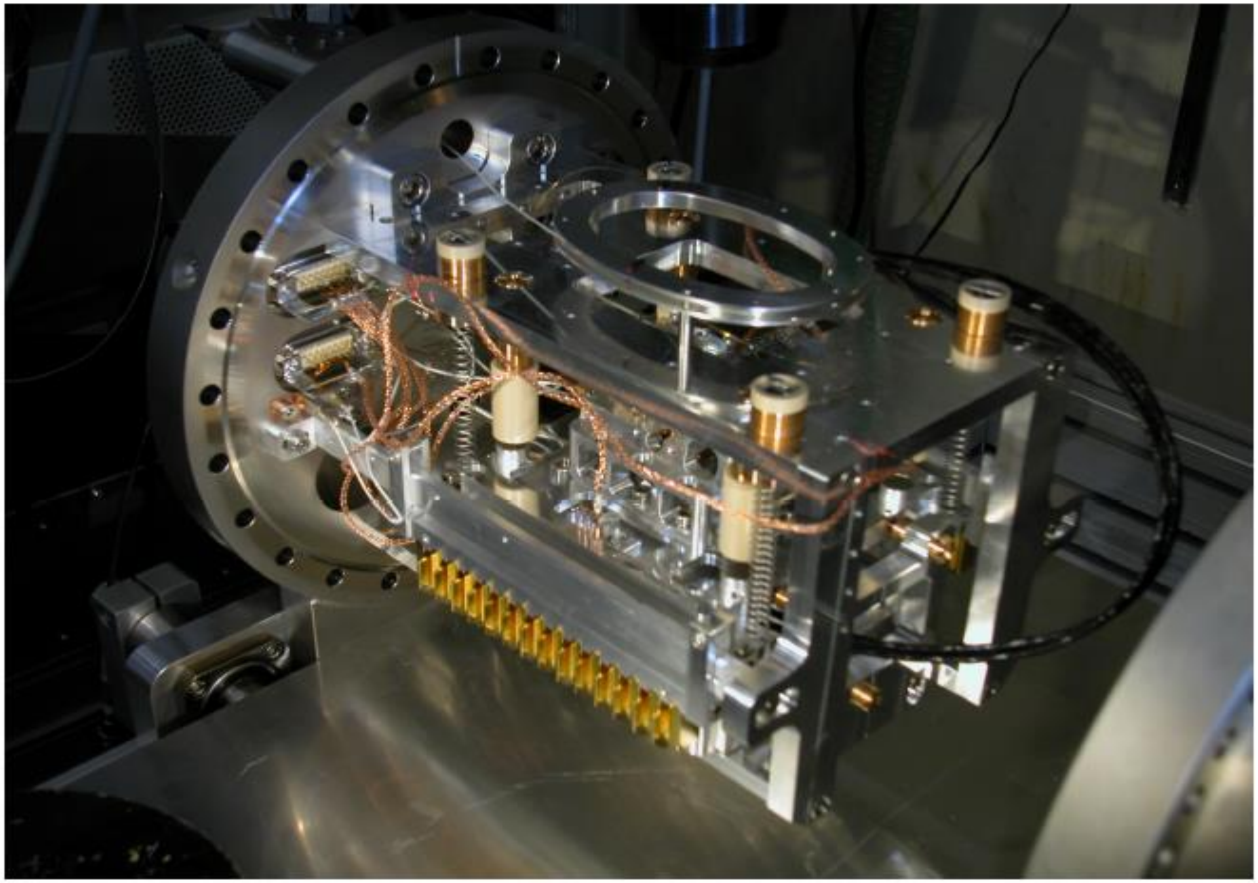

Relevant forces

- **short-range repulsive forces (Pauli exclusion) or ionic repulsion forces**
- **short-range chemical binding forces**
- **van der Waals forces (always present, retarded beyond 100 nm)**
- **electrostatic forces (long-ranged)**
- **magnetic forces**

- **interaction in liquids**
  - **hydrophobic / hydrophilic forces**
  - **steric forces**
  - **solvation forces**

Literature:
J. Israelachvili
Intermolecular and Surface Forces with Applications to Colloidal and Biological Systems, **Academic Press (1985)**
D. Tabor
***Gases, liquids and solids*, Cambridge University Press (1979)**

Force vs. Distance curve

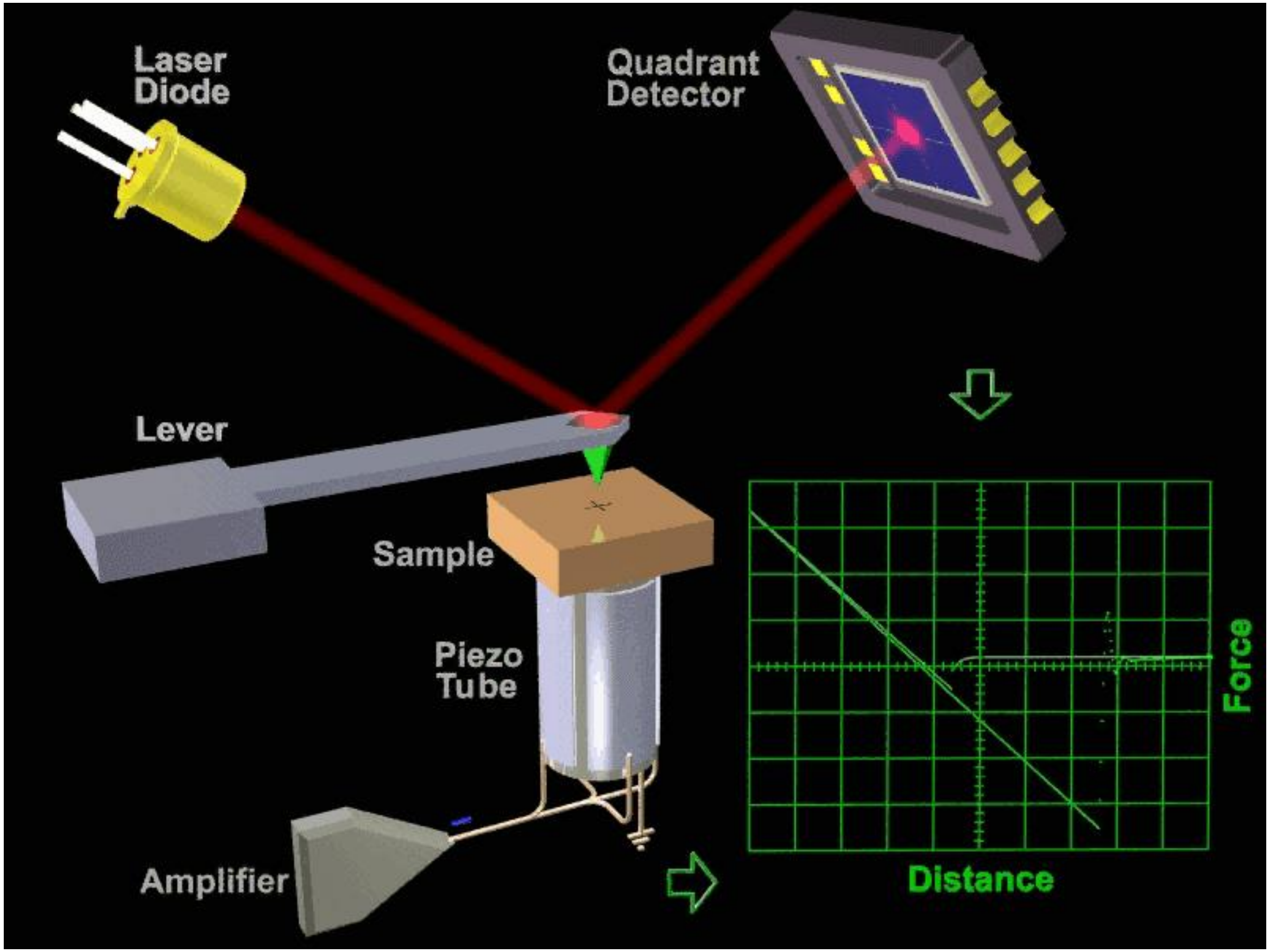

AFM on compact discs

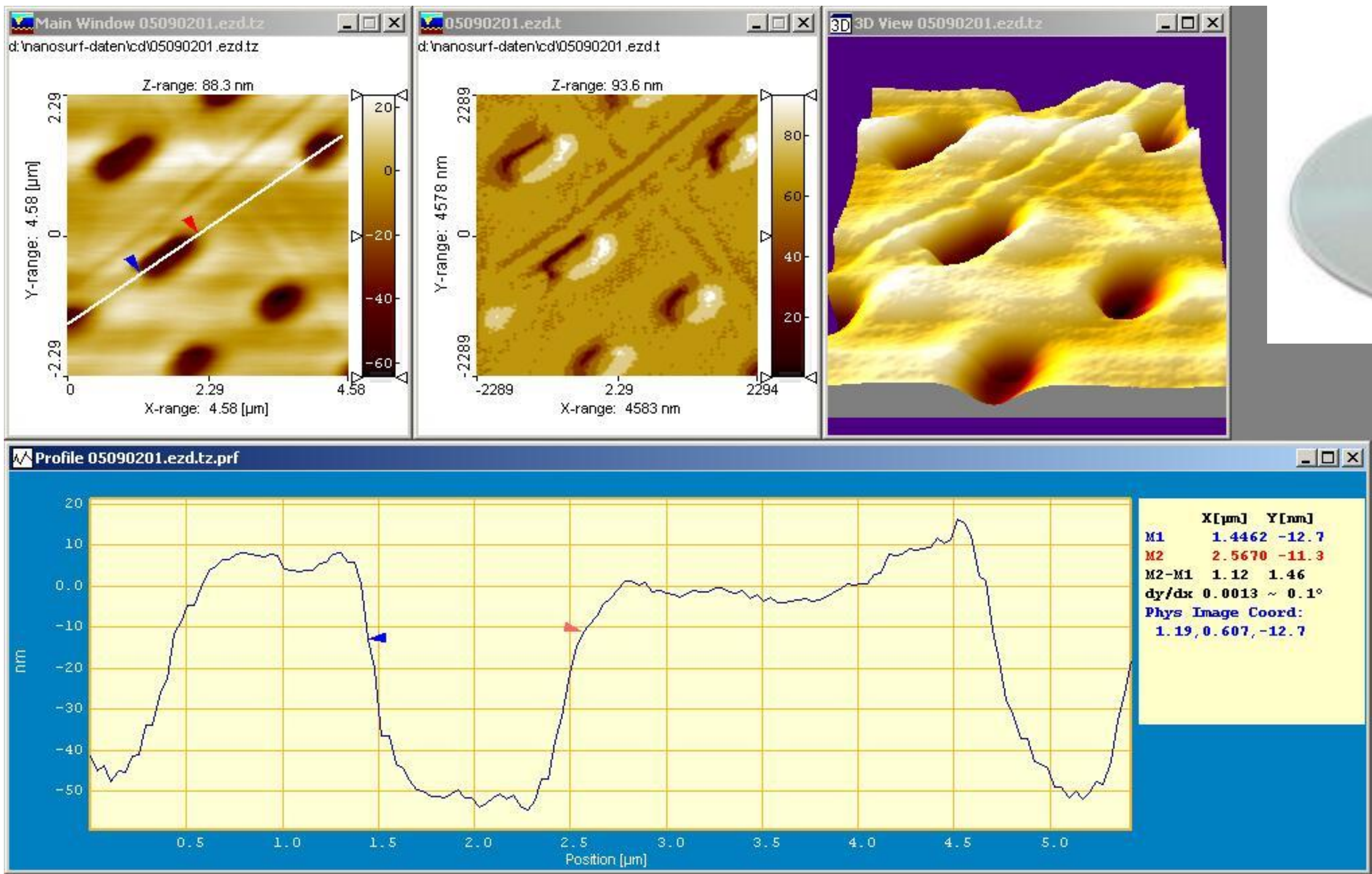

*nano**Surf***

Applications of AFM

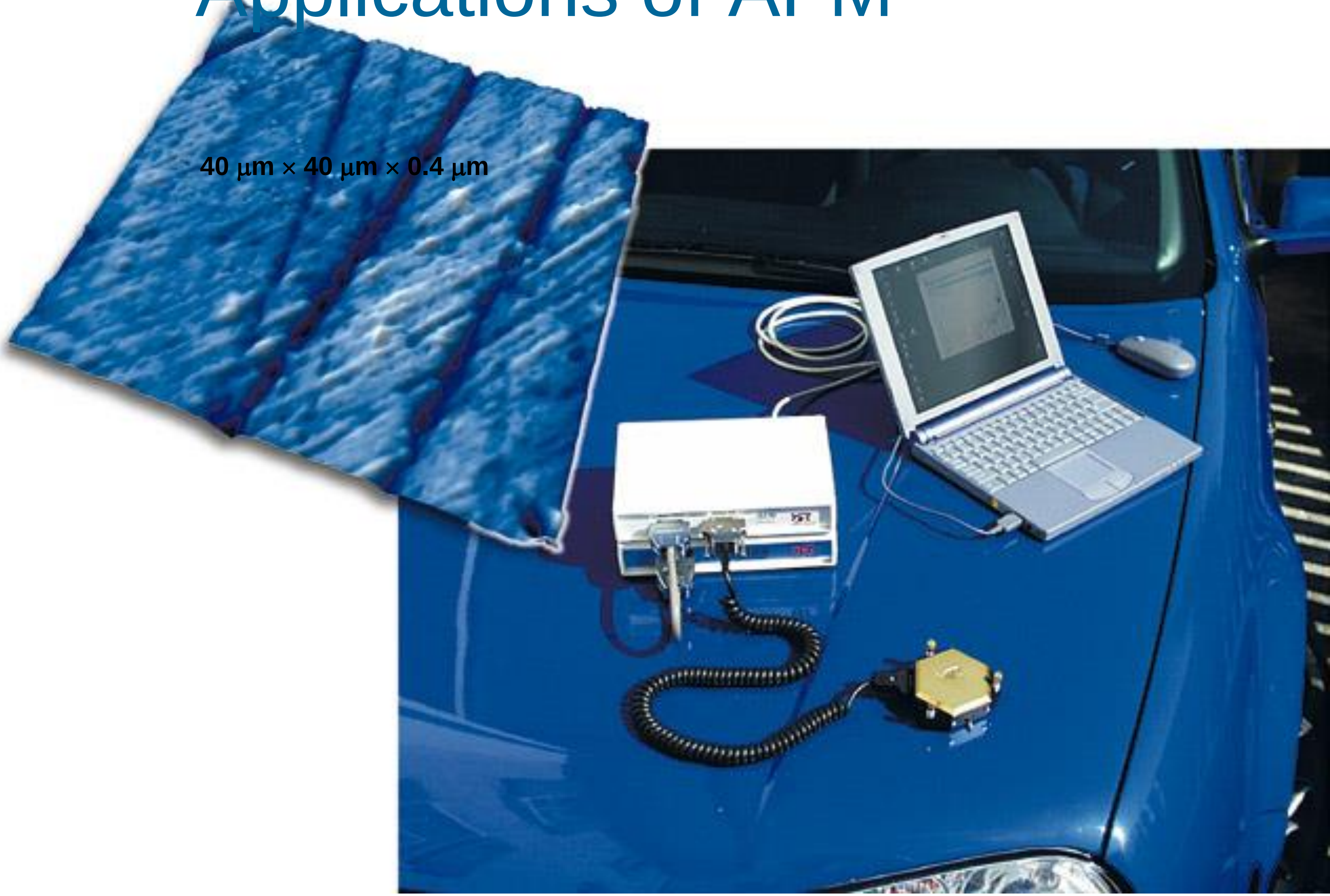

UNI BASEL

Single molecules

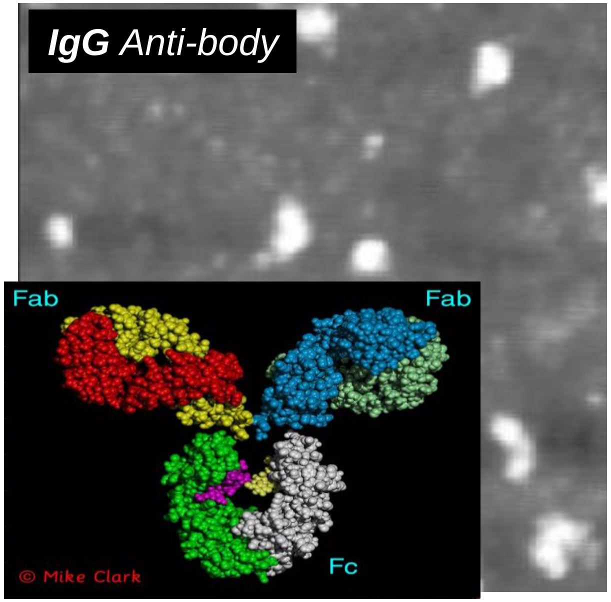

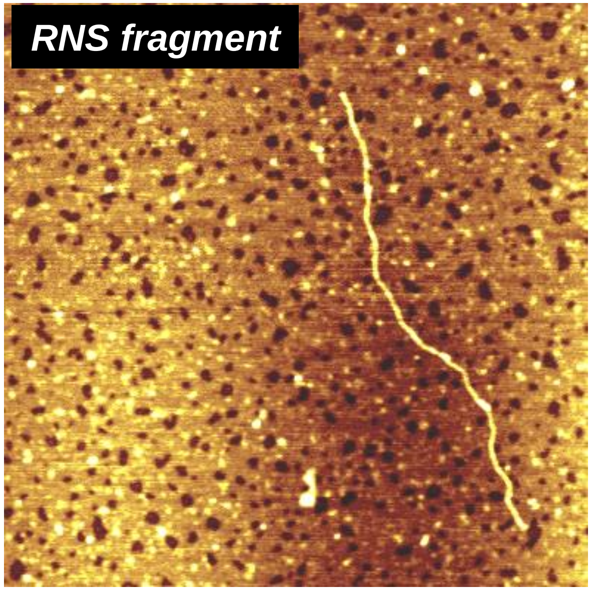

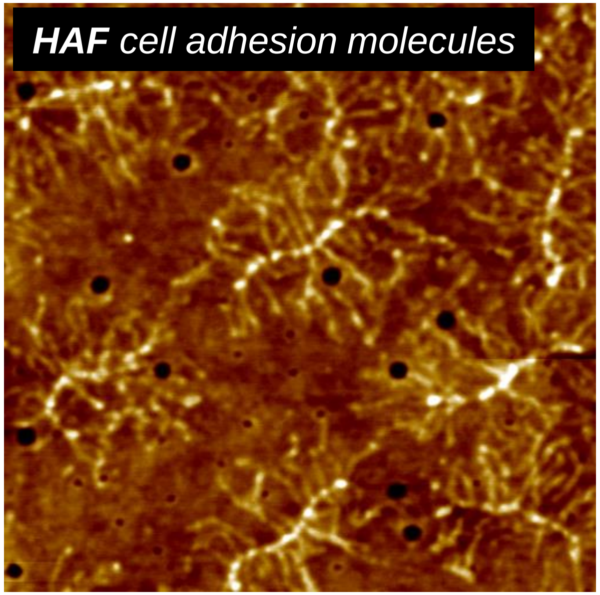

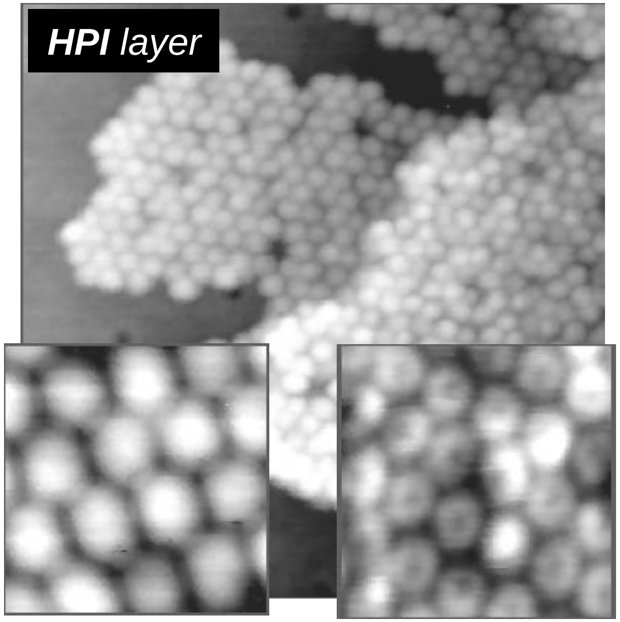

Atomic resolution on Si(111)7x7 by AFM

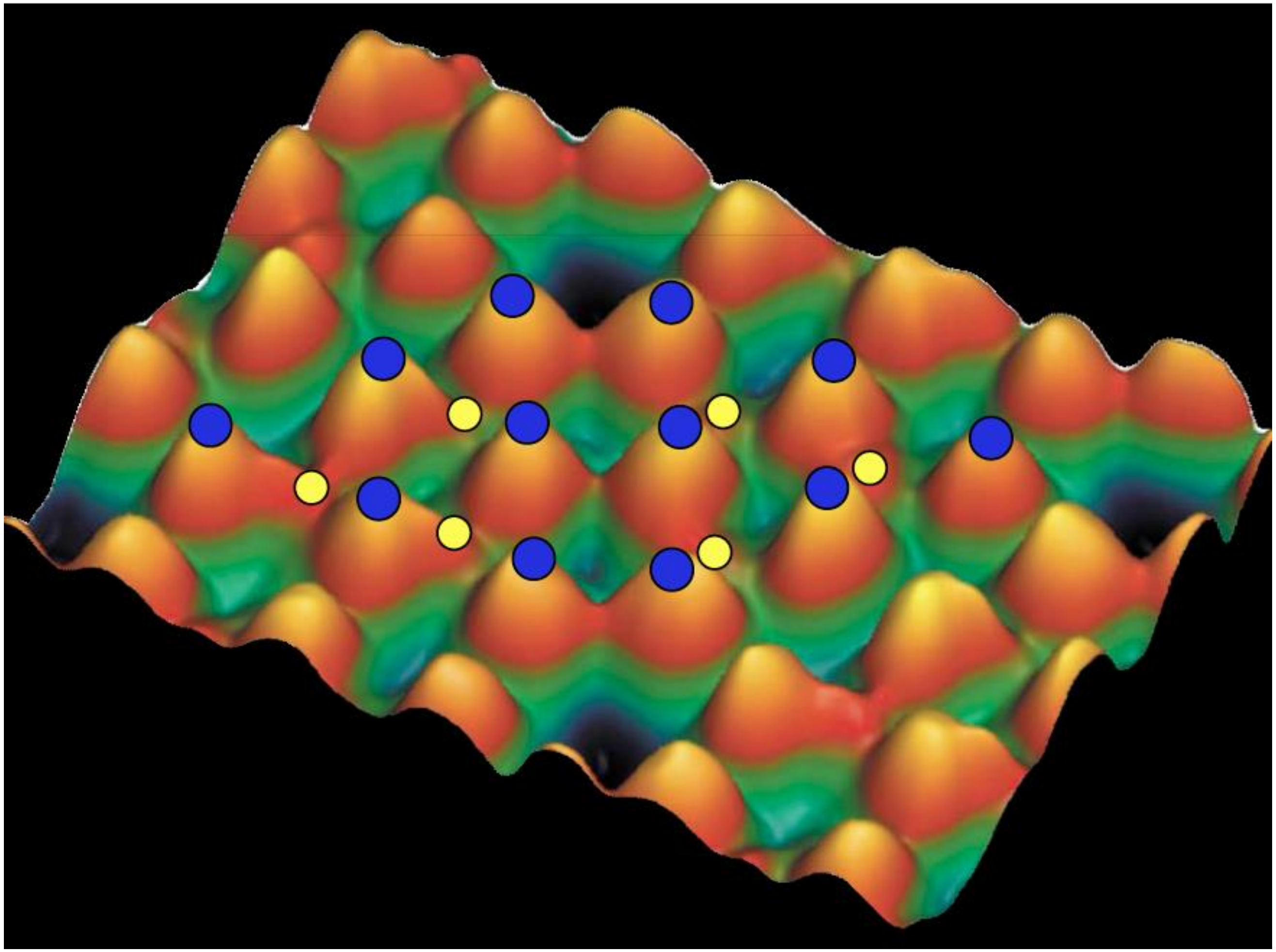

F. Giessibl et al. 267, 68 (1995), Science M. Lantz et al. Science 291, 2582 (2001)

True atomic resolution on NaCl(001)

(Insulator surface with point defects)

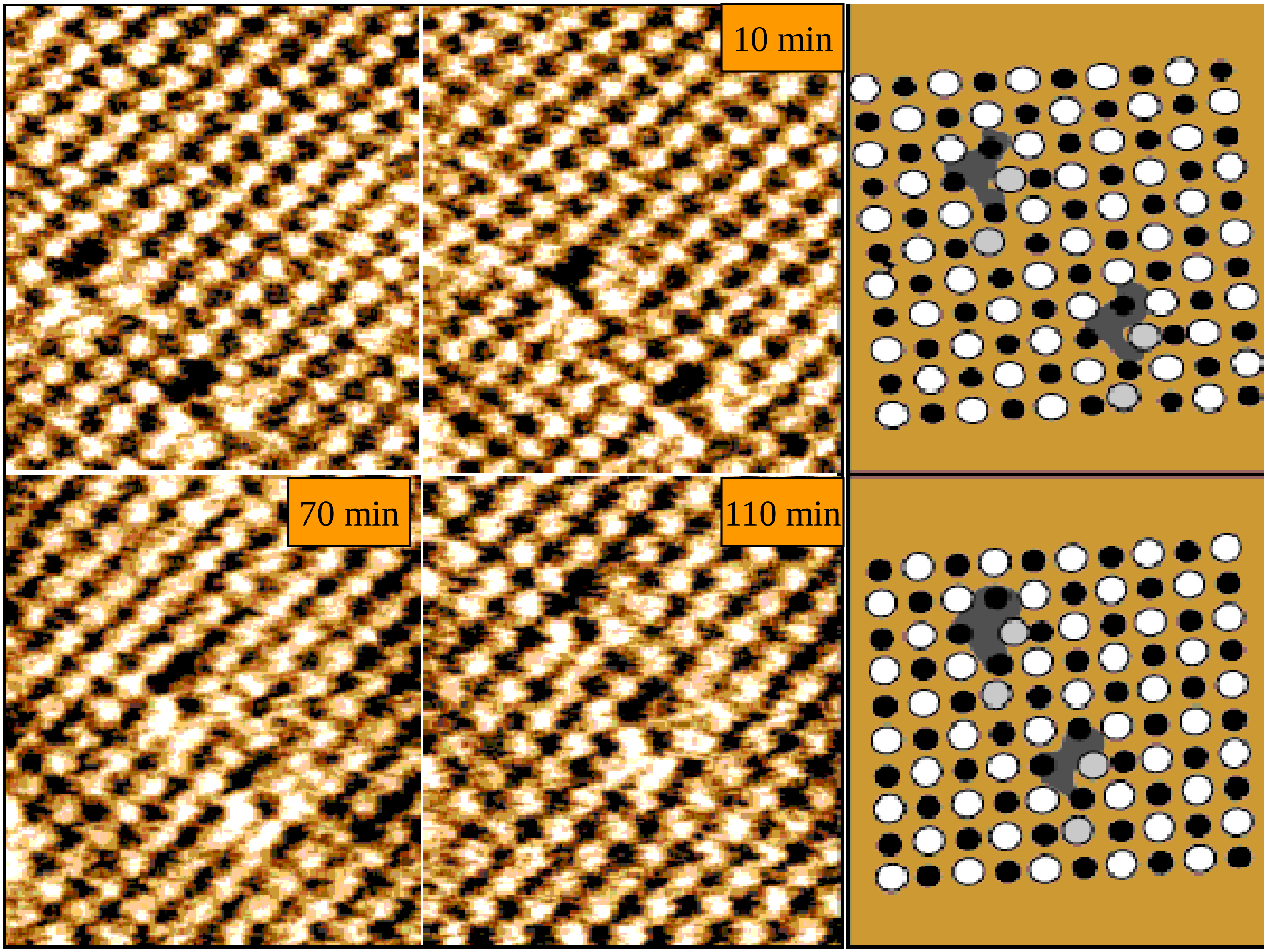

M. Bammerlin et al., *Probe Microscopy* **1**, 3 (1997)

Nano-Switzerland

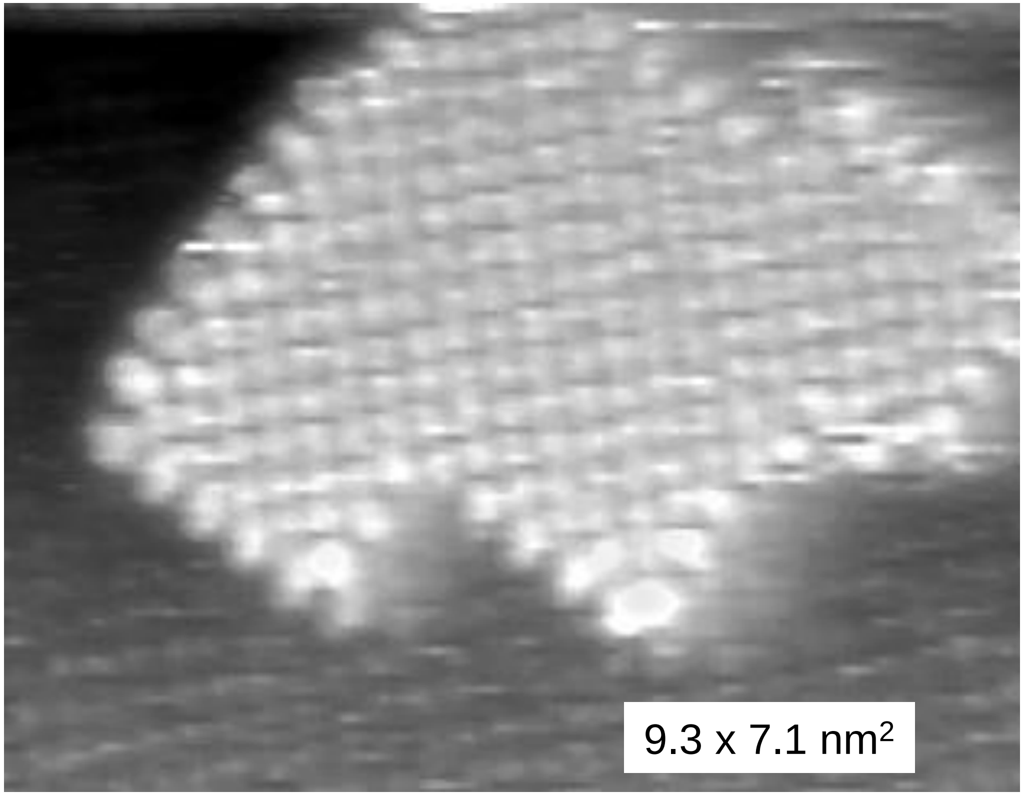

NaCl-Islands consisting of 120 atoms

Truxene molecules on insulators

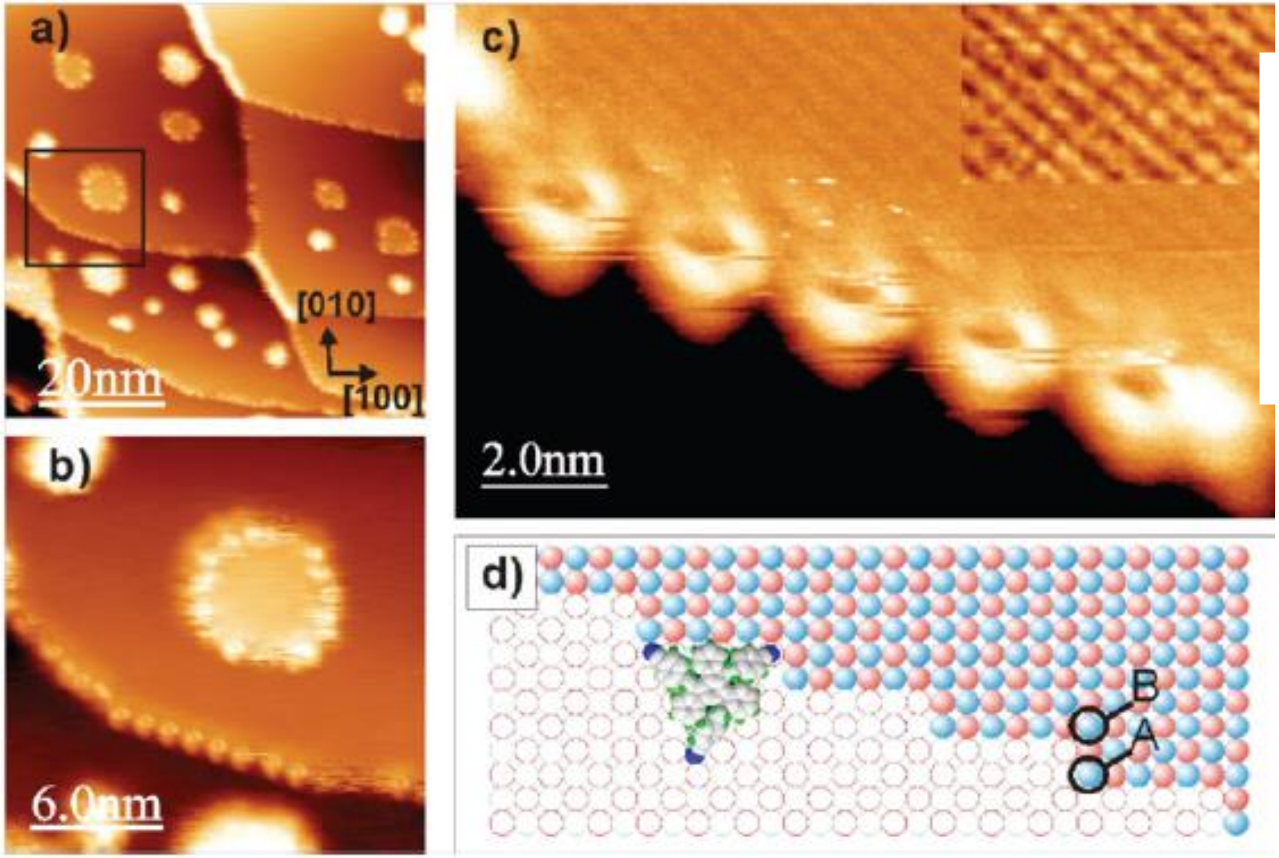

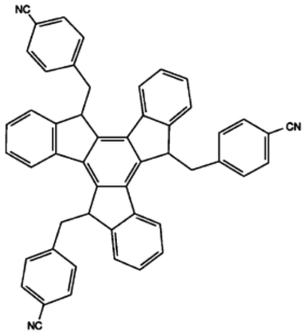

Stable adsorption at steps and kink sites of KBr(001)

B. Such et al., ACS Nano (2010).

Single truxene molecules on an insulator

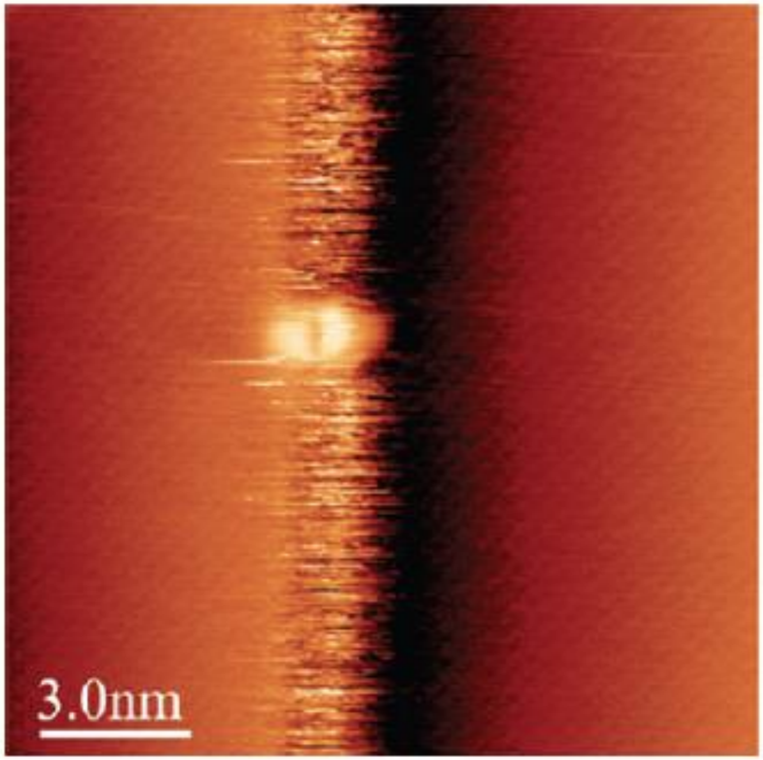

Br terminated, E_b=1.33eV

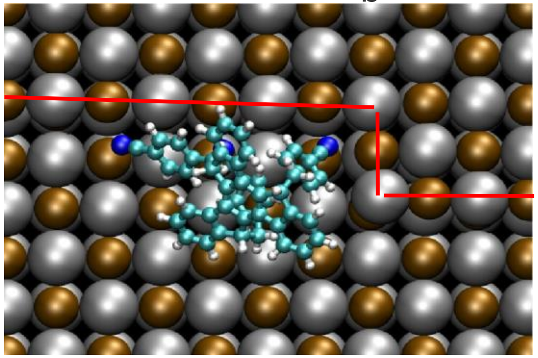

K terminated, E_b=1.17eV

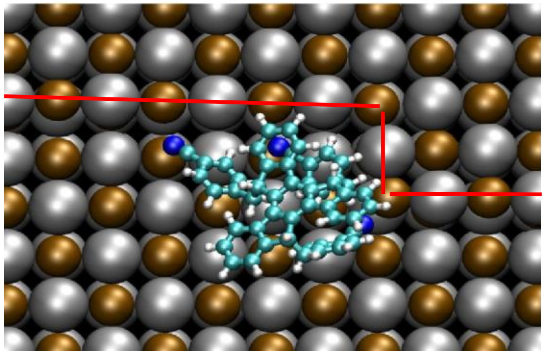

Truxene molecule on KBr at RT
Stable configuation at the kink sites

B. Such et al., ACS Nano (2010).

UNI BASEL

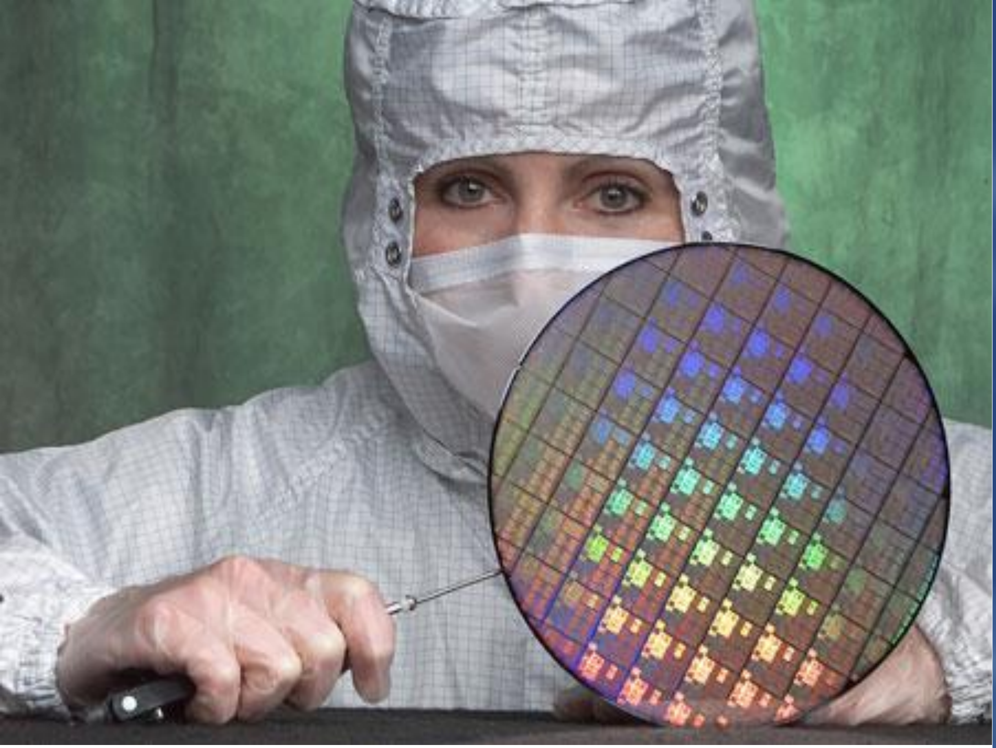

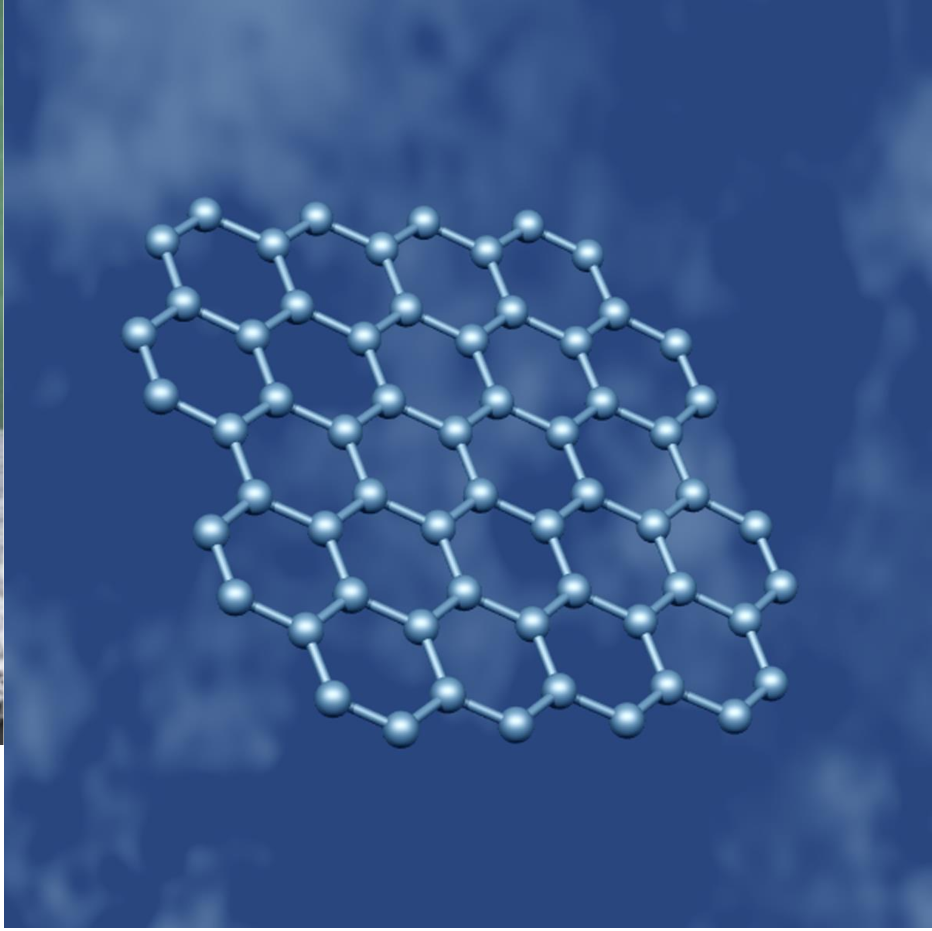

Graphene:
thickness of one atomic layer
interesting electronic and mechanical properties

High resolution of graphene nanoribbon with a CO tip

NC-AFM image (df map) @ 4.8 K Au(111)

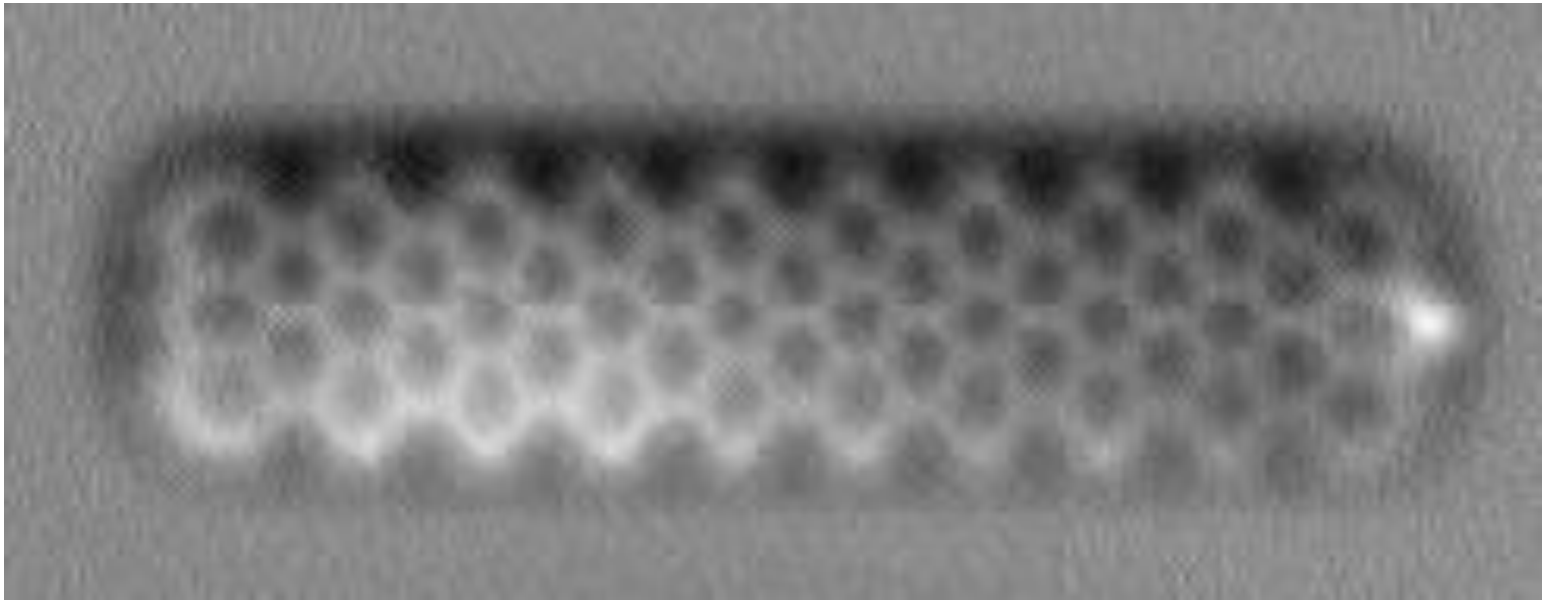

Tuning fork sensor

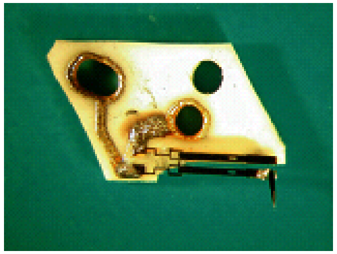

F.J. Giessibl, APL 73, 3956 (1998).

CO tip

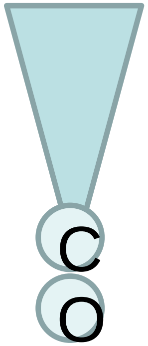

L. Gross et al Science 325, 1110 (2009).

Sharpen tip by FIB milling R_{tip}≈20 nm

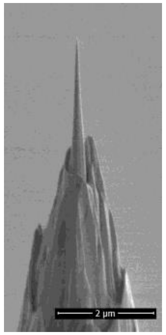

S. Kawai

STM on Nanodiamonds with light exposure

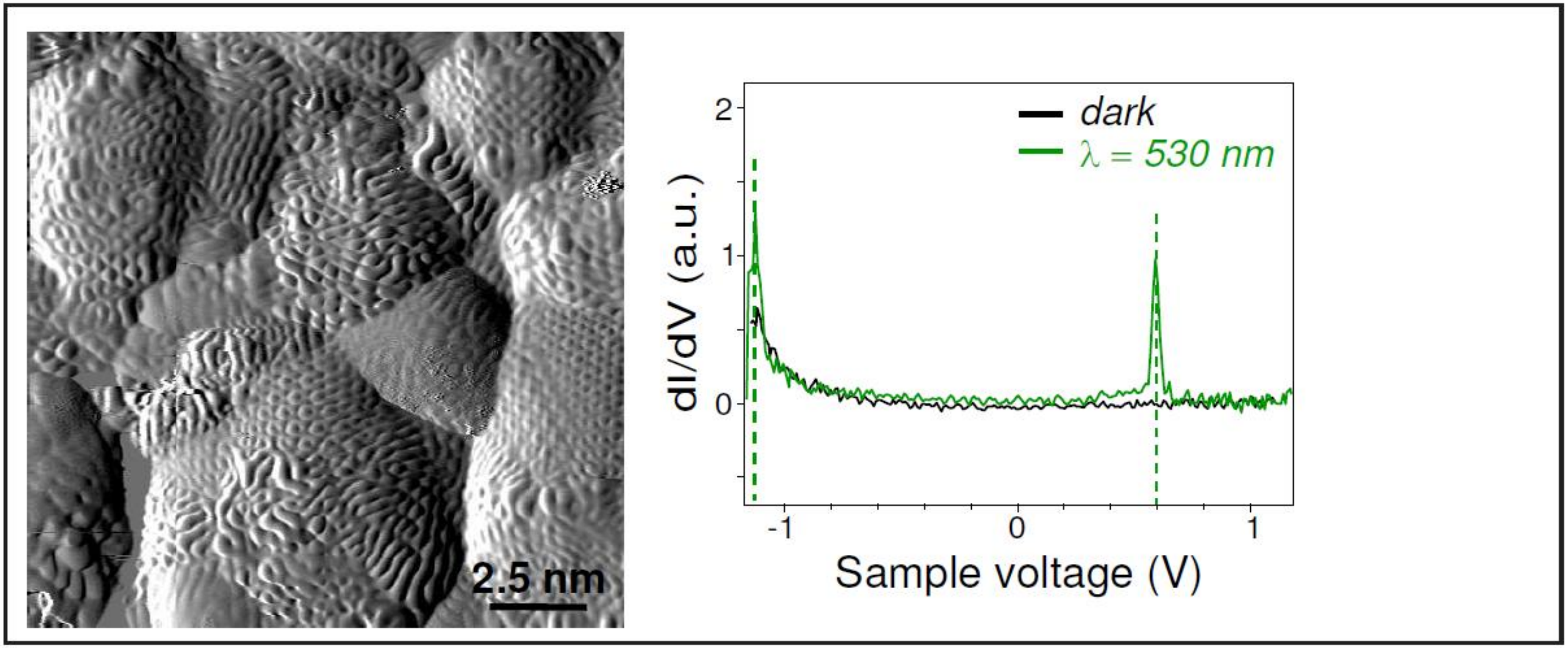

Rémy Pawlak, Thilo Glatzel, Vincent Pichot, Loïc Schmidlin, Shigeki Kawai, Sweetlana Fremy, Denis Spitzer et Ernst Meyer, **Local Detection of Nitrogen-Vacancy Centers in a Nanodiamond Monolayer** Nano Lett. DOI: 10.1021/nl402243s (2013)

UNI BASEL

Comparison of AFM and Simulations

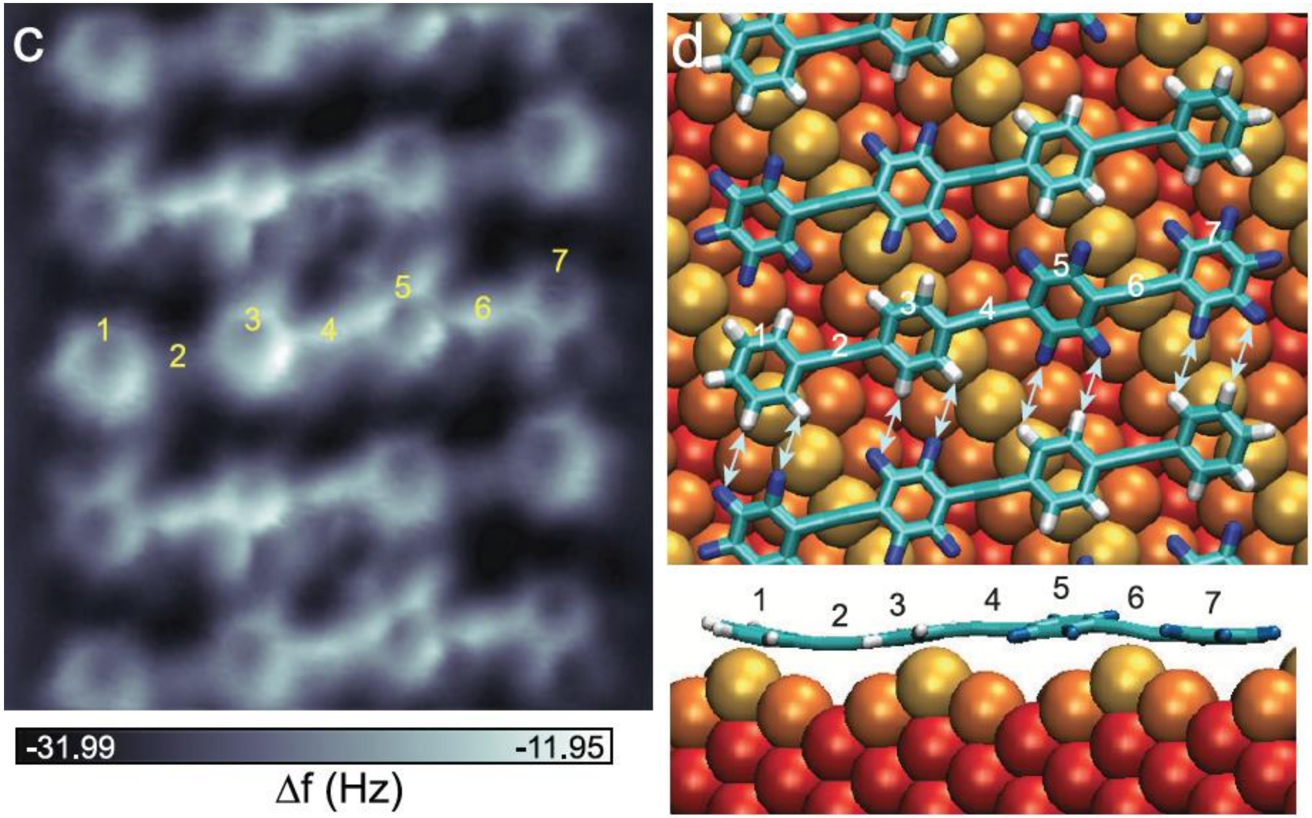

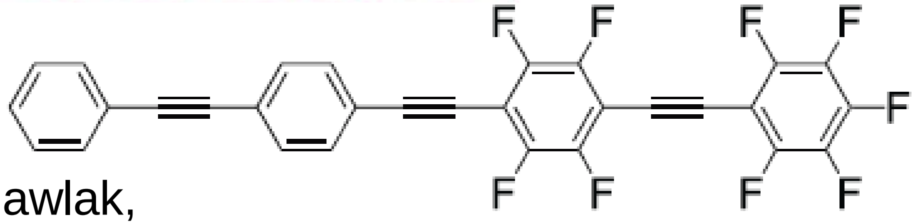

S. Kawai, A. Sadeghi, X. Feng, P. Lifen, R. Pawlak,
T. Glatzel, A. Willand, A. Orita, J. Otera, S. Goedecker, and E. Meyer
ACS Nano, 7, (10), (2013), 9098

Assembly of Swiss Cross at RT by vertical manipulation

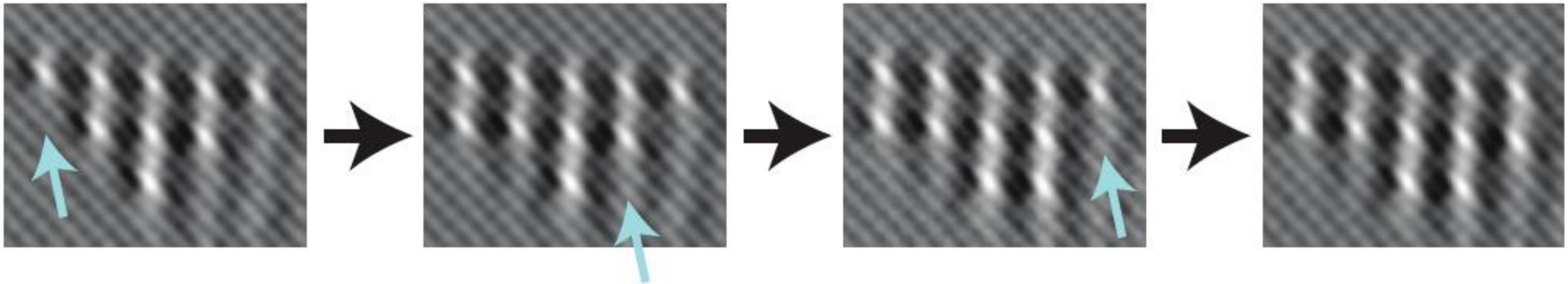

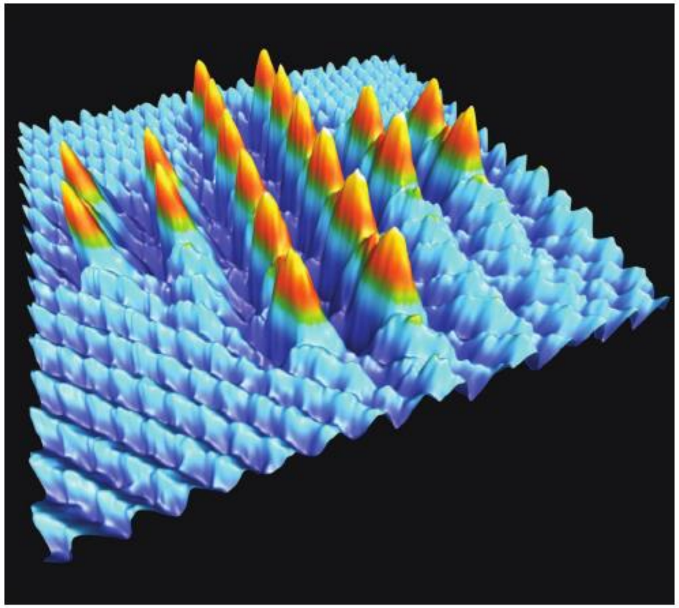

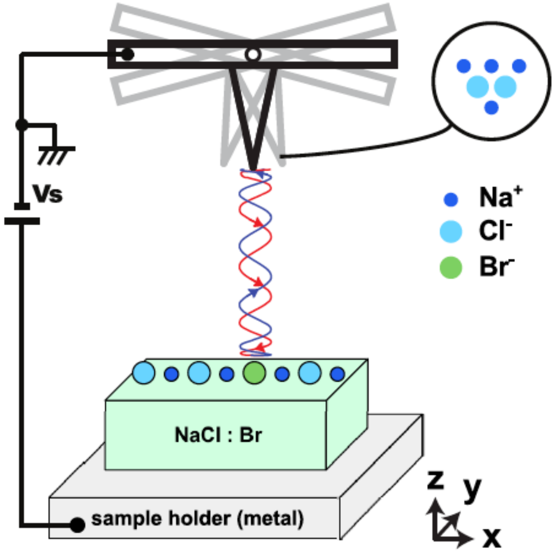

S. Kawai, Nat. Comm. 2014

Torsion frequency imaging
gives best contrast between Br and Cl

UNI BASEL

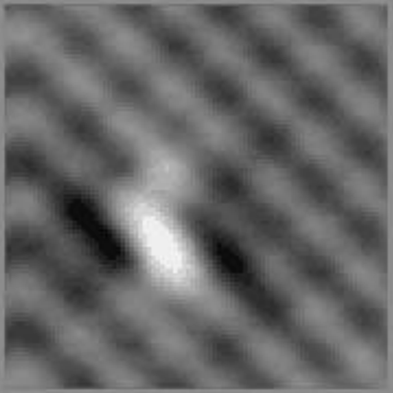

Besten Dank für
Ihre Aufmerksamkeit